SAPIENZA
UNIVERSITÀ DI ROMA

RAD52 prevents accumulation of Polα-dependent replication gaps at perturbed replication forks in human cells

Department of Molecular Medicine
Ph.D. program in Human Biology and Medical Genetics
XXXV cycle

Ludovica Di Biagi

Scientific Tutor:

Dr. Pietro Pichierri

Director of Doctoral Program:

Prof. Laura Stronati

Academic year 2021-2021

INDEX:

ABSTRACT

RAD52 (Radiation sensitive 52) is a highly conserved protein involved in DNA damage repair. In humans, RAD52 contributes to the stabilization of the replication forks after replication arrest and prevents an excessive reversion of the forks that may result in pathological strand degradation. Consequently, loss of the RAD52 function leads to excessive replication fork reversal, persistence of under-replicated regions and chromosome instability. However, the mechanisms that the cell uses to overcome the stalled forks and complete the DNA replication in the absence of RAD52 are still unknown. Here, we investigated how replication restarts in absence of a functional RAD52. As recent evidence suggests that an excessive fork reversion could limit the repriming-mediated replication restart, we asked whether the loss of RAD52 could affect this mechanism. Using multiple cell biology experiments, we demonstrated that, in response to hydroxyurea-mediated replication fork slowing or arrest, the impairment of RAD52 ssDNA-binding induces the accumulation of parental DNA gaps due to increased recruitment of DNA polymerase alpha (Polα) and that RAD52 deficiency stimulates Polα-mediated, but not PrimPol-mediated, replication repriming. Furthermore, we showed that Polα recruitment occurs downstream the remodelled reversed fork (RF) and depends on the function of RAD51. Finally, we demonstrated that the repair of ssDNA gaps derived from Polα-mediated repriming is delayed until the G2-phase of the cell cycle, and are filled by the post replicative

repair (PRR) mechanism mediated by PCNA ubiquitination. In this scenario, the ssDNA gaps repair is possibly mediated by a post-replicative activation of the checkpoint kinase 1 (CHK1). Collectively, our findings unveil a novel Polα-mediated repriming pathway acting when reversed forks undergo extensive degradation in the absence of fork cleavage. We proposed that the repriming mechanism driven by Polα in absence of RAD52 function is a novel rescue pathway to prevent DNA damage and promote viability under replication stress.

INTRODUCTION

DNA REPLICATION

Cellular DNA replication is initiated through the action of multiprotein complexes that recognize replication start sites in the chromosome and facilitate duplex DNA melting within these regions (Bell & Dutta, 2002). Research in the past two decades has identified an ensemble of 20 proteins involved in the process of replication initiation (Bell & Dutta, 2002). Initial unwinding of the DNA is confined to limited regions known as origins of replication. The enzyme that catalyses this process, the replicative helicase, is a primary target for the regulation of DNA replication in all domains of life. The core of the replicative helicase in eukaryotes is a hetero-hexameric ring-shaped complex called minichromosome maintenance (MCM), in which six related subunits (Mcm2–7) interact in a defined order. The first step, helicase loading, occurs in late mitosis and G1 phase, and involves the loading of MCM onto chromatin at origins of replication. This reaction is dependent on prior binding of the Origin Recognition Complex (ORC), comprised of ORC1–6, and the proteins Cdc6 and Cdt1 (Zhu et al., 2007), producing a double hexamer of MCM that encircles double-stranded DNA (dsDNA) and is inactive as a helicase. In the second step, helicase is activated upon progression into S-phase.

Here, the combined activities of cyclin-dependent kinase (CDK) and Dbf4-dependent kinase (DDK) recruit to MCM the firing factors Sld2/3/7, Cdc45, Dpb11, GINS, pol ε and Mcm10 (Yeeles et al., 2015) (Fig 1). Once recruited, the firing factors remodel the MCM double hexamer into two active CMG (Cdc45–MCM– GINS) helicases. Encircling each leading DNA strand, the active complex moves away from the centre of the origin and allows for the assembly of the remaining replisome components on the resulting single-stranded DNA (ssDNA) (Fu et al., 2011; Yeeles et al., 2015) (Fig 1).

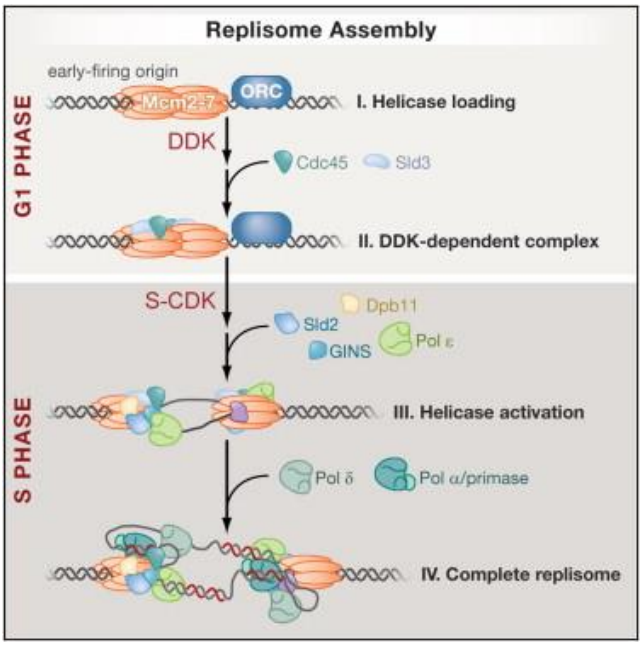

Fig. 1 - Model of Replication Initiation: The Mcm2–7 helicase is loaded to origin DNA in an inactive form during late M/G1 phase of the cell cycle. In late G1 or S phase, DDK targets Mcm2–7 for phosphorylation, allowing recruitment of Sld3 and Cdc45. S-CDK activation and phosphorylation of Sld2 and Sld3 trigger the recruitment of Sld2, Dpb11, GINS, Polε, and Mcm10. The formation of the Cdc45-Mcm2–7-GINS complex activates the helicase, triggering melting of origin DNA. Polα and Polδ are loaded on the unwound DNA to complete replisome assembly (Heller et al., 2011).

The synthesis is then completed by the major replicative DNA polymerases (Polδ and Polε). These enzymes have an advanced proofreading capacity, to ensure high fidelity synthesis (Bainbridge et al., 2021). They work by synthesizing DNA in 5′ to 3′ direction, however they lack the ability to initiate DNA synthesis de novo. Therefore, a short ribonucleotide primer is required, from which 3′ extension can be continued by the replicative polymerases (Kuchta & Stengel, 2010). In the conventional model, the initiating primers on both the leading and lagging strand are generated by the Polymerase α (Polα) - primase complex. The primase complex Pri1/Pri2 (PriS/L) synthesises de novo a short RNA primer of 8–12 ribonucleotides that Polα can extend by adding 10–20 DNA nucleotides to create an RNA-DNA hybrid primer (Kuchta et al., 1990; Perera et al., 2013). This primer is then further extended by the primary replicative polymerase (Polδ and Polε). Polymerase usage throughout replication is well-coordinated, with the majority of leading strand synthesis driven by Polε, while Polδ copies the lagging strand (Daigaku et al., 2015). All polymerases exclusively synthesise DNA in a 5′ to 3′ direction, for this reason, the lagging strand is synthesised in short, discontinuous fragments called Okazaki fragments (OF). OF synthesis is initiated by Polα-primase, which generates hybrid primers whose extension is executed by Polδ and regulated by PCNA binding. As Polδ-PCNA complex encounters the RNA primer of the preceding OF, it performs limited strand displacement (SD) synthesis and gives rise to a single-stranded 5′ flap structure (Maga et al., 2001.) that are cleaved by flap endonuclease-1 (FEN1), (Zaher et al., 2018) generating a nick product that can then be sealed by DNA Ligase 1 (Lig1) (Blair et al., 2022; Lin et al., 2013; Matsumoto et al., 2020). Termination

of DNA replication occurs either when converging replication forks meet or when the end of the chromosome is reached. Unlike replication initiation, which is well studied in eukaryotes, replication termination has received significantly less attention. For this reason, the current understanding of replication termination is somewhat incomplete (Bainbridge et al., 2021).

DNA DAMAGE RESPONSE

The DNA is constantly subjected to different types of lesions. These could derive from exogenous agents, like ionizing radiation (IR), ultraviolet light (UV), DNA damaging chemotherapeutics, or endogenous sources, including deoxyribonucleoside triphosphate (dNTP) misincorporation, spontaneous deamination, loss of DNA bases, and modification of DNA bases by alkylation. Additionally, oxidized DNA bases and DNA breaks can be generated by reactive oxygen species (ROS) derived from normal cellular metabolism (Pilzecker et al., 2019) Among the most harmful forms of DNA damage are the double-strand breaks (DBSs), which are deleterious lesions with the potential to cause cell death or genomic instability leading to cancer (Khanna & Jackson, 2001). DSBs can occur accidentally during normal metabolism, because of replication fork collapse, or after exposure to exogenous DNA-damaging agents, such as certain types of chemotherapeutic drugs or carcinogens (Pilzecker et al., 2019). Therefore, to ensure the stability of their genomes, the cells have developed refined mechanisms to signal and repair the DNA damages. The combination of these pathways is called DNA damage response (DDR), and it can be divided into:

- DNA damage repair
- DNA damage tolerance (DDT)
- DNA damage signalling

In this thesis, we will focus mainly on the DDT and DNA damage signalling pathways.

Replication stress tolerance (DDT)

If DNA damages are not repaired prior to replication, replication forks may run into these lesions and remain blocked. The replicative polymerases Polε and Polδ have an advanced proofreading capacity to prevent mis-incorporation of nucleotides. If in the DNA is present a lesion that cannot be accommodated in the catalytic site of replicative polymerases, they do not recognise the base pair with incoming nucleotides, and lead to replication fork stalling (Pilzecker et al., 2019). Other lesions that impair the progression of the replication forks include DNA damages created by exogenous agents or intrinsic replication obstacles such as secondary structures in the DNA template, tightly bound protein-DNA complexes and conflicts with the transcription machinery (Berti et al., 2020; Quinet et al., 2021). The slowing or stalling of replication forks in response to these challenges is called ''replication stress''. To prevent fork collapse, mutagenesis, and genome instability, cells must restore the stalled or damaged replication forks (Kobayashi et al., 2016). Thereby they have evolved different molecular pathways aimed at preserving the stability of stalled forks and promoting their accurate restart (Kondratick et al., 2021; Quinet et al., 2021). Altogether these pathways constitute the DNA damage tolerance (DDT) machinery. DDT includes repriming, translesion DNA synthesis (TLS) and homology-directed DDT pathways like fork reversal and template switching (TS). How cells choose among

these pathways is still unclear, however recent studies have demonstrated that different factors favour one pathway over the other, including the nature of the DNA lesion, extent of DNA damage, PCNA post-translational modifications, and changes in the genetic background (Quinet et al., 2021) (Fig.2).

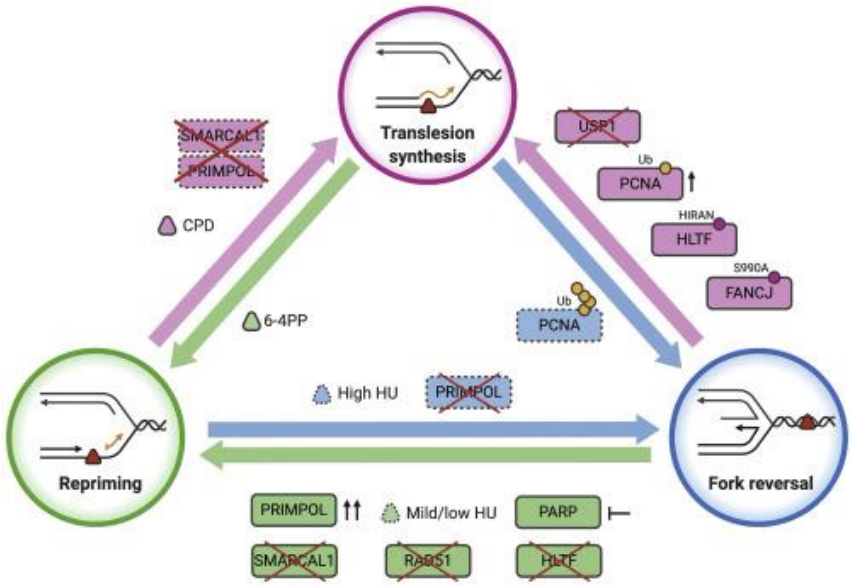

Fig. 2 - Factors influencing the choice among TLS, fork reversal, and repriming (Quinet et al., 2021)

Translesion synthesis (TLS)

Translesion synthesis (TLS) is a process by which a blocking lesion in the DNA is traversed by specialized DNA polymerases to ensure continued genome duplication and cell survival (Vaisman et al., 2012). These specialized TLS polymerases have active sites that are larger and more open than those of the high-fidelity replicative DNA polymerases, and allow the synthesis through the lesions in the DNA template (Stallons & McGregor, 2010). The skipping of the lesions by TLS occurs in two steps: at first a DNA base is inserted opposite to the lesion by Y-family DNA polymerases (REV1, Polη, Polι and Polκ), then the DNA synthesis is extended by the B-family Polz complex (REV3L/REV7/POLD2/POLD3) (J. A. Ling et al., 2022; Taglialatela et al., 2021; Vaisman & Woodgate, 2017; Yang & Gao, 2018). Despite their ability to synthesize DNA over a damage helps the cells to avoid double strand breaks (DSBs) derived by replication fork stalling, these proteins lack of proofreading activity, leading to the high probability of inducing mutations by incorrect base addition (Sale, 2013). Mammalian DNA polymerases with TLS capabilities include the Y and B-family polymerases, Polν, Polθ, Polζ and primase and DNA-directed polymerase (PrimPol) (J. A. Ling et al., 2022; Pilzecker et al., 2019; Sale et al., 2012). One of the main factors regulating the TLS pathway is proliferating cell nuclear antigen (PCNA) (Boehm et al., 2016). PCNA is a homotrimeric DNA clamp that acts as a key processivity factor for many DNA polymerases and central hub regulating several processes during DNA replication,

tolerance and repair (Moldovan et al., 2007; Choe & Moldovan, 2017). Regulation of TLS mostly occurs through PCNA monoubiquitination (PCNA-Ub) on lysine 164 (K164), which promotes polymerase switching from one of the replicative Polδ or Polε to a TLS polymerase (Friedberg et al., 2005) (Fig. 3). The E2/E3 ubiquitin ligases RAD6 and RAD18 constitute one of the main complex that is involved in PCNA-Ub (M. Li et al., 2020). One of the most important factors that regulate PCNA and RAD18 interaction is the protein BRCA1. BRCA1 is a key factor in DSBs and inter-strand crosslink repair, however it has been shown that its deficiency impairs also RAD18 recruitment and PCNA K164 ubiquitination. Similar to BRCA1, SIVA1 apoptosis inducing factor (SIVA1) directly mediates RAD6-RAD18 dependent PCNA ubiquitination (Han et al., 2014). In addition, SprT-like domain-containing protein SPRTN is involved in the recruitment of RAD18 and TLS polymerases (Centore et al., 2012). Beyond the RAD6-RAD18 pathway, several other proteins are known to mediate PCNA-Ub. The $CRL4^{Cdt2}$ E3 ubiquitin ligase complex promotes PCNA-Ub in a pathway independent on RAD18, and is counteracted by the action of the ubiquitin-specific protease 1 (USP1) (Terai et al., 2010). Additionally, spliceosome-associated factor 3 (SART3) has also been reported to affect PCNA monoubiquitination and Polη recruitment into foci (M. Huang et al., 2018). Furthermore, PCNA-associated factor 15 (PAF15) is double monoubiquitinated and regulates polymerase switching through its interaction with PCNA (Povlsen et al., 2012). E3 ubiquitin ligase HECT, UBA And WWE Domain Containing 1 (HUWE1) has been shown to interact with PCNA, though the exact mechanism remains unclear (Choe et al., 2016). Another important protein that is able

to recruit TLS polymerases and regulate TLS is the polymerase REV1. Altough some evidences suggest that REV1 could functions in a PCNA-Ub-independent manner (Guo et al., 2006), the REV1 pathway is mostly dependent on PCNA ubiquitilation. REV1 first bind to PCNA-Ub through its BRCT and UBM domains, then recruits Polζ and TLS polymerases through its C-terminal domain (Rizzo & Korzhnev, 2019).

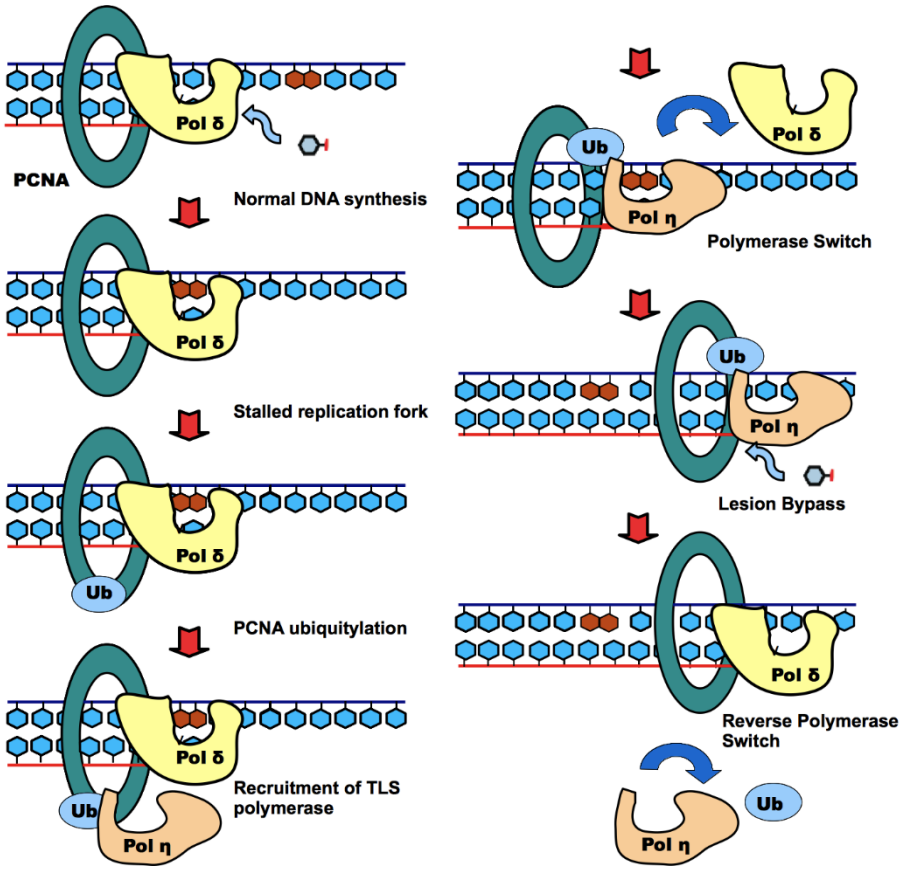

Fig 3 - Mechanism of translesion synthesis driven by PCNA ubiquitination (Zhuang Research Group - University of Delaware)

Repriming

A mechanism that cells have evolved to bypass an impediment is to reinitiate the replication downstream the lesion through the generation of a new primer that is successively extended by the replicative polymerases. This process, termed repriming, allows the restart of the stalled forks but accumulates regions of single-stranded DNA (ssDNA) that could trigger recombination or lead to subsequent formation of DSBs (Branzei, 2011). The phenomenon of repriming was first observed in bacteria, when it was demonstrated that UV radiation leads to the accumulation of ssDNA discontinuities on the daughter strands (Howard-Flanders et al., 1968). However, the mechanisms leading to the formation of these ssDNA gaps remained unknown. Successive studies in bacteria showed that the DnaG primase ensures replication fork restart downstream of a UV lesion in both the lagging and the leading strands (Heller et al., 2011). These findings suggested that the replisome was able to reinitiate DNA synthesis downstream of leading strand lesions and that the repriming activity of DnaG leads to the formation of a ssDNA gap between the lesion and the point at which synthesis restarts (Yeeles & Marians, 2011). The same ssDNA gaps generated by the repriming were then observed in *Saccharomyces cerevisiae* and in mammalian cells upon exposure to a wide range of DNA-damaging agents(Lopes et al., 2006; Quinet et al., 2016). In budding yeast it was demonstrated that the repriming is carried out by polymerase α (Polα)/primase complex and Ctf4, a replisome factor that bridges the

MCM helicase and the Polα /primase complex (Fumasoni et al., 2015). It was also demonstrated that the ssDNA gaps generated by the repriming of Polα/primase were located behind the replication fork and repaired by a post-replicative repair (PRR) mechanism (T. A. Guilliam, 2021). In higher eukaryotes, it has been shown that the repriming is catalysed by primase and DNA directed polymerase (PrimPol), a TLS primase/polymerase that is absent in budding yeast (Bianchi et al., 2013; T. Guilliam & Doherty, 2017; Mourón et al., 2013) (Fig. 4). This protein is known to operate in both the nucleus and mitochondria and, in contrast with other primases, is able to initiate DNA synthesis de novo using deoxynucleotides and discriminating against ribonucleotides (Díaz-Talavera et al., 2022). PrimPol is a member of the archaeo-eukaryotic primase (AEP) superfamily. It has two functional domains: an archaeo-eukaryotic primase (AEP) polymerase domain, that is required for both catalytic activities, and a DNA-binding, zinc-finger domain, required only for primase activity. PrimPol polymerase activity is limited, since it is able to synthesizes DNA incorporating only about four nucleotides on an undamaged template (Keen et al., 2014), so is its primase domain that is essential for the functions of PrimPol in the nucleus (Kobayashi et al., 2016; Quinet et al., 2020; Schiavone et al., 2016). In human cells, deletion of PrimPol under replicative stress is not lethal, but results in replication fork slowing, delayed recovery, increased mutagenesis, and sister chromatid exchanges (Kobayashi et al., 2016). Loss of PrimPol in human cells lacking Polη or Polζ significantly increases sensitivity to damaging agents (Bailey et al., 2019; Kobayashi et al., 2016), suggesting that it is required for the tolerance of impediments not efficiently bypassed by TLS, including

chain-terminating nucleosides (Kobayashi et al., 2016), DNA secondary structures (Schiavone et al., 2016), R-loops (Šviković et al., 2019), cisplatin-induced adducts and hydroxyurea (Quinet et al., 2020), bulky DNA adducts that induce recombination (Piberger et al., 2020), and interstrand crosslinks (ICLs) (González-Acosta et al., 2021). Additionally, PrimPol repriming in human cells deficient for BRCA2 protects the stalled replication forks from pathological degradation by suppressing reversed fork (RF) formation (Quinet et al., 2020). The ssDNA regions derived from PrimPol repriming under BRCA1/2 deficiency are then repaired by the TLS factors RAD18 and REV1 (Taglialatela et al., 2021).

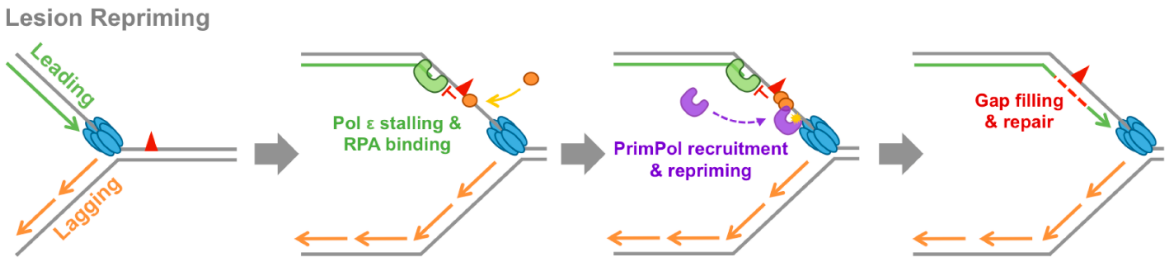

Fig. 4 - PrimPol-repriming in nuclear DNA replication. PrimPol is able to reprime and reinitiate leading strand replication downstream of a range of obstacles. Following repriming, replication can proceed and the resulting single-stranded DNA (ssDNA) gap is filled through translesion synthesis (TLS) or template switching mechanisms, permitting subsequent repair or removal of the obstacle. (Modified from Guilliam and Doherty, 2017)

Homology-directed DNA damage tolerance

Another group of pathways belonging to the DNA damage tolerance (DDT) mechanism is that of homology-directed DDT. Contrary to the error-prone TLS, in these pathways the newly synthesized DNA strand of the sister chromatid is used as template in order to repair and bypass the DNA lesions, therefore are considered relatively error-free (Pilzecker et al., 2019). They could act either at the ongoing replication fork or in a post-replicative gap repair (PRR) (Pilzecker et al., 2019). Two main pathways are thought to perform homology-directed DDT: fork reversal and template switching (TS) (Branzei & Szakal, 2016). In yeast, the prevalent homology-directed pathway is the TS. In mammals, fork reversal seems the dominant mechanism (Vujanovic et al., 2017), even though, in some cases, the formation of reversed forks (RFs) itself is able to stimulate the TS. While the TLS mechanism is mediated by PCNA-Ub, both fork reversal and TS depend on the polyubiquitination of PCNA (PCNA-Ubn) accomplished by the SNF2 histone linker PHD RING helicase (SHPRH) or the helicase like transcription factor (HLTF) (Krijger et al., 2011; Pilzecker et al., 2019).

Template switching (TS)

Template switching (TS) is a mechanism involved in the post-replicative repair (PRR) of single-stranded DNA gaps in an error-free manner (Branzei & Szakal, 2016). TS involves the switch of one strand to the undamaged sister chromatid, making structures resembling double holiday junctions, similar to those forming during a homologous recombination reaction (Branzei & Szakal, 2016; Giannattasio et al., 2014). In *S. cerevisiae*, TS is driven by the cohesion/condensing-like Smc5/6 complex and the helicase Pif1, that function in expanding the ssDNA gaps in PRR (García-Rodríguez et al., 2018), and is promoted the SUMOylation of PCNA by UBC13, an E2 ubiquitin-conjugating enzyme, and MMS2, a ubiquitin-conjugating enzyme variant (Pilzecker et al 2019). In humans, after the first monoubiquitylation of PCNA at K164 generated by RAD6 and RAD18, the protein complex MMS2-UBC13 add an ubiquitin chain on the same residue through the function of RAD5 (human HTLF), that associates with RAD18 and acts as a ubiquitin ligase (Ulrich, 2000). Both in *S. cerevisiae* and humans, has been proposed a role of the homologous recombination protein RAD51 in the TS events driven by RAD18 and RAD5 (Branzei & Szakal, 2016). One hypothesis is that RAD18-RAD5 complex interacts with RPA present both at ssDNA gaps and at stalled replication forks. After being loaded on ssDNA, this complex could promote PCNA-Ubn and triggers the RAD51-dependent TS (Prado, 2014). An alternative hypothesis is that RAD18 mediates TS steps only after the strand invasion performed by RAD51

(Branzei & Szakal, 2016). Downstream strand invasion, RAD18-RAD5 mediated PCNA-Ubn regulates the function of Polδ to extend the 3′ end of the invading strand, and the consequent intermediates are cleaved by MUS81 nuclease Branzei & Szakal, 2016). In yeast, important factors promoting the TS mechanism are the replication and damage checkpoint kinases (Branzei & Foiani, 2009). For example, the phosphorylation of the RAD51-paralog, RAD55, by the replication checkpoint, stabilizes the RAD51 filament and facilitates its strand-invasion activity (Symington, 2002). Checkpoint-mediated phosphorylation of the nuclease EXO1 inhibits EXO1 degradation of replication fork intermediates, preventing faulty template switching events at inverted repeats (Kaochar et al., 2010). In higher eukaryotes, the role of replication checkpoint in modulating the RAD18-dependent TS mechanism is still under debat (Branzei & Szakal, 2016). Some studies demonstrated that RAD18 is a potential target of ATR-ATM (Matsuoka et al., 2007), and that the inhibition of S-phase checkpoint kinases in human stimulates the recruitment of RAD18 at stalled or damaged forks (Branzei & Szakal, 2016), Moreover, in eukaryotic cells, TS is promoted by SUMOylation of PCNA at Lys164 (K164) driven by the E3-type small ubiquitin-like modifier (SUMO) ligase PIAS1 and PIAS4 (Mohiuddin et al., 2018) (Fig.5).

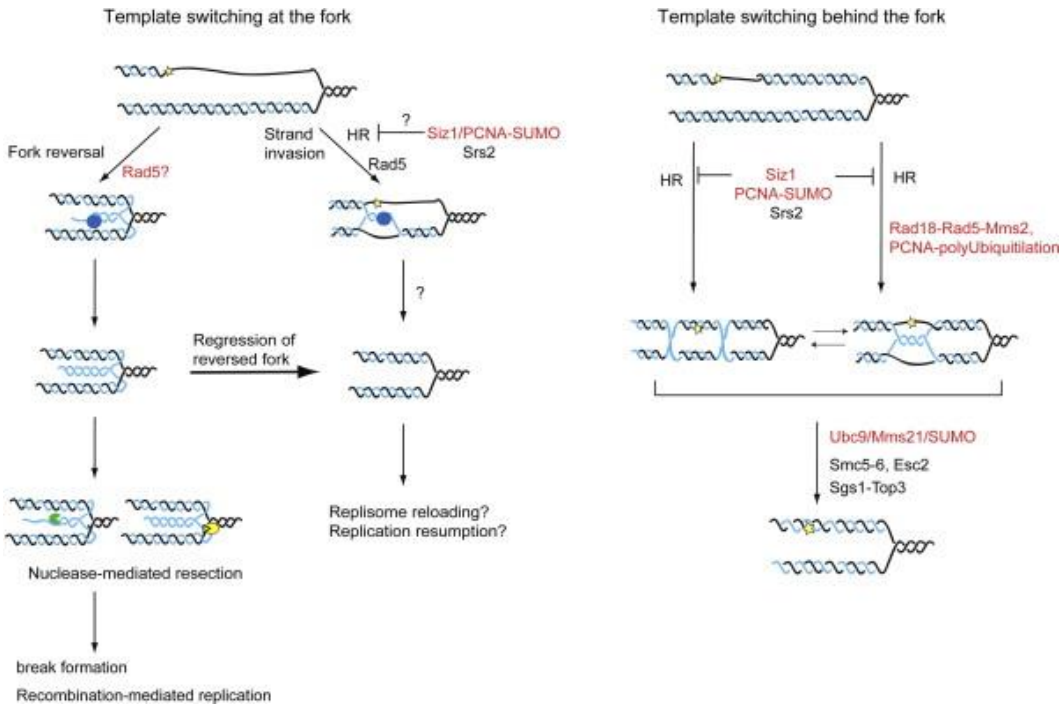

Fig. 5 - Representation of mechanisms that promote template switch (TS). TS can take place at the fork or behind the fork, through strand annealing or strand-invasion mediated mechanisms. The factors with Ubiquitin and SUMO-related activities are highlighted in red. (Branzei, 2011)

Fork reversal

One version of TS that has been shown to be crucial for recovery after replication arrest is the replication fork reversal. It involves the remodelling of the stalled replication fork and its conversion into a four-way Holliday junction by reannealing of nascent strands, generating the so-called reversed fork (RF). Replication fork reversal was initially proposed as a pathological result of fork destabilization, but now has been

accepted as a DNA damage tolerance (DDT) mechanism that is indispensable for maintaining genome stability in eukaryotic cells (Berti et al., 2020; Neelsen & Lopes, 2015). When a lesion occurs on the leading strand, the synthesis of the leading strand is inhibited at the blockage point due to polymerase dissociation (also called fork uncoupling), while the helicase continues to generate ssDNA for hundreds of bases (Berti et al., 2020). Thus, stalling the synthesis of the leading strand results in an accumulation of ssDNA that works as a platform for the loading of multiple enzymes, thereby promoting RF formation (Kolinjivadi et al., 2017). Critical Enzymes in RF formation in human are the SNF2 family chromatin remodelers, including SWI/SNF-related, matrix-associated, actin-dependent, regulator of chromatin, and subfamily A-like 1 (SMARCAL1), zinc finger, RAN-binding domain containing 3 (ZRANB3), and helicase like transcription factor (HLTF) (Poole & Cortez, 2017). Mutations in SMARCAL1 lead to Schimke immuno-osseous dysplasia (SIOD), while HLTF/ZRANB3-deficient cells are vulnerable to replication stress and contribute to tumorigenesis (Helmer et al., 2019; Weston et al., 2012). These helicase-like proteins are recruited to the stalled replication forks by interactions with other proteins, like RPA or PCNA, bind DNA via substrate-recognition domains and then use energy from ATP hydrolysis to remodel chromatin structure (Hargreaves & Crabtree, 2011). All three of these DNA translocases can catalyze replication fork regression both in vitro and in vivo, and have specific, distinct functions in fork remodeling (Achar et al., 2011; K. P. Bhat et al., 2015). SMARCAL1 interacts with RPA to catalyzes replication fork regression, and the process is regulated by the ATM and Rad3-related (ATR) protein kinase (K. P. Bhat &

Cortez, 2018; Couch et al., 2013). ZRANB3 contains a PCNA-interacting PIP motif and an AIkB homology 2 PCNA interaction motif (APIM) to bind PCNA, which facilitates its localization to stalled forks (Ciccia et al., 2012; Weston et al., 2012). Moreover, its NPL4 zinc-finger motif preferentially interacts with K63-linked polyubiquitinated PCNA (PCNA-Ubn) and is also required for the localization of ZRANB3 at stalled replication forks (Vujanovic et al., 2017). ZRANB3 has functions similar to SMARCAL1, including annealing complementary DNA strands and catalyzing fork reversal. Unlike SMARCAL1, however, RPA inhibits the fork reversal ability of ZRANB3 on the leading-strand gaps substrates (Bétous et al., 2013). Moreover, unlike other SNF2 family proteins, ZRANB3 exhibits structure-specific ATP-dependent endonuclease activity and can cleave fork DNA structures (Weston et al., 2012). Exactly how these enzymatic activities work together at stalled replication forks remains unknown. Similar to SMARCAL1 and ZRANB3, HLTF can catalyze fork reversal via ATP hydrolysis. HLTF binds the leading strand via its N-terminal HIRAN domain to stimulate fork regression (Kile et al., 2015). In addition, it has been reported that HLTF partly counteracts the activity of the DNA helicase FANCJ at stalled forks to maintain fork remodeling and prevent unlimited replication (Peng et al., 2018). Unlike the other two DNA translocases, no protein interaction motifs have been discovered in HLTF, and how it is recruited to stalled forks requires further investigation. Although a study has demonstrated that RPA interacts with HLTF, future research should examine their roles in replication stress (MacKay et al., 2009). Since simultaneously depletion of SMARCAL1, ZRANB3, and HLTF did not show an additive effect on reversed fork

frequency, these three DNA translocases may function at different stages of a common pathway (Taglialatela et al., 2017; Tian et al., 2021). It is also possible that each translocase works preferentially on specific substrates or genomic regions, which need further investigation (Taglialatela et al., 2017; Tian et al., 2021). In addition to the SNF2 family proteins, it has been reported that RAD51 is required for replication fork regression. RAD51 is a highly conserved DNA recombinase that is recruited to the sites of ssDNA exposed as a result of DNA damage or replication problems (Holloman, 2011). RAD51 recruitment is dependent on BRCA2, that modulates the formation of stable RAD51 filaments on ssDNA. Here it protects ssDNA from nuclease degradation and mediate DNA repair by promoting homologous recombination (Laurini et al., 2020; Sinha et al., 2020). Unlike homologous recombination repair, RAD51 function in fork reversal is independent on BRCA2 function, since BRCA2-dependent RAD51 filaments are not needed in this process (K. P. Bhat & Cortez, 2018). Although the mechanisms are not clear, it has been suggested that RAD51 paralogs (RAD51B, RAD51C, RAD51D, XRCC2, and XRCC3) may assist RAD51 and DNA translocases in promoting replication fork reversal (Berti et al., 2020; Rodrigue et al., 2006). Although many related enzymes and molecules have been discovered, it is not clear whether these proteins work together to promote fork remodeling, or if they work independently in response to different replication obstacles. Moreover, the activity of these enzymes must be tightly regulated, as too little or too much of their activities at stalled forks is deleterious for genomic stability (Qiu et al., 2021). For example, ATR phosphorylates SMARCAL1 at Ser652 to limit its fork regression activity, thereby

preventing replication fork collapse (Couch et al., 2013). Apart from ATR, RAD52 also limits SMARCAL1 activity at stalled forks by counteracting its loading (Malacaria et al., 2019). Additionally, the RPA-like single-strand DNA binding protein RADX antagonizes RAD51 filament formation to prevent inappropriate replication fork reversal (Adolph et al., 2021; H. Zhang et al., 2020) (Fig. 6).

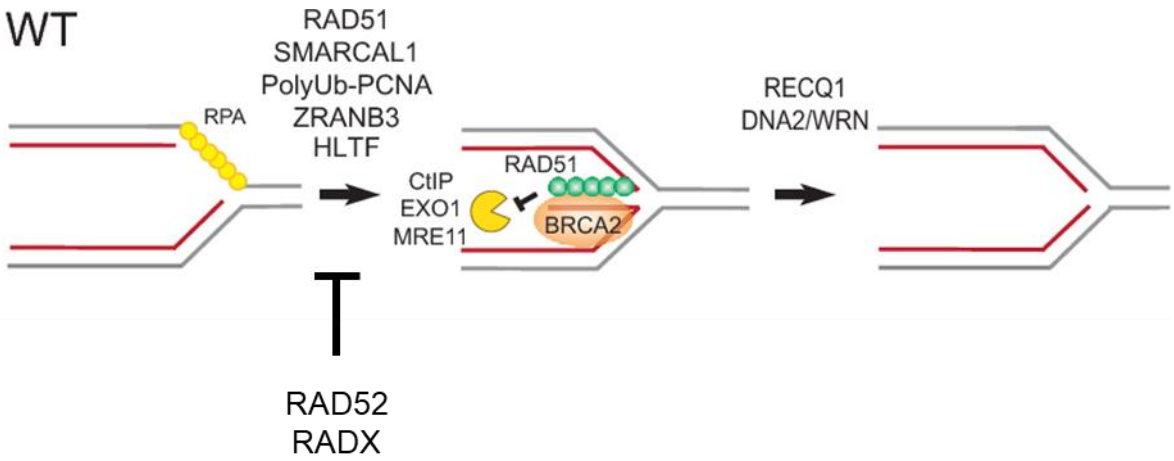

Fig. 6 – Mechanisms of Reversed Replication Fork Protection and Restart
(Modified from Quinet et al., 2017).

DNA damage signaling

The hallmark of DDR is the activation of cellular checkpoints that temporarily delay cell cycle progression through inhibition of cyclin-dependent kinase activity, activate DNA repair system or induce cellular apoptosis/senescence (Maréchal & Zou, 2013; Zhou & Bartek, 2004). These coordinated events help preventing replication or segregation of damaged DNA, and to induce transcription of genes that are involved in DNA repair and metabolism (Friedberg et al., 2006), therefore maintaining overall genomic integrity. The DNA damage checkpoint transduction cascade consists of a group of proteins acting in concert to relay the signal from damaged DNA to the cellular processes that promote cell-cycle arrest and DNA repair (Maréchal & Zou, 2013) (Fig. 7).

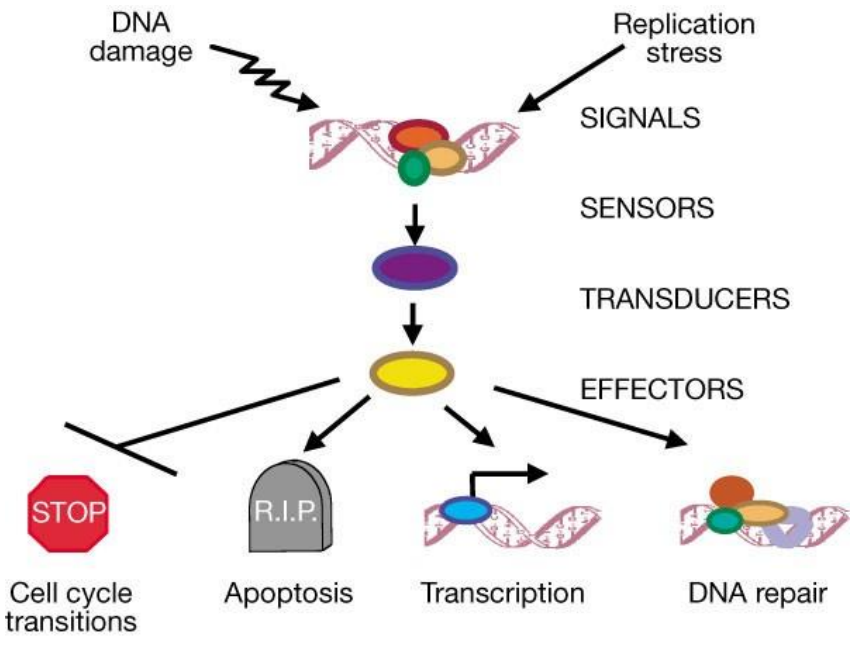

Fig. 7 - Model of DDR signal-transduction pathway. (Zhou 2000)

Checkpoint responses are primarily mediated through members of the phosphoinositide three-kinase-related kinase (PIKK) family that includes ataxia-telangiectasia mutated (ATM), ATM and Rad3-related (ATR), DNA-dependent protein kinase catalytic subunit (DNA-PKcs), mammalian target of rapamycin (mTOR) and suppressor with morphological effect on genitalia family member (SMG1) (Lovejoy & Cortez, 2009). In humans, mutations in ATM cause ataxia telangiectasia, a rare autosomal recessive disorder characterized by genome instability, immunodeficiency and predisposition to cancer (McKinnon, 2004). One of the main functions of ATM pathway is to signal the presence of DSBs during all phases of the cell cycle (Uziel, 2003). In this context, ATM is recruited to the damage sites after the interaction with the MRN complex, which consists of MRE11, RAD50 and NBS1, then is activated by auto trans-phosphorylation at residue serine 1981 (Uziel, 2003). One of the major targets of ATM is the histone variant H2AX, which allows further accumulation of MRN complex and increases checkpoint signals (Uziel, 2003). Another role of ATM is to response to DNA lesions other than DSBs, like that derived from endogenous sources of oxidative stress (Lee et al., 2018; Lee & Paull, 2021; Y. Zhang et al., 2018). ATR, on the other hand, can be activated by the presence of long stretches of single-strand DNA (ssDNA) derived from the resection of DSBs or from the uncoupling between replicative helicase and DNA polymerase movement at the stalled forks (Branzei & Foiani, 2009). It has been reported that checkpoint signaling could be elicited also by the remodelling and regression of the stalled forks. Similar to DSBs and telomeres, the end of the extruded arm of the regressed fork could trigger signaling by the ATM kinase.

In support of this hypothesis, ATM was found activated following TopI inhibition or nucleotide depletion, even in the absence of detectable DSBs (Fugger et al., 2015). Furthermore, the processing of the regressed arm by MRE11, DNA2 or other nucleases, could generate ssDNA gaps on the reversed arm that contribute to ATR signaling (Thangavel et al., 2015). Downstream to the signal transduction chain, soon after ATR and ATM, are found the checkpoint kinases CHK1 and CHK2. CHK1 is activated by phosphorylation at serine (Ser) 345 and Ser 317, both in S- and in G2–M phase of the cell cycle, and serves to mediate chromatin remodelling, DNA replication and repair (Zhou & Bartek, 2004).

MECHANISMS OF REPLICATION FORK MAINTENANCE AND STABILITY

The nascent strands exposed in the RF structure resemble a one-ended DSB, which is susceptible to the degradation by nucleases such as MRE11, exonuclease1 (EXO1), DNA replication helicase/nuclease 2 (DNA2), and MUS81 (Lemaçon et al., 2017; Mijic et al., 2017; Thangavel et al., 2015). To prevent the excessive degradation of the stalled forks, cells evolved protective mechanisms to avoid the nucleolytic activity of these enzymes and maintain replication fork structure and genomic stability.

BRCA2 and RAD51

One mechanism of stalled fork protection is the generation of RAD51 filaments on the ssDNA exposed on the reversed arm of the RF. This pathway is mediated by the protein BRCA2 (Carreira & Kowalczykowski, 2011) and is required to protect the regressed arm from MRE11-mediated degradation (Kolinjivadi et al., 2017; Mijic et al., 2017; Malacaria et al., 2019). Moreover, WRN interacting protein 1 (WRNIP1), a member of the AAA + ATPase family, interacts with BRCA2-RAD51 complex and participates in

the stabilization of RAD51 filaments (Leuzzi et al., 2016). However, how RAD51 protects regressed forks from nuclease-mediated degradation is still unclear. One hypothesis is that RAD51 physically blocks the binding of nucleases. In alternative scenario, RAD51 may cooperate with other inhibitory proteins (Vallerga et al., 2015). Furthermore, the RAD51 paralogs also participate in replication fork protection against MRE11 over-resection (Somyajit et al., 2015). Whether RAD51 paralogs dampen nucleases via the same mechanism as the BRCA2- RAD51 complex requires further study.

FA pathway components

The Fanconi anemia (FA) proteins are a family of proteins that, when mutated, are responsible for the onset of Fanconi anemia disease (Xu et al., 2021). One of the most relevant is the FA core complex, an ubiquitin ligase that, following DNA damage, monoubiquitinates the downstream proteins FANCD2 and FANCI and regulates HR and repair of inter-strand crosslinks (ICL) (Xu et al., 2021). In addition to their canonical role in ICL repair, several FA proteins are known to stabilize stalled forks. For example, FANCD2 prevents MRE11-mediated fork processing by stabilizing RAD51 nucleofilaments, similarly to BRCA2 (FANCD1 homolog) (Kim et al., 2015;

Schlacher et al., 2012). Also BOD1L, a protein that acts downstream of FANCD2/BRCA2, is involved in the maintenance of fork stability by inhibiting BLM/FBH1 helicases and stabilizing RAD51 nucleoprotein filaments (Higgs et al., 2015). However, unlike FANCD2, BOD1L suppressed DNA2-mediated degradation rather than that of MRE11 (Higgs et al., 2015).

RECQ family of DNA helicases

The RecQ family of DNA helicases, including RECQL1/4/5, Werner syndrome protein (WRN), and Bloom's syndrome helicase (BLM), have been shown to be important for protecting the stalled replication forks and maintaining genome integrity (Croteau et al., 2014). A previous study showed that WRN helicase and exonuclease catalytic activities were needed to prevent MUS81-mediated cleavage after HU-induced replication fork stalling (Murfuni et al., 2013). A more recent finding suggested that WRN is able to prevent MRE11/EXO1-dependent over-resection of nascent ssDNA (Iannascoli et al., 2015), possibly by stabilizing RAD51 (Su et al., 2014). Also the protein BLM has been implicated in replication fork protection upon replication stress. It was reported that BLM and FANCD2 co-localized at stalled forks in response to replication fork stalling agents (Pichierri et al., 2004). Moreover, the FA pathway was shown to be

essential for BLM phosphorylation and assembly in nuclear foci in response to DNA ICL (Pichierri et al., 2004). Recently, it was demonstrated that BLM helicase activity was also indispensable for FANCM recruitment and function at stalled forks (C. Ling et al., 2016). Therefore, it is reasonable to hypothesize that BLM and the FA pathway form a positive feedback loop to ensure sufficient protection of the stalled forks. Other proteins, such as ABRO1, PALB2, and WRNIP, have also been implicated in stalled replication fork protection (Liao et al., 2018; Berti et al., 2020). However, it is still unclear how these factors interact or function in response to different replication obstacles.

RAD52: A "LESS" MYSTERIOUS PROTEIN IN HUMAN CELLS

Radiation sensitive 52 (RAD52) is emerging as an important factor in the maintenance of genome stability. RAD52 structure is highly conserved from yeast to human, where it self-associates to form ring structures of different size that can range between 4–13 subunits (West, 2003). This conformation allows the protein to bind both ssDNA and dsDNA, and mediate single strand annealing (SSA) (Fig. 8).

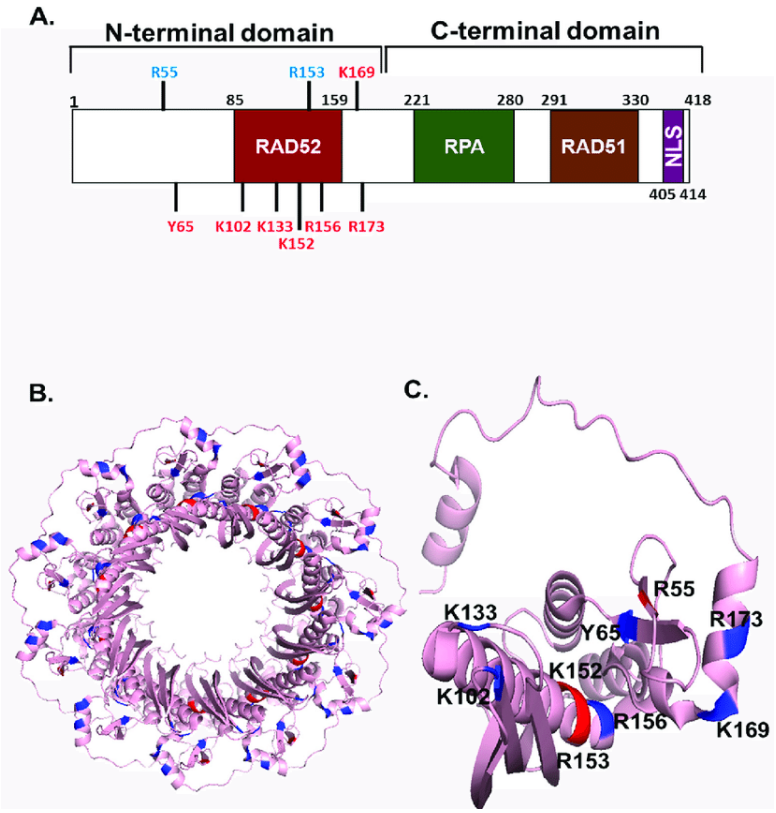

Fig. 8 - Structure of human RAD52: (A) The domain map of human RAD52. The N-terminal domain (NTD) contains the DNA binding region, a self-associating region; the C-terminal domain (CTD) contains RPA and RAD51 interacting regions and a

nuclear localization signal. (B) The structure of the undecamer ring formed by RAD52 NTD_{1-212} (PDB ID:1KN0). (C) The structure of RAD52 NTD_{1-212} monomer. Amino acid residues marked with red bind to both ssDNA and dsDNA; amino acid residues marked with blue bind to ssDNA only (Hanamshet et al., 2016).

Even though its biochemical features are mostly conserved, RAD52 function slightly changes among these species. While in yeast Rad52 has an essential role in all the homologous recombination (HR) pathways, including DSBs repair, RAD52 knock-out (KO) mammalian cells show only a mild decrease in HR and DNA damage sensitivity (Hanamshet et al., 2016; Malacaria et al., 2020). Indeed, in mammals the role of yeast Rad52 is played by the tumor suppressor protein BRCA2 (Kojic et al., 2002; Pellegrini & Venkitaraman, 2004). Despite RAD52 KO in mammals does not impair cells viability (Hanamshet et al., 2016) , its deficiency induces synthetic lethality in cells with a mutation on BRCA1, BRCA2 or other HR proteins, including PALB2 and RAD51 paralogs (Chun et al., 2013; Hanamshet et al., 2016; Malacaria et al., 2020), suggesting that RAD52 may drive a rescue pathway when HR mechanisms are unavailable. Since RAD52 alone is not enough to prevent HR defects, the hypothesis is that in BRCA-deficient cells, RAD52 could repair the DSBs through alternative repair pathways like single strand annealing (SSA), break induced replication (BIR) or Microhomology-mediated end joining (MMJ) (Malacaria et al 2020). A recent work demonstrated that the function of RAD52 in both SSA and BIR is modulated by the protein DSS1, which interaction modifies RAD52 conformation and modulates its DNA binding and strand invasion activities (Stefanovie et al., 2020). Moreover, some studies have shown that

RAD52-mediated BIR takes place also during mitosis, either to mediate the mitotic DNA synthesis (MiDaS) at fragile sites, or to perform the alternative maintenance of telomeres (ALT) to prevent cell senescence (Claussin & Chang, 2016; Verma et al., 2019). RAD52 recruitment to telomeres during ALT is dependent on the interaction with RAD51AP1 (Barroso-González et al., 2019). A recent work proposed that in absence of BRCA2, RAD52 could promote cell survival by regulating the function of the theta-mediated end joining (TMEJ) driven by Polθ (Llorens-Agost et al., 2021). Specifically, they demonstrate that, in BRCA2-deficient cells, RAD52 prevents the premature usage of TMEJ before the onset of mitosis and limits the formation of chromosomal fusions (Llorens-Agost et al., 2021). Another well characterized function of RAD52 is to modulate MRE11 dependent degradation of the nascent ssDNA exposed on the regressed arm of the RF. When BRCA2 is absent or deregulated, RAD52 directly recruits MRE11 to the unprotected ssDNA, and allows DNA degradation (Mijic et al., 2017; Schlacher et al., 2011). Conversely, in a WT background, RAD52 protects the exposed ssDNA by MRE11-mediated degradation (Malacaria et al, 2019). This duality of RAD52 function could be explained by the fact that, in WT cells, RAD52 can bind the stalled replication fork before RF formation and prevent the loading of RF factors like SMARCAL1, ZRANB3, and RAD51 (Malacaria et al, 2019). Hence, the absence or the inhibition of RAD52 leads to an excess of fork reversal that exhausts the pool of RAD51 necessary to protect nascent DNA from MRE11-dependent degradation (Malacaria et al, 2019). Both RAD52 and SMARCAL1 bind RPA through a RQK sequence (Bhat et al., 2015; Grimme et al., 2010), suggesting that the two proteins may

compete for the DNA binding. Therefore, the loading of RAD52 could prevent RF generation by impeding SMARCAL1 recruitment (Malacaria et al, 2020). Furthermore, RAD52 has a role in the replication restart under pathological conditions, such as BRCA-deficiency or checkpoint inactivation (Malacaria et al, 2020). This pathway involves the degradation of the reversed arm by MRE11 and the RAD52-dependent generation of a D-loop that is successively cleaved by MUS81. Eventually, has been reported a function of RAD52 in promoting both transcription-associated and transcription-coupled homologous recombination repair (TA/TC-HR) by regulating R-loop processing (Yasuhara et al., 2018). A summary of RAD52 function and the phase of the cell cycle in which they are active is reported on Fig. 9.

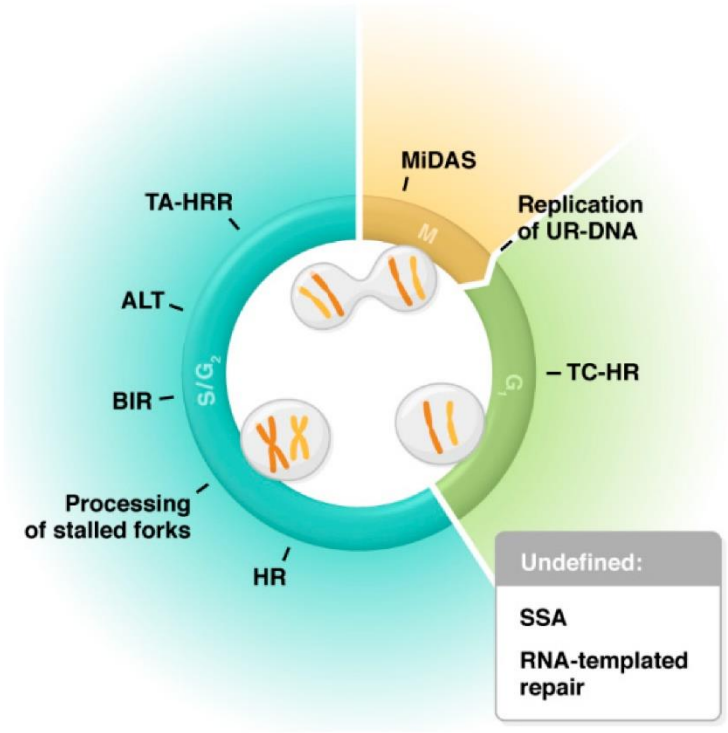

Fig. 9 - RAD52 functions along the cell cycle. TC-HR (transcription-coupled homologous recombination), HR (homologous recombination), Processing of stalled forks (MUS81-dependent fork cleavage and protection against excessive fork reversal), BIR (break-induced replication), ALT (alternative lengthening of telomeres), TA-HRR (transcription-associated homologous recombination repair), MiDAS (mitotic DNA synthesis), Replication of UR-DNA (replication of under-replicated DNA in 53BP1 nuclear bodies), SSA (single-strand annealing), and RNA-templated repair (Jalan et al., 2019).

In human, the regulation of RAD52 functions is mediated by a number of post-translational modifications. RAD52 SUMOylation and phosphorylation are known to modulate the SSA activity of RAD52 (Altmannova et al., 2010). Phosphorylation of RAD52 occurs at tyrosine 104 and is driven by the c-ABL1 kinase (Honda et al., 2011). This modification on one end enhances RAD52-mediated SSA, on the other inhibits its dsDNA binding ability (Lord & Ashworth, 2016). In response to DNA damage, RAD52 is methylated on serine 147 (S147). Mutations in this residue destabilize and reduce RAD52 foci formation in cells subjected to hydroxyurea (HU) (Wray et al 2014). A recent paper demonstrated that the histone acetyltransferase (HAT) p300/CBP-mediated acetylation of RAD52 stabilizes the binding of the protein to the DSBs site, and this activity is counteracted by the deacetylation mediated by SIRT2 and SIRT3. It has been shown that RAD52 mutants unable to being acetylated dissociate prematurely from the DSBs (Yasuda et al., 2018). In this background, the premature dissociation of RAD52 impaired also RAD51 binding to the DSBs, and as consequence, the HR pathway (Yasuda et al 2018). Moreover, it was demonstrated that RAD52 acetylation was dependent on ATM, since it promotes the formation of RAD52, p300/CBP, SIRT2,

and SIRT3 foci at DSB sites (Yasuda et al 2018). Due to its involvement in many DNA damage repair pathways, RAD52 has emerged as an interesting target for developing new anticancer therapies targeting HR deficient tumors (D. S. Bhat et al., 2022; Ha et al., 2016; Hanamshet & Mazin, 2020; Toma et al., 2019).

RESULTS

PART 1 - RAD52 DEFICIENCY TRIGGERS Polα-DEPENDENT ssDNA GAPS EXPOSURE

It was demonstrated that in human cells subjected to replication stress, the absence of RAD52 cause the persistence of under-replicated regions of DNA that are not resolved even after many hours of recovery from the exposure to the stressing agent (Malacaria et al, 2019). However, the defect in replication completion observed under RAD52 deficiency was previously attributed only to the pathological degradation of the nascent single-stranded DNA (ssDNA) exposed at the reversed forks (RF) mediated by the nuclease MRE11 (Malacaria et al, 2019). Recent works reported a strong correlation between the remodelling of the stalled replication forks and their restart through the repriming mechanism (Quinet et al., 2020). Since RAD52 depletion under replicative stress drives a strong remodelling of the stalled forks (Malacaria et al, 2019), we asked whether the unreplicated DNA gaps raised in this situation would derive also from repriming events.

RAD52 deficiency stimulates a PrimPol-independent repriming mechanism

To detect under-replicated regions of DNA in our cellular model, we first analysed the presence of parental ssDNA regions left behind the stalled replication forks. To inhibit RAD52 function, we treated U2OS WT cells with Epigallocatechin (EGC), a compound that blocks the RAD52-ssDNA interaction (Ha et al., 2016), prior to stalling of the replication with 2mM Hydroxyurea (HU) (Fig. 10A). We then triggered the restart of the replication by incubating the cells with fresh medium (Fig. 10A). We detected the presence of parental ssDNA by immunofluorescence by means of antibodies directed against the DNA labelled with the 5-Iodo-2′-deoxyuridine (IdU) under non-denaturing conditions. The treatment of WT cells with the high dose of HU elicited a IdU signal that disappeared after 18 hours from replication release (Fig. 10A), while the cells that were inhibited for RAD52 presented a IdU signal higher than that of mock-inhibited control that persisted also at 18 hours of recovery (Fig. 10A), suggesting that the repair of this ssDNA gaps was delayed until a late phase of the cell cycle. Fork repriming is a process by which DNA replication is restarted by de novo primer synthesis downstream of the stalled replication forks (Bainbridge et al., 2021). This process allows the completion of the replication, however it causes the accumulation of unreplicated parental ssDNA gaps that has to be resolved through either translesion synthesis (TLS) or template switching (TS) mechanisms (Quinet et

al., 2021; Tirman et al., 2021). In bacteria, the repriming is mediated by the DnaG primase (Heller & Marians, 2006), in yeast it is carried out by the polymerase α (Polα)-primase complex and Ctf4 (Fumasoni et al., 2015), and in mammalian cells by the primase and DNA-directed polymerase (PrimPol) (Bianchi et al., 2013; Mourón et al., 2013). To understand whether the ssDNA observed under RAD52 inhibition was generated by events of repriming, we exposed the cells to a lower concentration of HU, in order to slow down the replication without completely blocking it (Van et al., 2010). To detect presence of ssDNA gaps, we performed a modified DNA fibers assay by pulse-labeling the cells with a thymidine analog, CldU (red), for 20 minutes, followed by the labeling with a second thymidine analog, IdU (green), for 4 hours, in concomitance with the treatment with 0.5 mM HU (Fig. 10B). We used the ssDNA-specific S1 nuclease to determine whether the IdU-labeled tracts contained ssDNA gaps. The reduction in the ratio between the IdU and CldU tracts of S1 treated cells respect to the – S1 was used as a readout for the presence of gaps. We found that HU treatment led to ssDNA gap accumulation in RAD52i U2OS cells, but not in WT, suggesting that RAD52 deficiency stimulates the repriming pathway and ssDNA gap formation (Fig 10B). It is established that RAD52 depletion in cells subjected to HU stimulates MRE11-dependent degradation of the nascent ssDNA exposed at the RF (Malacaria et al., 2019). To see if the parental ssDNA gaps derived from RAD52 deficiency were dependent on the RF degradation, we exposed the cells to MIRIN, a specific MRE11 inhibitor, before fork slowing and analyzed the presence of parental ssDNA. As expected, exposure of parental ssDNA was stimulated by RAD52

inhibition, however, it was not abrogated by the treatment with MIRIN (Fig. 10C), suggesting that the accumulation of ssDNA did not derive from the extensive degradation of the RF.

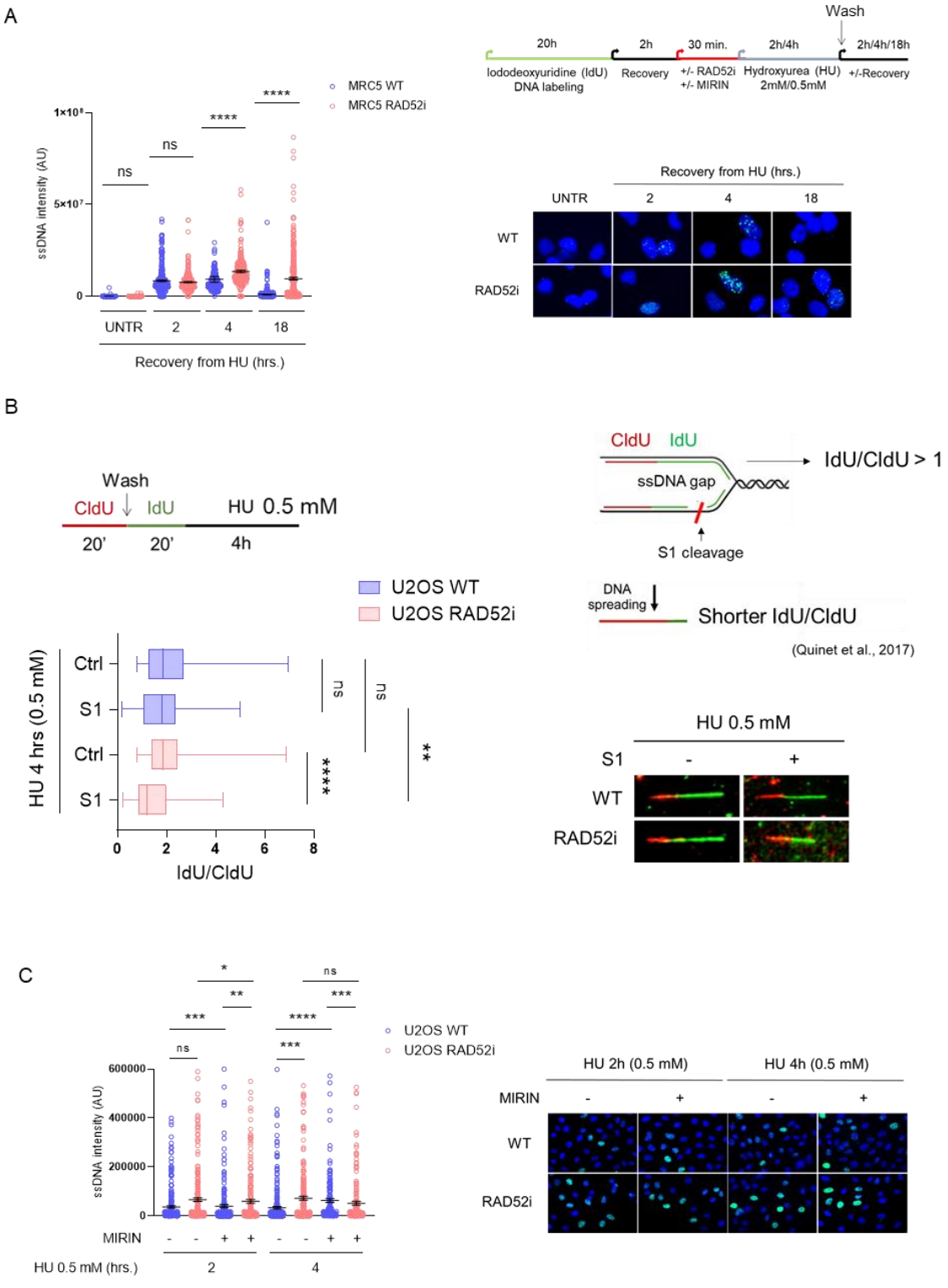

Fig. 10 - (A-C) RAD52 deficiency stimulates repriming. A. Analysis of parental ssDNA after 2 mM hydroxyurea (HU) treatment. MRC5 WT were treated as indicated on the experimental scheme. Replication recovery was given by adding fresh medium. The ssDNA was detected by IdU immunofluorescence. Graph shows the mean intensity of ssDNA staining. Representative images are shown. **B.** Detection of ssDNA gaps in U2OS through S1 fibers assay. On top and right: schemes describing the experiment. Briefly, it was done a first Clorodeoxyuridine (CldU) pulse of 20 min and a second pulse with IdU that was kept for all the duration of the experiment. The cells were treated with the S1 nuclease to cut the ssDNA on the IdU labeled tract. The graph reports the mean IdU/CldU ratio. Representative images of single DNA fibers are shown. **C.** Analysis of parental ssDNA after 0.5 mM hydroxyurea (HU) exposure. The treatments were carried out following the experimental scheme depicted above. The graph shows the mean fluorescence intensity (AU). Representative images are shown. All the values above are presented as means ± SE (ns = not significant; *P < 0.1; **P<0.1; ***P < 0.001; ****P < 0.0001; Mann–Whitney test;).

It has been shown that the repriming mediated by PrimPol aims to rescue the stalled forks when fork reversal is impaired, as it occurs upon loss of the SMARCAL1 or HLTF translocases (Bai et al., 2020; Quinet et al., 2020), and protects excessive RF degradation in BRCA2 deficient cells by suppressing fork reversal (Quinet et al., 2020). Since RAD52 deficiency is known to induce a fork remodeling that results in the increase of both fork reversal and degradation (Malacaria et al., 2019), we wanted to exclude that the parental ssDNA accumulating in the absence of RAD52 derives from the repriming mediated by PrimPol. We first evaluated the presence of ssDNA gaps with the S1-fiber assay in MRC5 WT and MRC5$^{-/-PrimPol}$. In MRC5$^{-/-PrimPol}$, the ratio between the IdU/CldU tract length was higher than the one of WT cells, indicating that low doses of HU are sufficient to stimulate PrimPol repriming, however, the inhibition of RAD52 still induced a significant reduction in IdU/CldU ratio, suggesting that a portion of parental

ssDNA gaps accumulating are independent on PrimPol-mediated repriming (Fig. 10D). We checked also PrimPol recruitment at parental ssDNA by proximity ligation assay (PLA). The PLA reaction was carried out by labeling the DNA with IdU and transfecting the MRC5$^{-/-PrimPol}$ with a GFP-tagged PrimPol, and the analysis was done by counting the PLA-spot per nucleus. PLA detected a substantial interaction between PrimPol and the parental ssDNA after 4 hours of HU treatment. Interestingly, the recruitment of PrimPol was not affected by RAD52 inhibition (Fig. 10E), as it occurs when BRCA2 was depleted (Fig. 10F). Altogether, these results indicate that the ssDNA gaps that accumulate in absence of a functional RAD52 derive from a PrimPol-independent repriming.

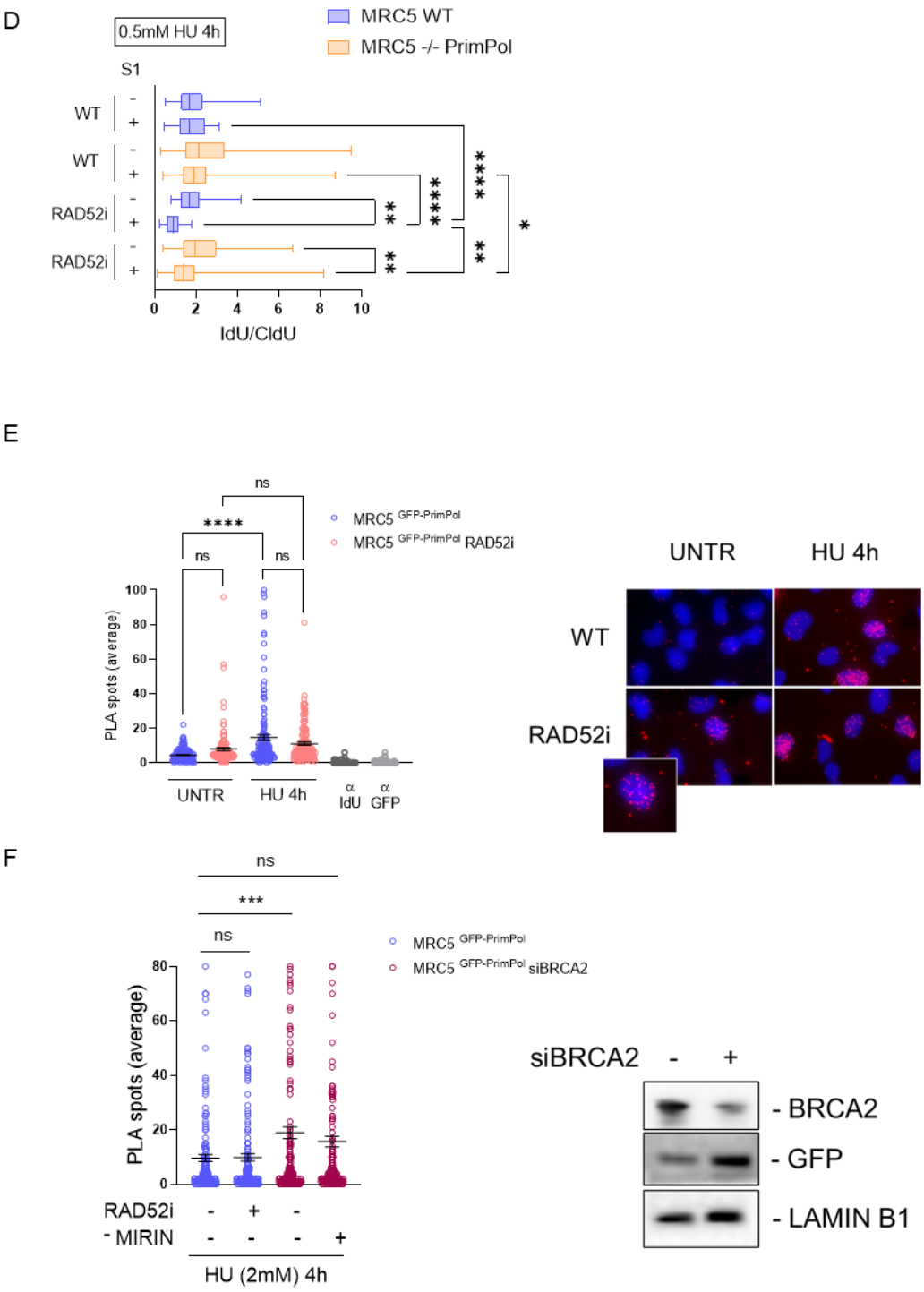

Fig. 10 (D-F) - D. Analysis of ssDNA gaps through S1 fiber assay. The cells were treated with 0.5 μM HU for 4 hours. RAD52i (Epigallocatechin, 50μM) was given 30 min before replicative stress induction. The graph reports the mean IdU/CldU ratio. **E** and **F.** Analysis of PrimPol-IdU interaction using Proximity Ligation Assay (PLA). MRC5 -/- PrimPol were transfected with a peGFP-PrimPol prior the silencing of BRCA2 with a siRNA. 24 hours after transfection the cells were treated with 100 μM IdU for 20 hours, released for 2 hours in fresh medium and subjected to RAD52i and HU. PLA

reaction was carried out using antibodies against GFP and IdU. Controls were subjected to PLA with anti-IdU or anti-GFP only. Western blot shows the level of BRCA2 and GFP expression in transfected cells. LAMIN B1 was used as loading control. All the values above are presented as means ± SE (ns = not significant; *P < 0.1; **P<0.1; ***P < 0.001; ****P < 0.0001; Mann–Whitney test;)

The repriming is mediated by Pol*α* on the lagging strand

Having demonstrated that, under RAD52 deficiency, PrimPol is not involved in the excessive ssDNA production, we wanted to investigate which protein is involved in the repriming events that we observed in RAD52i cells. The only other polymerase known to initiate DNA replication in humans is the Polymerase alpha (Pol*α*). In complex with a primase, Pol*α* initiates the synthesis of the leading strand at each origin of replication and the synthesis of each Okazaki fragment in the lagging strand (Mourón et al., 2013; Bainbridge et al., 2021). The primase synthesizes RNA oligonucleotides that are extended with dNTPs by Pol*α* until a length of about 30 nucleotides, then the primers are elongated by the polymerases Polδ and Polε (Mourón et al., 2013). The recruitment of Pol*α* to parental ssDNA was assessed by PLA in cells treated with HU at different times. RAD52 inhibition alone was enough to enhance the association between Pol*α* and ssDNA, and this further increased following the treatment with HU (Fig. 11A). To exclude that in this context, Pol*α* was involved in new origin firing, we treated the cells with the CDC7 inhibitor, and we did not observe any reduction in Pol*α*-ssDNA interaction (Fig. 11B). Under physiological conditions or in situations of replicative stress, the human CTF4-orthologue, AND-1 (WDHD1), promotes the correct positioning of Pol*α*/primase complex on the lagging-strand template at the replication fork (Kilkenny et al., 2017). Thus, we analysed if Pol*α*

recruitment stimulated by the absence of RAD52 was also dependent on the function of AND-1. To this aim, we depleted AND-1 with a siRNA in U2OS WT and RAD52i cells and checked Polα-ssDNA association. The depletion of AND-1 reduced the number of Polα-ssDNA spots in RAD52-deficient cells, but it did not affect that of WT (Fig. 11C). As confirmation, RAD52 deficiency enhanced also the recruitment of AND-1 at parental ssDNA (Fig. 11D). To validate if the parental ssDNA raised from the inhibition of RAD52 was directly dependent on the higher Polα recruitment in chromatin, we treated the cells with the Polα inhibitor ST1926 (Abdel-Samad et al., 2018; Ercilla et al., 2020). It is known that Polα depletion in WT cells stimulates high ssDNA accumulation and RPA recruitment due to the blocking of the lagging strand synthesis and the consequent strand uncoupling (Ercilla et al., 2020). Thus we decided to titrate the amount of inhibitor with a 5-ethynyl-2'-deoxyuridine (EdU) incorporation assay, to select a concentration that did not significantly impair lagging strand synthesis. We found that 0.3μM of Polα inhibitor only partially reduced EdU incorporation (Fig. 11E), so we decided to use this concentration to evaluate the presence of parental ssDNA at 0.5mM HU. The treatment with the low dose of Polαi strongly elicited the exposure of ssDNA in WT cells. In RAD52-deficient cells, Polαi reduced the ssDNA exposed, and the effect was independent on the firing of new origins (Fig. 11F). To support this data, we did also the S1-fiber assay, where we observed a high amount of ssDNA gaps formation in WT cells, as indicated by the lower IdU/CldU tract length ratio (Fig. 11G). On the contrary, in cells deficient for RAD52, the treatment with Polαi decreased the presence of ssDNA gaps (Fig. 11G),

suggesting that in absence of a functional RAD52 there is a strong correlation between Polα recruitment and ssDNA gaps formation. Interestingly, the same phenotype was obtained in -/- PrimPol cells (Fig. 11G), indicating that even in absence of PrimPol RAD52 deficiency is enough to stimulate an alternative repriming mechanism driven by Polα.

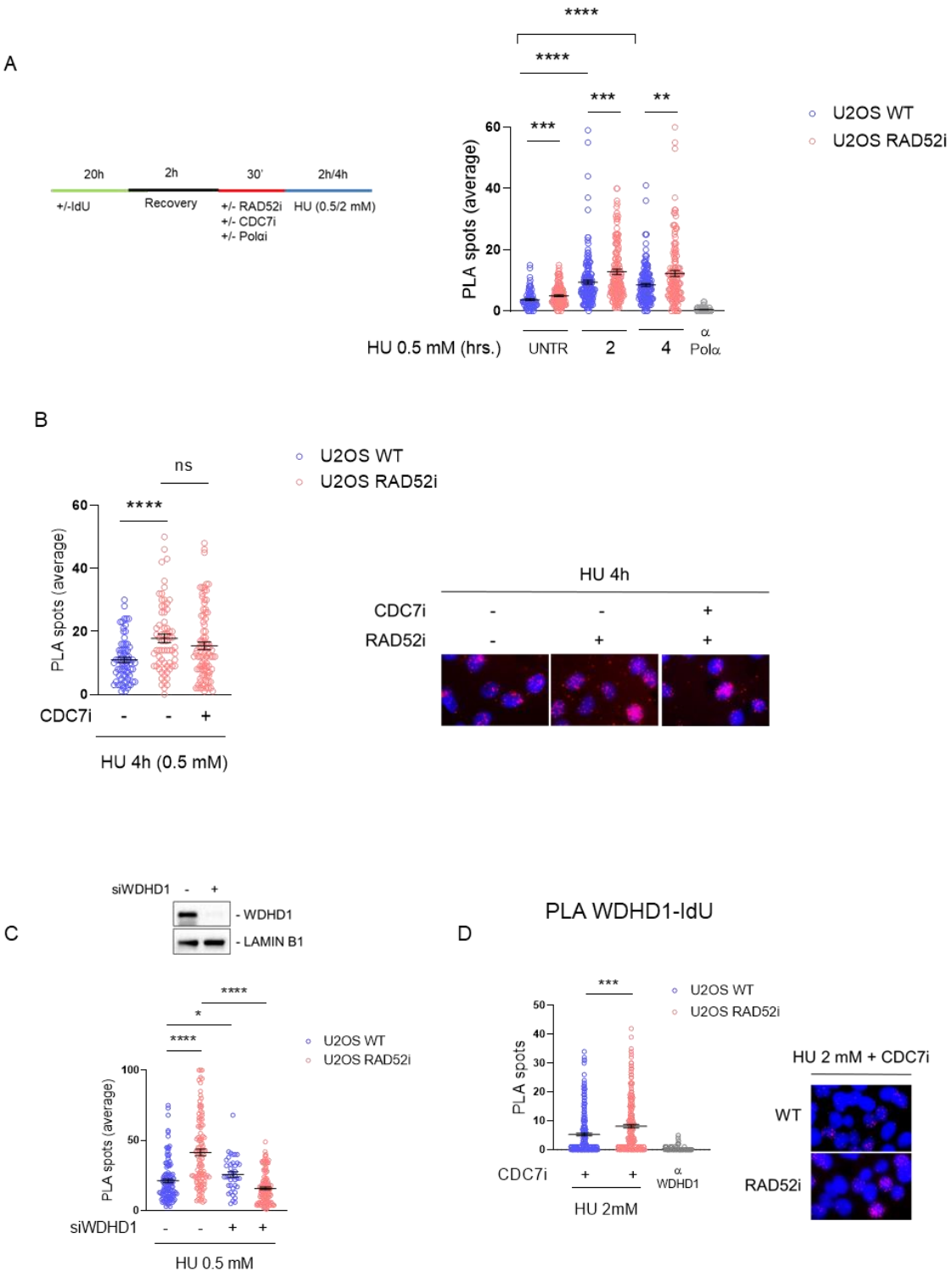
A
20h
2h
30'
2h/4h
+/-IdU
Recovery
+/- RAD52i
+/- CDC7i
+/- Polαi
HU (0.5/2 mM)
PLA spots (average)
HU 0.5 mM (hrs.)
UNTR
2
4
α Polα
U2OS WT
U2OS RAD52i
B
ns
****
CDC7i
HU 4h (0.5 mM)
HU 4h
RAD52i
C
siWDHD1
- WDHD1
- LAMIN B1
HU 0.5 mM
D
PLA WDHD1-IdU
PLA spots
HU 2mM
α WDHD1
HU 2 mM + CDC7i
WT
RAD52i

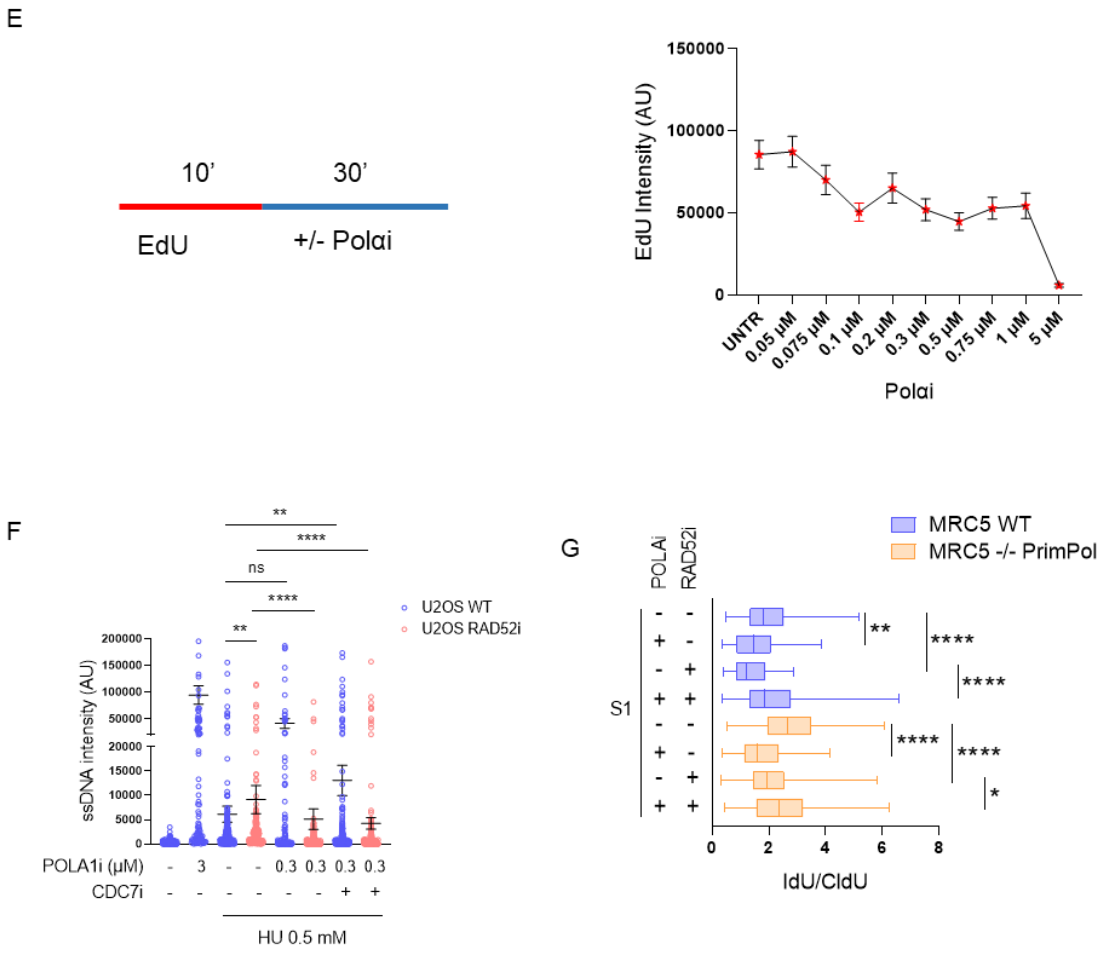

Fig. 11 - The repriming is mediated by Pol*α* on the lagging strand. A-C. Analysis of Pol*α*-IdU association by PLA. U2OS WT were treated as indicated on the experimental scheme above. AND-1 (WDHD1) siRNA was transfected 48 hours before the experiment. WDHD1 silencing was assessed by western blot. LAMIN B1 was used as loading control. PLA reaction was carried out using antibodies against POLA1 and IdU. The graphs report the mean PLA spots per cell. **D.** Analysis of WDHD1-IdU interaction by PLA. Cells were treated with CDC7i as indicated above. PLA reaction was carried out using antibodies against WDHD1 and IdU. Graph shows the mean PLA spots per cell. Representative images are reported. **E.** 5-ethynyl-2'-deoxyuridine (Edu) incorporation assay for the titration of Pol*α* inhibitor (ST1926). ST1926 was tested at the concentrations reported on the graph. The cells were treated as indicated on the scheme on the left. Graph shows the mean EdU intensity. **F.** Analysis of parental ssDNA exposure in U2OS WT. Both RAD52i and Pol*α*i were given 30 minutes before HU. Pol*α*i was used at 0.3 μM. Graph shows the mean fluorescence intensity (AU). **G.** S1 fiber assay for ssDNA gaps detection. Cells were treated as written above. Graph reports the mean IdU/CldU ratio. Controls were subjected to PLA with anti-Pol*α* and anti-WDHD1 only. All the values are presented as means ± SE (ns = not significant; *P < 0.1; **P<0.1; ***P < 0.001; ****P < 0.0001; ANOVA or Mann–Whitney test;).

Upon RAD52 deficiency, Polα recruitment depends on replication fork remodeling

Next, we wanted to understand if the binding of Polα at parental ssDNA occurred downstream the replication fork remodeling that occurs in absence of RAD52. First we analyzed if Polα-ssDNA interaction was dependent on RF formation. We transfected U2OS cells with a Tet-On system for the doxycycline-inducible silencing of SMARCAL1 ($U2OS^{shSMARCAL}$) and gave HU at high dose. The exposure of $U2OS^{shSMARCAL}$ to doxycycline slightly reduced Polα recruitment, but a greater reduction was observed in RAD52i cells, where Polα-ssDNA interaction was brought back at WT level (Fig. 12A). A decrease in Polα recruitment in chromatin was observed also in cells depleted of ZRANB3 through chromatin fractionation (Fig. 12B.). Since the silencing of SMARCAL1 and ZRANB3 had a major effect in reducing Polα binding only in RAD52-deficient cells, we asked whether Polα recruitment was strictly dependent on the excess of RF that is observed under RAD52 deficiency (Malacaria et al., 2019). To mimic an excess of RF in WT cells, we transfected U2OS with a doxycycline-inducible PiggyBac transposon system for the overexpression of SMARCAL1, and we exposed the cells to HU. Unexpectedly, the treatment with doxycycline greatly reduced Polα-ssDNA interaction (Fig. 12C). To exclude that the lower Polα-ssDNA interaction was due to DSBs raised by the cleavage of RF by the endonuclease MUS81 (Wyatt et al 2013, Lugli et al 2017), we silenced MUS81 with a siRNA in doxycycline-treated cells, but we

did not obtain any changes in the interaction phenotype (Fig. 12C). This results indicate that, under RAD52 deficiency, the excessive RF formation is necessary but not enough to enhance Polα recruitment. To understand if Polα binding occurred downstream RF degradation by MRE11, we analyzed Polα-ssDNA interaction by treating the cells with MIRIN before HU exposure. As shown in Fig. 12D, in U2OS WT Polα-ssDNA interaction was not affected by MRE11 inhibition, but it was slightly reduced in RAD52i cells. Altogether these results suggest that, in absence of a functional RAD52, at least a portion of Polα is engaged after the MRE11-mediated degradation of the nascent ssDNA exposed on that RF.

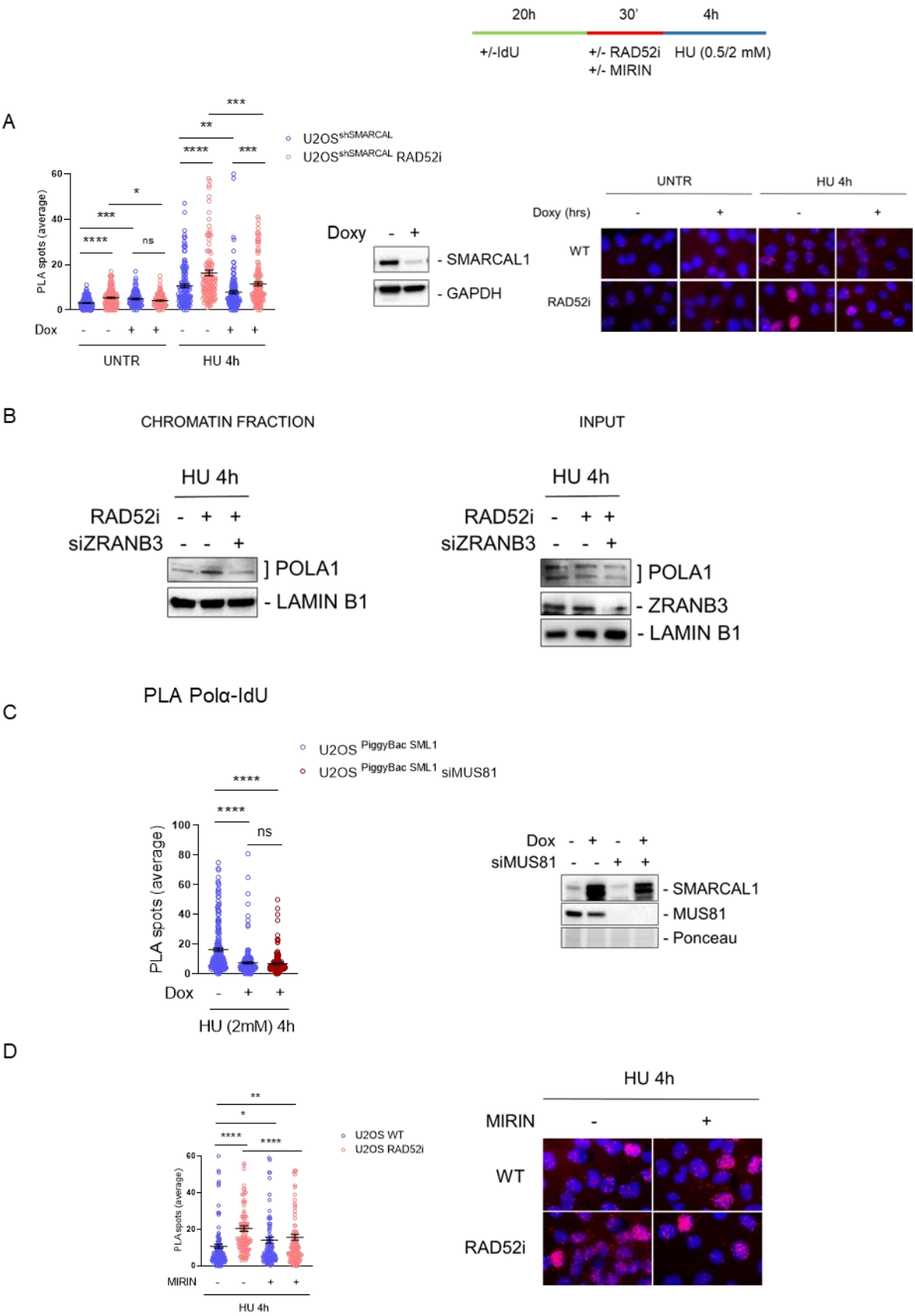
20h
30'
4h
+/-IdU
+/- RAD52i
+/- MIRIN
HU (0.5/2 mM)
A
PLA spots (average)
U2OS shSMARCAL
U2OS shSMARCAL RAD52i
Dox
UNTR
HU 4h
Doxy
- SMARCAL1
- GAPDH
Doxy (hrs)
WT
RAD52i
B
CHROMATIN FRACTION
INPUT
RAD52i
siZRANB3
] POLA1
- LAMIN B1
- ZRANB3
C
PLA Polα-IdU
U2OS PiggyBac SML1
U2OS PiggyBac SML1 siMUS81
HU (2mM) 4h
siMUS81
- SMARCAL1
- MUS81
- Ponceau
D
U2OS WT
U2OS RAD52i
MIRIN

Fig. 12 - Polα recruitment under RAD52 deficiency depends on replication fork remodelling. **A.** Analysis of Polα-IdU interaction by PLA in U2OS shSMARCAL1. SMARCAL1 silencing was induced by giving Doxycycline (Dox) 48 hours before to treat the cells as indicated on the scheme above. Western blot shows the expression level of SMARCAL1. GAPDH was used as loading control. PLA reaction was carried out using antibodies against POLA1 and IdU. Graph shows the mean PLA spot per nucleus. Representative images are shown. **B.** Analysis of Polα recruitment in chromatin by chromatin fractionation. Cells were transfected with the ZRANB3 siRNA 48 hours before treatments. RAD52i was given 30 min before HU. After treatment, cell pellets were subjected to chromatin fractionation and the protein extracts were quantified by Western Blotting. Polα was identified by using an antibody directed against the Polα subunit POLA1, and LAMIN B1 was used as loading control. The whole cell extracts were used as control (INPUT). **C.** Analysis of Polα-IdU interaction by PLA in U2OS overexpressing SMARCAL1. SMARCAL1 overexpression was obtained by giving Doxycycline (Doc) 48 hours before treatments, in concomitance with the transfection with MUS81 siRNA. Western blot shows the expression level of SMARCAL1 and MUS81. PLA reaction was carried out using antibodies against POLA1 and IdU. Graph shows the mean PLA spots per nucleus. **D.** Analysis of Polα-IdU interaction by PLA in U2OS WT. Both RAD52i and MIRIN were given 30 min before HU. PLA reaction was carried out using antibodies against POLA1 and IdU. Graph shows the mean PLA spots per nucleus. Representative images are reported. All the values are presented as means ± SE (ns = not significant; *P < 0.1; **P<0.1; ***P < 0.001; ****P < 0.0001; ANOVA or Mann–Whitney test;).

Polα engagement is mediated by RAD51

Experiments performed in *Xenopus* egg extracts demonstrated that RAD51 directly interacts with Polα to promote its association with stalled replication forks (Kolinjivadi et al., 2017), so we wondered whether RAD51 could be involved in the recruitment of Polα to ssDNA in cells lacking of a functional RAD52. First we examined Polα-parental ssDNA association in cells treated with the RAD51 inhibitor B02. RAD51i reduced Polα-ssDNA interaction only in RAD52i cells, starting from 2 hours of treatment with HU (Fig. 13A). In accordance with the PLA result, also the parental ssDNA exposure was reduced by the treatment with B02 only under RAD52 deficiency (Fig 13B). It is now established that, in response to various genotoxic treatments, RAD51 binding to ssDNA can mediate the reannealing of the nascent strands and drive the equilibrium toward the RF formation (Zellweger et al., 2015). Thus we investigated if the reduction of Polα recruitment at ssDNA was a consequence of the impaired RF formation. To this aim we silenced RAD51 with the J11 siRNA (K. P. Bhat et al., 2018). When used at the low concentration of 2pmol, J11 interference should affect only the expression of RAD51 pool involved in fork protection, maintaining a physiological level of RF. When used at a higher dose, the siRNA would impair also the expression of the part of RAD51 involved in RF formation (K. P. Bhat et al., 2018). As shown in Fig. 13C, we observed a decrease in Polα-ssDNA PLA spots in cells treated with both 2 and 20 pmol

of J11 siRNA, so we excluded that the decrease in Polα recruitment dependent on RAD51i was caused only by loss of RF. Next, we tested if RAD52 deficiency could modulate the physical interaction between Polα and RAD51. Interestingly, we found that RAD52i was sufficient to increase Polα-RAD51 association already at 2 hours of HU exposure (Fig. 13D).

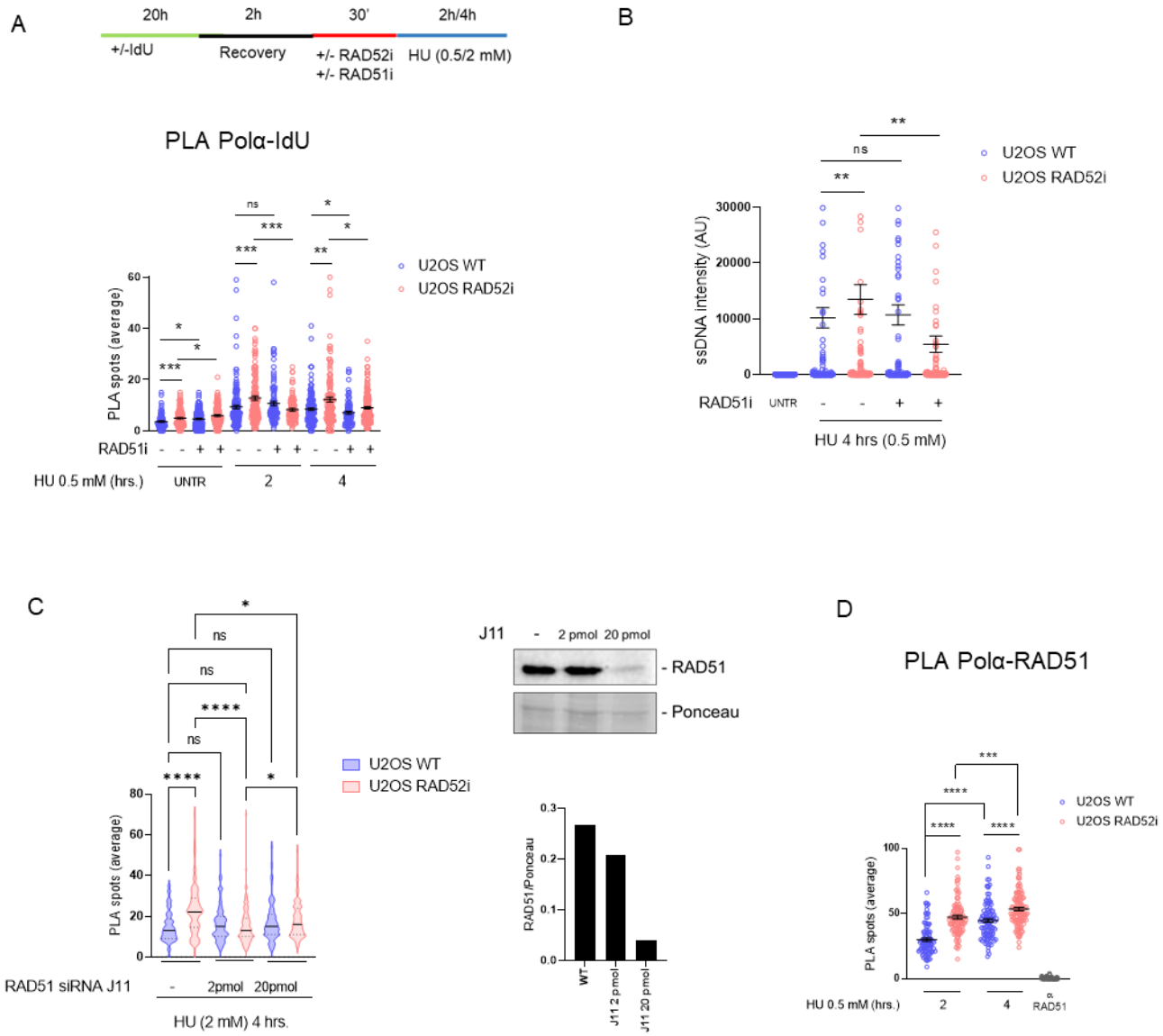

Fig. 13 - Polα engagement is mediated by RAD51. A. Analysis of IdU-Polα PLA in U2OS WT. Cells were treated as indicated in the experimental scheme. PLA reaction

was carried out using antibodies against POLA1 and IdU. The graph shows the mean PLA spot per cell. **B.** Analysis of parental ssDNA by immunofluorescence. U2OS WT were treated as above. The graph shows the mean fluorescence intensity (AU) **C.** Analysis of IdU-Polα PLA in U2OS WT treated with the RAD51 siRNA J11. The siRNA was transfected at two different concentrations (2 and 20 pmol) and the treatments with RAD52i and HU were performed after 48h from transfection. Both the western blot image and the quantification graph show the level of RAD51 expression in transfected cells. **D.** Analysis of RAD51-Polα interaction by PLA in U2OS WT. The cells were treated with RAD52i 30 min before HU. PLA reaction was carried out using antibodies against POLA1 and RAD51. The control was subjected to PLA with only one primary antibody. The graph shows the mean PLA spot per cell. All the values above are presented as means ± SE (ns = not significant; *P < 0.1; **P<0.1; ***P < 0.001; ****P < 0.0001; Mann–Whitney test;)

Polα recruitment occurs downstream RAD51-dependent strand invasion

We have previously demonstrated that a portion of Polα was recruited downstream the RF formation and MRE11 degradation of nascent DNA strand, therefore we asked whether Polα could bind parental ssDNA behind the digested replication forks. To study Polα position with respect to the active replication, we did a single-cell assay for in-situ protein interaction with nascent DNA replication forks (SIRF) (Lazarchuk et al., 2019), with which we studied Polα interaction with the dsDNA labeled with EdU. As shown by the experimental scheme in Fig. 14A, we labeled the cells with EdU, then gave a recovery in fresh medium for different times before treating with HU at low dose. Since it has been shown that the velocity of replication in U2OS is about 1 kb per minute (Parplys et al., 2015), we expected that after 0/5 minutes of recovery the EdU labeled portion of DNA was found slightly behind the active replication forks (Fig. 14B). The treatment with HU slowed down the replication and stimulated RF formation, potentially exposing the nascent ssDNA labeled with EdU. When RAD52 was inhibited, we observed a significant increase in Polα-dsDNA interaction (Fig. 14B). Interestingly, Polα recruitment under these conditions was independent on MRE11-mediated degradation (Fig. 14B). After a recovery of 10/15 minutes from EdU, we expected that the labeled DNA was far behind the active replication forks. Also in this case, we observed in RAD52i cells a higher recruitment of Polα at dsDNA (Fig.

14C). Surprisingly, the treatment with MIRIN significantly reduced Polα-EdU PLA spots only in RAD52 inhibited cells. Altogether these results suggest that, under RAD52 deficiency, Polα could be engaged both at the stalled replication forks, in a pathway that is independent on MRE11, and behind them, probably on the nascent ssDNA exposed by MRE11-dependent degradation. We observed also that both at early and late time from EdU-recovery, Polα recruitment triggered by RAD52 inhibition was strictly dependent on the function of RAD51 (Fig. 14D and 14E). Since RAD51 is known to be involved in the strand invasion phase of template switching (TS) mechanism in a BRCA2 dependent manner, we asked if BRCA2 depletion could mimic RAD51i effect in reducing Polα-dsDNA association under RAD52 deficiency. We monitored Polα-dsDNA interaction in the ovarian cancer cell line PEO1, that possess a missense mutation in BRCA2 gene (5193C>G), that makes the protein unable to mediate RAD51-foci formation (Guillemette et al 2015). As a control we used the PEO4 cell line, that has a reversion mutation in BRCA2 gene, and express BRCA2 WT (Fig. 14F). We observed that the treatment with RAD52i in PEO1 resulted in a lower number of cells positive for EdU-Polα interaction. At the same time, we observed also a BRCA2-dependent engagement of RAD51 at dsDNA in a cell line inducible for the silencing of BRCA2 (Fig. 14G). Analysis of super resolution microscopy allowed us to visualize the spatial distribution of Polα and RAD51 on the EdU-labelled DNA. After replication fork arrest, cells were subjected to Click-iT™-mediated detection of EdU and antibody-mediated detection of Polα and RAD51 prior to acquire immunofluorescence by dSTORM. Multiple stacks of images were processed and

single nuclei showing dual or triple localisation quantified. As shown in Fig. 14I, after a treatment of 0.5 mM HU, Polα and RAD51 are localized in correspondence of nascent DNA. The treatment with RAD52i reduced the number of dual localisation between DNA and RAD51, while increased that of triple localisation of DNA-RAD51-Polα, suggesting that in this background a significant portion of RAD51 is headed to the Polα-mediated repriming. Altogether our results indicate that, under RAD52 deficiency, Polα and RAD51 could promote a PRR mechanism by a strand invasion similar to that of TS.

A

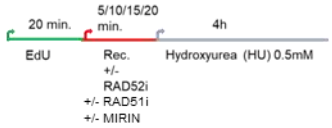
20 min.
5/10/15/20 min.
4h
EdU
Rec.
+/-
RAD52i
+/- RAD51i
+/- MIRIN
Hydroxyurea (HU) 0.5mM

B

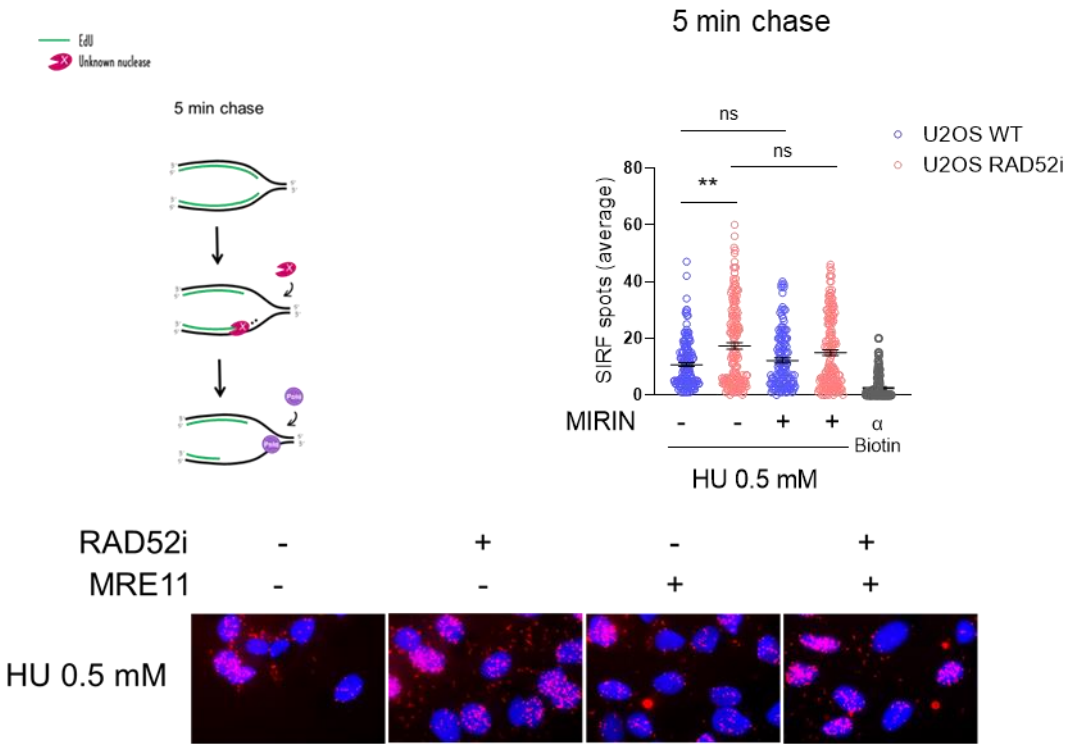
5 min chase
EdU
Unknown nuclease
5 min chase
ns
ns
**
U2OS WT
U2OS RAD52i
SIRF spots (average)
80
60
40
20
0
MIRIN
-
-
+
+
α Biotin
HU 0.5 mM
RAD52i
-
+
-
+
MRE11
-
-
+
+
HU 0.5 mM

C

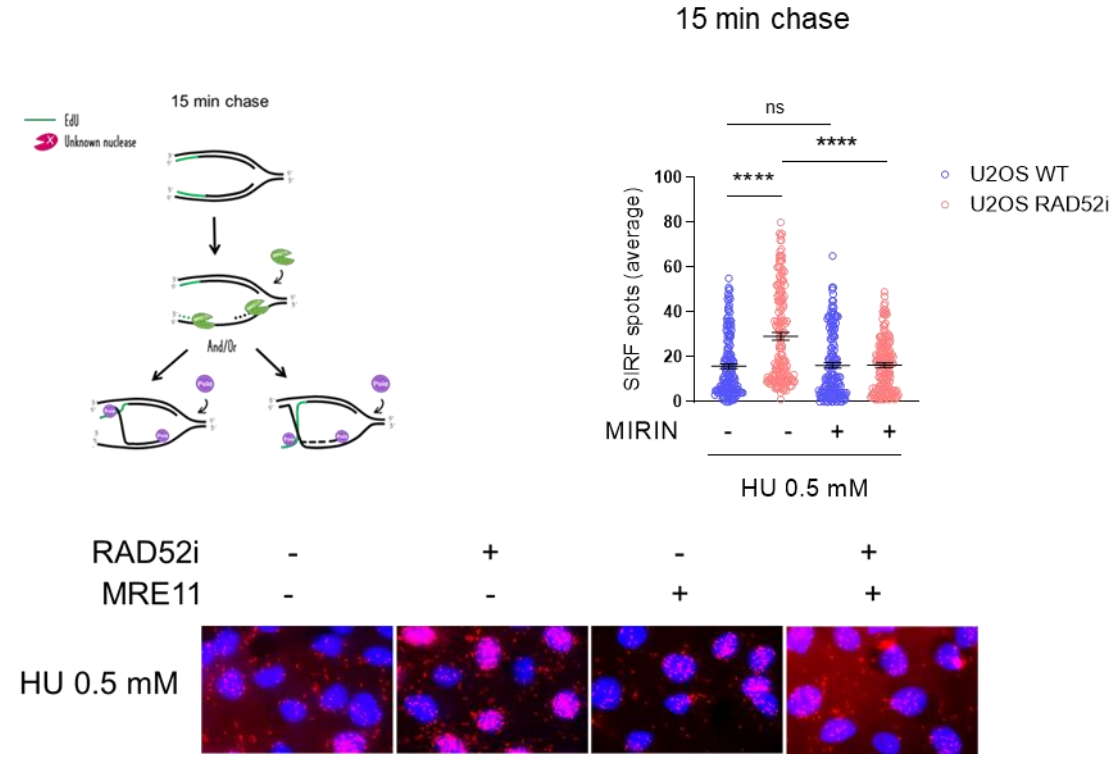
15 min chase
EdU
Unknown nuclease
15 min chase
And/Or
ns
****
****
U2OS WT
U2OS RAD52i
SIRF spots (average)
100
80
60
40
20
0
MIRIN
-
-
+
+
HU 0.5 mM
RAD52i
-
+
-
+
MRE11
-
-
+
+
HU 0.5 mM

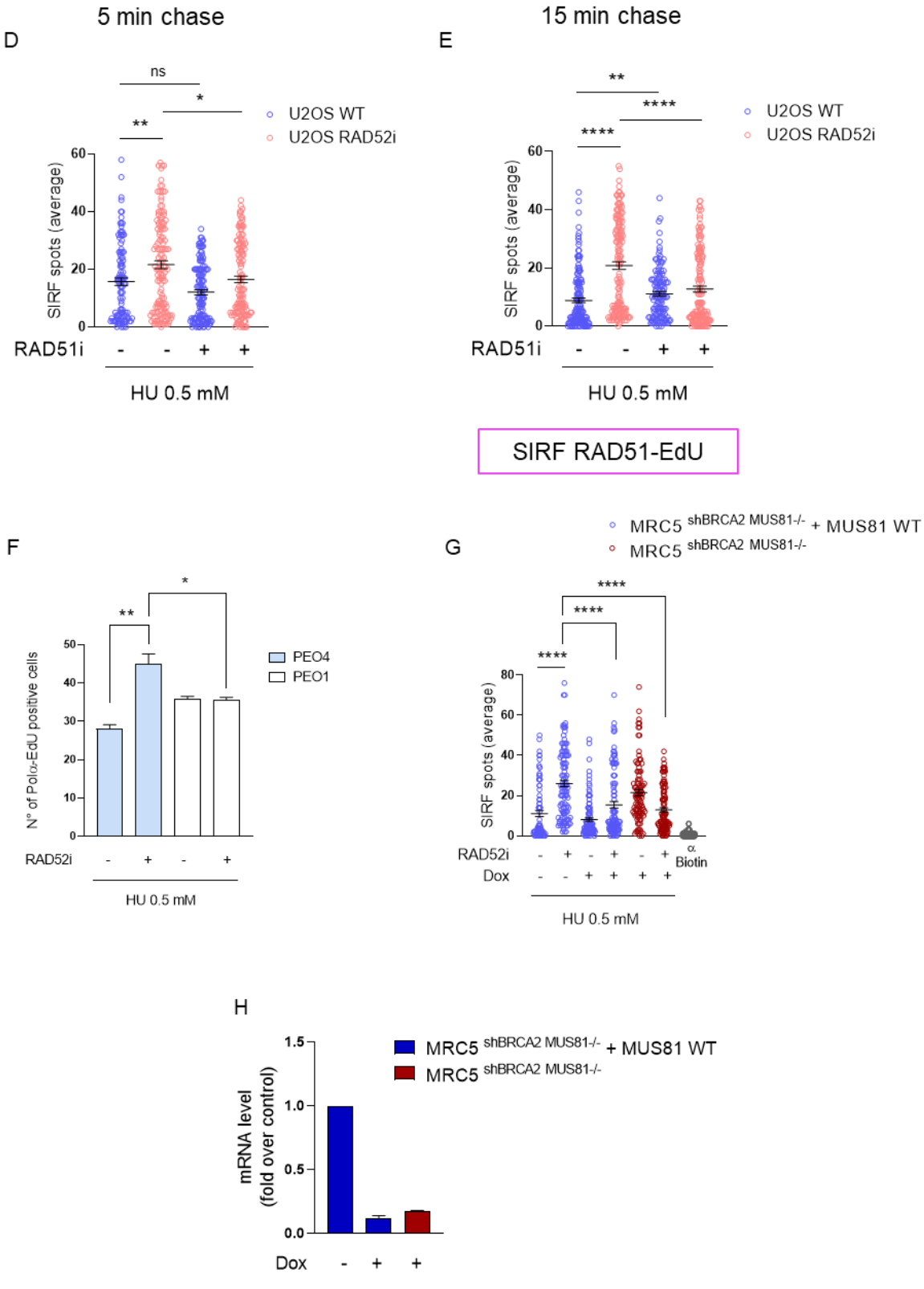
D
5 min chase
ns
*
**
U2OS WT
U2OS RAD52i
SIRF spots (average)
60
40
20
0
RAD51i - - + +
HU 0.5 mM
E
15 min chase
**
****
****
U2OS WT
U2OS RAD52i
SIRF spots (average)
RAD51i - - + +
HU 0.5 mM
SIRF RAD51-EdU
F
*
**
PEO4
PEO1
N° of Polα-EdU positive cells
50
40
30
20
10
0
RAD52i - + - +
HU 0.5 mM
G
MRC5 shBRCA2 MUS81-/- + MUS81 WT
MRC5 shBRCA2 MUS81-/-
****
****
****
SIRF spots (average)
80
60
40
20
0
RAD52i - + - + - + α Biotin
Dox - - + + + +
HU 0.5 mM
H
MRC5 shBRCA2 MUS81-/- + MUS81 WT
MRC5 shBRCA2 MUS81-/-
mRNA level (fold over control)
1.5
1.0
0.5
0.0
Dox - + +

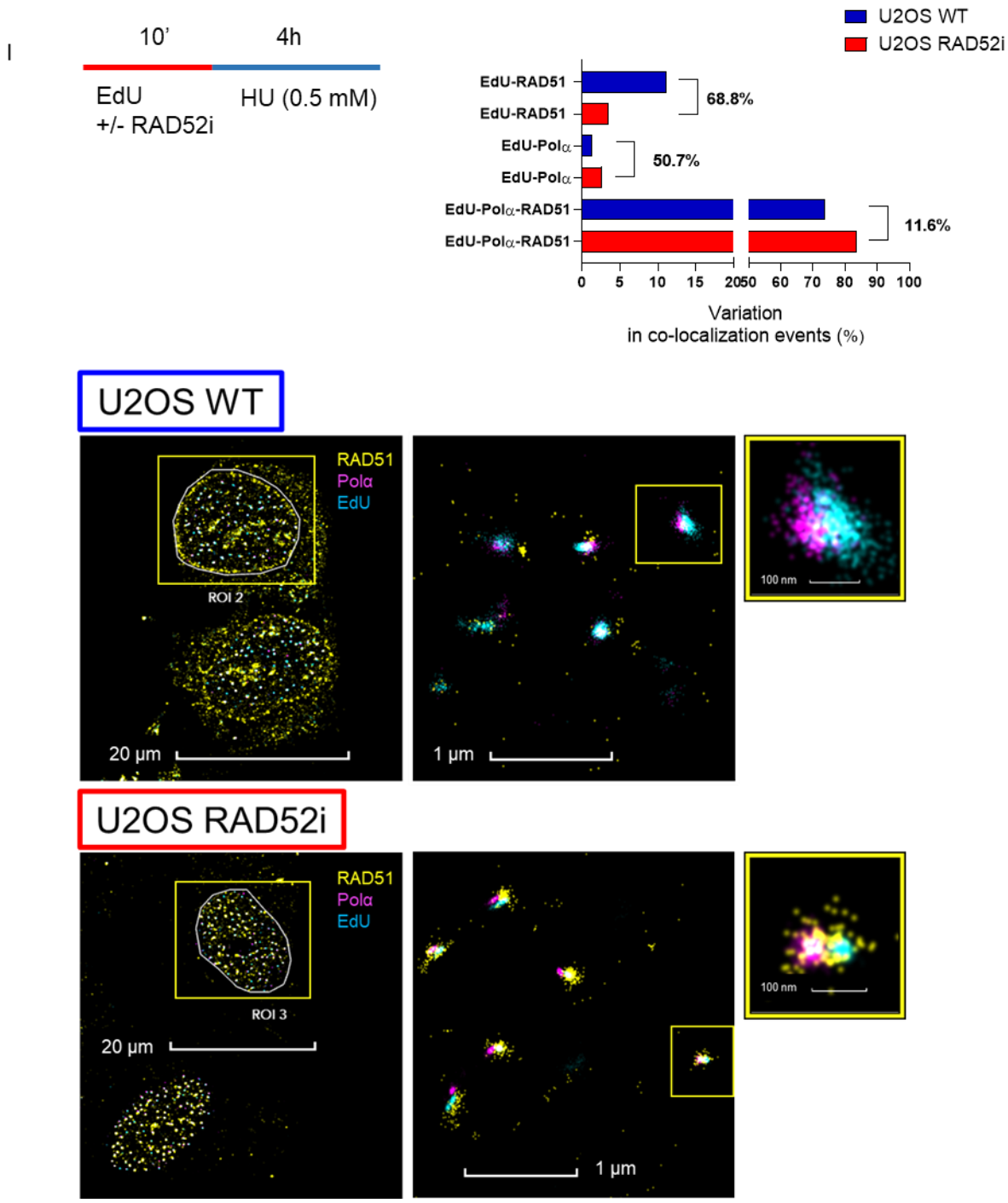

Fig. 14 - Pol*α* recruitment could be involved in gaps post replicative repair through template switching (TS). A. Experimental scheme of single-cell assay for in situ Protein Interaction (SIRF). **B**, **C**, **D** and **E.** Analysis of EdU-Pol*α* interaction by SIRF. SIRF was performed in U2OS WT treated as indicated above. SIRF reaction was carried out using antibodies against POLA1 and Biotin. Controls were subjected to SIRF with anti-biotin only. The graphs show the mean number of SIRF spots per cell after 5 or 15

minutes of recovery from EdU labelling. The models on the left represent the expected background. Where present, the representative images are shown under the respective graph. **F.** Analysis of EdU-Polα interaction by SIRF in PEO1 and PEO4 cell models. Cells were exposed to EdU labelling that was left for all the HU treatment. The graph shows the mean number of SIRF spots per cell. **G and H.** Analysis of EdU-RAD51 interaction by SIRF in MRC5 shBRCA2 +/-MUS81. Cells were exposed to EdU labelling that was left for all the HU treatment. SIRF reaction was carried out using antibodies against POLA1 and Biotin. The graph shows the mean number of SIRF spots per cell. BRCA2 silencing was induced by giving Doxycycline (Dox) 48 hours before the experiment. BRCA2 silencing was confirmed by qRT–PCR analysis of BRCA2 mRNA level 48 hours after doxycycline induction. Expression levels were normalized versus Beta-Actin gene. Relative expression levels are shown with respect to the basal level of BRCA2 in cells, which is considered as 1 (mean ±S.D. for n=2). **I.** Quantification of EdU-RAD51-Polα interaction by super-resolution (SR) microscopy. U2OS WT were treated as indicated on the scheme on the left. The graph represents the percentage of variation in co-localization events of Edu-RAD51, EdU- Polα and EdU-RAD51-Polα. Below the graph are shown representative dSTORM images of two nuclei immunolabeled for nascent DNA (cyan), Polα (magenta) and RAD51 (yellow). Scale bars = 20μm, 1μm and 100nm) All the values are presented as means ± SE (ns = not significant; *P < 0.1; **P<0.1; ***P < 0.001; ****P < 0.0001; ANOVA or Mann–Whitney test;).

Polα-repriming under RAD52 deficiency prevents DSBs formation

Having demonstrated that loss of RAD52 leads to an unusual, origin-independent engagement of Polα, we asked if this mechanism might limit the effects of RAD52 depletion on DNA damage and genome instability accumulation. To detect the presence of DSBs at 18 hours of recovery from HU, we did an immunofluorescence against the phosphorylated histone variant H2AX (γ-H2AX). RAD52i treated cells displayed the same amount of DSBs as the control, as there was no significant difference in γ-H2AX positive cells (Fig. 15A). The treatment with Polαi greatly increased the level of γ-H2AX in cells that were inhibited for RAD52, while did not affect that of WT. We next analyzed if loss of Polα together with RAD52 could impair chromosome stability. We analyzed the presence of chromosomal aberration in terms of unrepaired chromatid breaks and chromatid fusions. Cells inhibited for RAD52 showed a general higher level of chromosome aberrations respect to the control, and this was further increased by Polαi (Fig. 15B). Interestingly, we observed that the majority of chromosome aberrations characterizing the cells previously depleted of RAD52 are chromosomal fusions, while the overall quantity of chromosomal breaks seems the same for all the samples (Fig. 15B). Altogether these results indicate that, in a background in which RAD52 is absent, the recruitment of Polα may compensate for the loss of RAD52 by protecting the cells from DSBs formation. However, even if

RAD52 is depleted for a short period of time, the ssDNA lesions raised during its absence could last the whole cell cycle and stimulate chromosomes fusion.

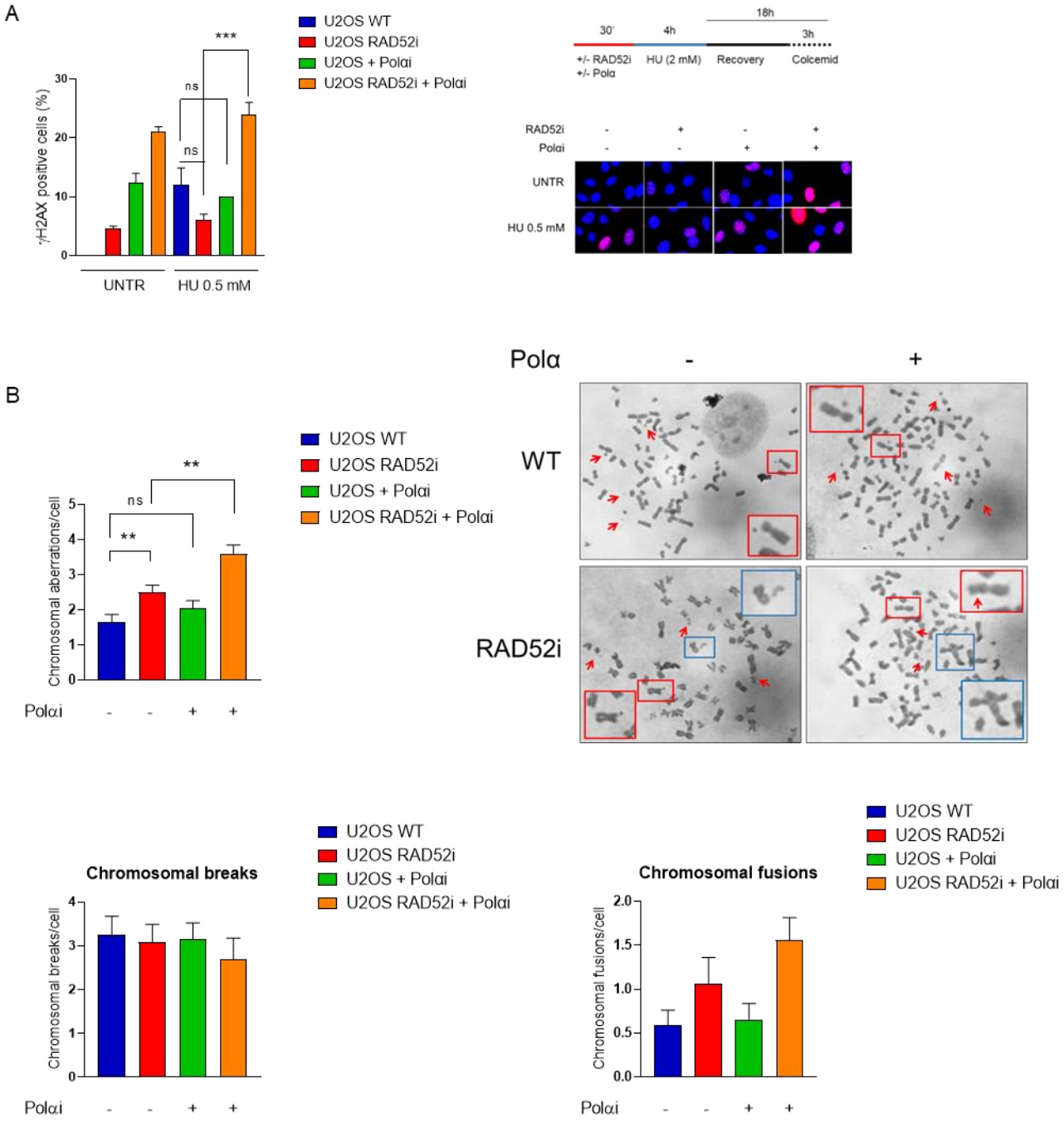

Fig. 15 - Pol*α*-repriming under RAD52 deficiency prevents DSBs formation but induces chromosomal aberrations. A. DSBs detection by immunofluorescence. U2OS WT were treated as indicated in the experimental scheme. Immunofluorescence was

carried out by using an antibody against γH2AX. The graph shows the percentage of γH2AX positive cells. Representative images are shown. **B.** Analysis of chromosomal aberrations in U2OS WT treated as in the experimental scheme above. The graphs show the mean of total chromosomal aberrations per cell and the mean of chromosomal breaks and fusions per cell. Representative images of Giemsa-stained metaphases are given. Red arrows indicate chromosomal breaks; blue arrows indicate chromosomal fusions. Insets show an enlarged portion of the metaphases for a better evaluation of chromosomal aberrations. All the values above are presented as means ± SE (ns = not significant; *P < 0.1; (**P<0.1; ***P < 0.001; ****P < 0.0001; ANOVA or Mann–Whitney test;)

PART 2 - PROCESSING AND HANDLING OF ssDNA GAPS DERIVED FROM RAD52 DEFICIENCY

We have previously demonstrated that the slowed or stalled replication forks, in absence of a functional RAD52, leave behind regions of unreplicated ssDNA that are dependent on a peculiar Polα-mediated repriming mechanism, and persist even after replication recovery. If not adequately repaired, these ssDNA gaps could be processed into DSBs and lead to genome instability. Recent works demonstrated that persistent ssDNA gaps play a role in the toxicity of several genotoxic agents (Panzarino et al., 2021), moreover, it has been shown that gap suppression conferred therapy resistance to BRCA1 and BRCA2 mutated tumors (Panzarino et al., 2021). Therefore, studying how ssDNA gaps are handled or repaired following RAD52 depletion could be of fundamental importance to find new biomarkers or targets to the development of new combined therapies or to treat therapy-resistant diseases. In these second part of the thesis, we sought to study the fate of the ssDNA gaps raised from RAD52 inhibition and how they are processed and repaired by the cells.

RAD52-dependent ssDNA gaps elicit a post-replicative checkpoint response

We have shown that the ssDNA gaps raised during the treatment with HU, in presence of RAD52i, persisted also after replication recovery. To test in which phase of the cell cycle the ssDNA gaps were found after 18 hours of recovery, we performed a quantitative image-based cytometry (QIBC) analysis of the ssDNA exposed. As shown in Fig. 16A, the ssDNA formation in RAD52i cells subjected to high dose HU was limited to the S-phase of the cell cycle. On the contrary, after 18 hours of recovery, the ssDNA signal persisted up to the G2-phase (Fig. 16A). Formerly, it was believed that stalled replication forks were the only source of ssDNA capable of activating the replicative-checkpoint signaling (Byun et al., 2005; Walter and Newport, 2000). However, studies in yeast have uncovered a post-replicative checkpoint activation pathway that senses long stretches of unreplicated DNA, and that is mechanistically and spatially separated from that arising from the stalled replication forks during the S-Phase (García-Rodríguez et al., 2018). Based on these evidences in yeast, we wanted to determine whether RAD52-dependent ssDNA gaps exposed during recovery from HU could increase CHK1 phosphorylation. To this aim, we analysed CHK1 activation by Western blot after treatment with HU and at different hours of recovery. Phosphorylation of CHK1 at S345 was used as readout of checkpoint activation. In accordance with the ssDNA exposure, we observed an enhanced CHK1

phosphorylation in cells recovering from the combined treatment with HU and RAD52i compared to the mock-inhibited cells (Fig. 16B). This suggests that the ssDNA gaps raised from the inhibition of RAD52 during replicative stress could elicits CHK1 activation also during cell recovery. To examine in which phase of the cell cycle CHK1 was activated, we labeled the cells with EdU 20 minutes prior the end of the treatment and performed combined EdU detection with the immunofluorescence of pS345CHK1. In cells treated with 2mM HU, the pCHK1 signal was almost completely confined to EdU-labelled cells, suggesting that the activation of the replication-checkpoint was taking place during S-phase (Fig. 16C). During replication recovery, the pCHK1 signals did not co-localize with that of the EdU, on the contrary, it localized with the cyclin B, a well-known marker of G2/M phase of the cell cycle (Fig. 16D). Taken together, these results show that the ssDNA gaps derived from RAD52 loss elicit a post-replicative checkpoint response in G2-phase of the cell cycle.

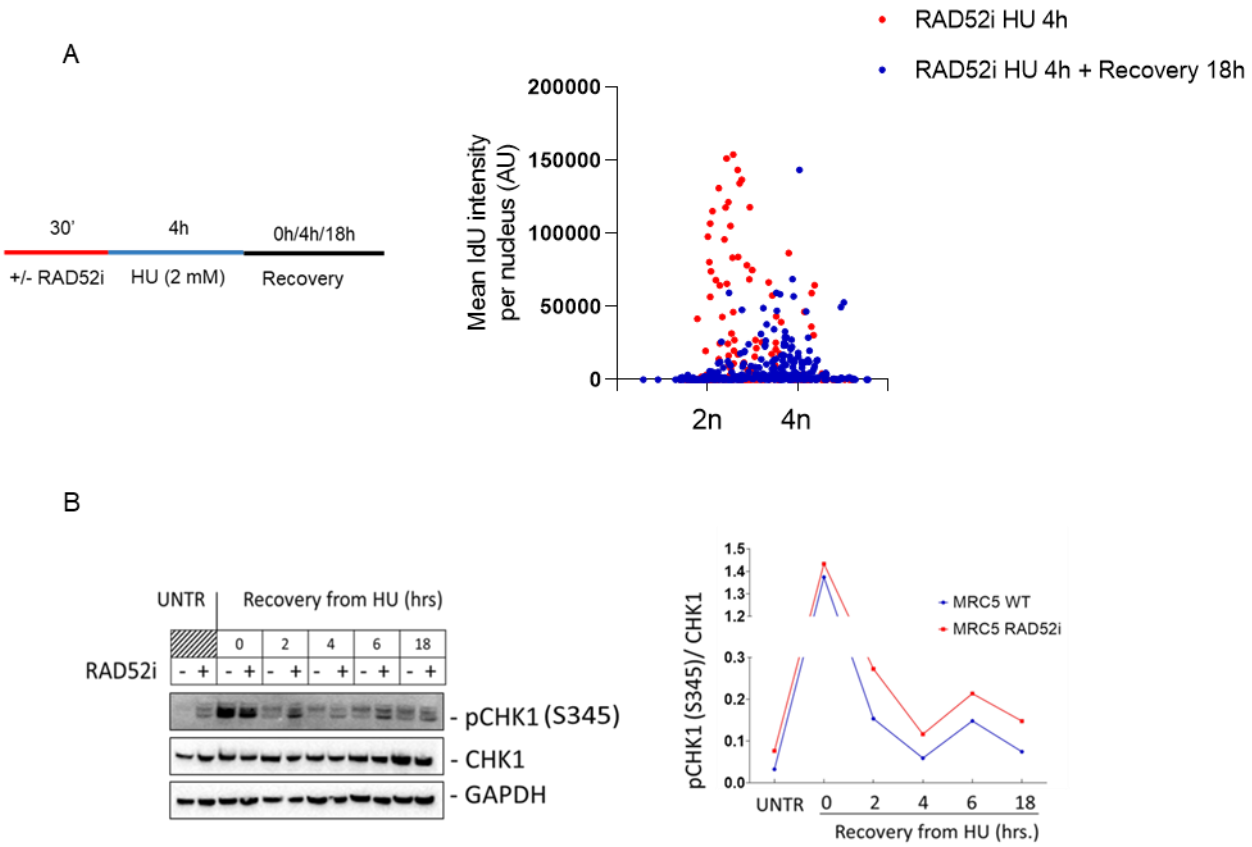
A
30'
4h
0h/4h/18h
+/- RAD52i
HU (2 mM)
Recovery
RAD52i HU 4h
RAD52i HU 4h + Recovery 18h
Mean IdU intensity per nucleus (AU)
200000
150000
100000
50000
0
2n
4n
B
UNTR
Recovery from HU (hrs)
RAD52i
0
2
4
6
18
- pCHK1 (S345)
- CHK1
- GAPDH
pCHK1 (S345)/ CHK1
MRC5 WT
MRC5 RAD52i
UNTR
Recovery from HU (hrs.)
C
RAD52i
UNTR
Recovery from HU (hrs.)
10μM
D
pCHK1
Merge
Cyclin B1
Negative cells
Recovery from HU (hrs.)
N° of cells (tot. 100)
Recovery from HU (hrs.)

Fig. 16 – RAD52-dependent ssDNA gaps elicit a post-replicative checkpoint response. A. Quantitative image-based cytometry (QIBC analysis) of ssDNA exposure during each phase of the cell cycle. The experiment was done by treating the cells as reported on the experimental scheme. Images were acquired and analysed with the Nikon NIS-Elements software (Total cell number = 700, N=2). The graph reports the mean IdU intensity per nucleus over the mean intensity of DAPI staining (2n = G1-phase, 4n =G2-phase). **B.** Western blot analysis of whole cell extracts from MRC5 WT. Cells were treated as indicated on the figure. Phosphorylation of CHK1 at S345 (pCHK1) was used as readout of checkpoint activation. GAPDH and total CHK1 were used as loading controls. **C.** Analysis of pS345-CHK1 and EdU by co-immunofluorescence in MRC5 WT. Cells were treated following the experimental scheme above. To mark cells in the S-phase, they were labelled with EdU 20 minutes before samples collection. Immunofluorescence was carried out by combining the pCHK1 immunostaining with the Click-iT™ reaction. Scale bar = 10μm. **D.** Analysis of pS345-CHK1 and Cyclin B by co-immunofluorescence. Cells were treated following the experimental scheme above. Immunofluorescence was carried out by combining the pCHK1 immunostaining with that of Cyclin B, to detect the cells in G2/M-phase. The graph on the right reports the quantity of cells in which the two staining co-localize compared to the total amount of cells analysed (N=100).

RAD51 protects DNA gaps from MRE11-dependent excessive degradation

Previous studies in *Xaenopus* Egg extracts have demonstrated that RAD51 recognizes and binds the ssDNA gaps left behind the replication forks and protects the DNA from the pathological MRE11 nuclease activity (Hashimoto et al 2010). Therefore, we asked if RAD51 could be involved also in the protection of the ssDNA gaps generated by RAD52 disfunction. The treatment with B02 during replication recovery strongly elicited ssDNA exposure in WT cells, and it further increased after RAD52 inhibition (Fig. 17A). The treatment with MIRIN reduced the IdU signal in RAD52i cells starting from 4 hours of replication recovery (Fig. 17B), suggesting that, in absence of a functional RAD52, RAD51 may prevent the excessive digestion and enlargement of the ssDNA gaps driven by MRE11.

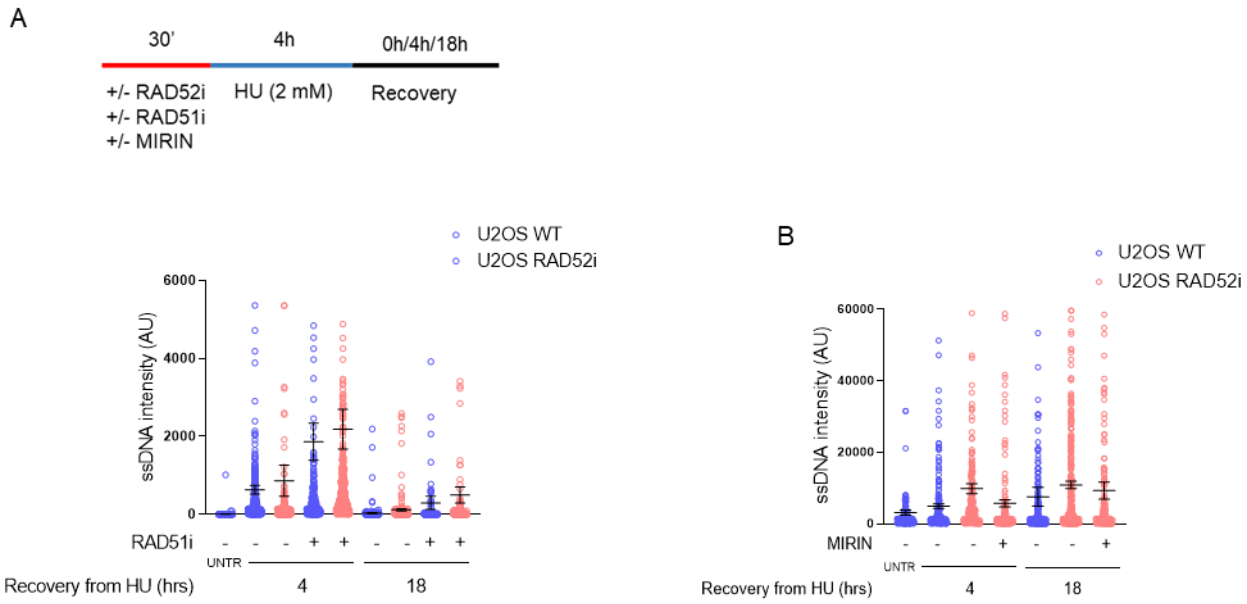

Fig. 17 - RAD51 protects DNA gaps from MRE11-dependent degradation. A and **B.** Analysis of parental ssDNA exposure in U2OS WT. The cells were treated as indicated by the scheme. The graphs show the mean ssDNA fluorescence intensity (AU). All the values are presented as means ± SE (ns = not significant; *P < 0.1; **P<0.1; ***P < 0.001; ****P < 0.0001; ANOVA or Mann–Whitney test;).

RAD52-dependent ssDNA gaps repair is delayed until G2-phase of the cell cycle

In human, the monoubiquitination of PCNA (PCNA-Ub) is mediated by the E3 ubiquitin ligase RAD18, and drives the recruitment of TLS enzymes to allow DNA damage bypass via polymerase switching (Kannouche et al., 2004). A work from Tirman et al. recently proposed that PCNA monoubiquitination by RAD18 promotes ssDNA gap filling dependent by REV1-POLζ in G2-phase of the cell cycle, and this pathway was only limited to the treatment with cisplatin (Tirman et al. 2021). Based on these evidences, we wanted to investigate whether the RAD52-dependent gaps released under the exposure to the high dose of HU could be repaired by the RAD18 pathway during G2-phase. In accordance with the cell cycle analysis, RAD18 depletion did not affected significantly the ssDNA exposure during fork stalling (Fig. 18A), but increased IdU signal after 18 hours of recovery only in RAD52i cells (Fig. 18A). This result suggests that also the ssDNA gaps derived from RAD52i cells treated with a high dose of HU may be filled post-replicatively by the RAD18/PCNA pathway, and

the failure of the repair could lead to the excessive processing of the gaps. UBC13 is an E2 ubiquitin-conjugating enzyme that in yeast drives the polyubiquitination of PCNA (PCNA-Ubn) in association with RAD5 and RAD18 (Ulrich, 2000). Contrary to its mono-ubiquitinated counterpart, PCNA-Ubn triggers the template switching (TS) mechanism. Intriguingly, we observed an impairment in gaps filling also when the protein UBC13 was depleted after 18 hours from replication stress recovery, although this occurred also in mock-inhibited cells. This suggest that the repair of ssDNA gaps left by RAD52 depletion during HU is delayed until G2-phase, where they are filled by either TLS or TS.

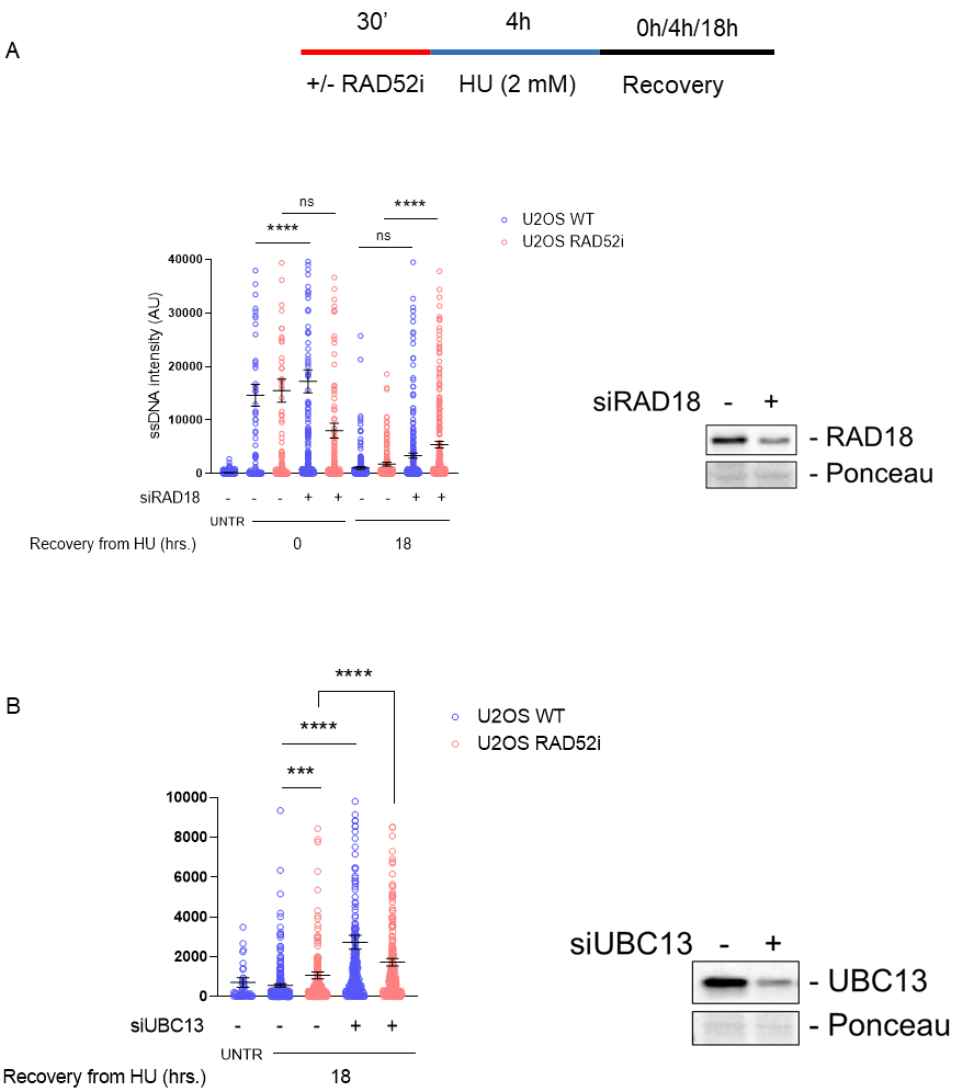

Fig. 18 - RAD52-dependent ssDNA gaps repair is delayed until G2-phase of the cell cycle. A and **B.** Analysis of parental ssDNA exposure in U2OS WT. The cells were treated as indicated by the scheme. The silencing of RAD18 and UBC13 with the siRNA was obtained by transfecting the cells 48 hours before the experiments. The silencing of the proteins was confirmed by western blot. The graphs show the mean ssDNA fluorescence intensity (AU). All the values are presented as means ± SE (ns = not significant; *P < 0.1; **P<0.1; ***P < 0.001; ****P < 0.0001; ANOVA or Mann–Whitney test;).

DISCUSSION

Our experiments demonstrate that the loss of RAD52 function in human cells subjected to a replication stalling dose of hydroxyurea (HU) drives the accumulation of parental ssDNA regions that are detectable until late time from replication recovery. ssDNA gaps usually accumulate on newly synthesized DNA under conditions of replication stress (Tirman et al., 2021), and can derive from nuclease-dependent digestion of the stalled forks, defects in Okazaki fragment processing or from repriming events (Wong et al., 2021). In human cells, repriming seems the prevalent mechanism leading to parental gap accumulation, especially under pathological conditions such as loss of BRCA1 or BRCA2 (Quinet et al., 2020). In these conditions, gaps derive from the repriming activity of primase and DNA directed polymerase (PrimPol), a specialized polymerase-primase that has been shown to be activated after different kinds of replication perturbations (Quinet et al., 2020). While in yeast the only protein that could mediate the repriming is the polymerase α (Polα) (Quinet et al., 2021), PrimPol was considered the only protein involved in the repriming mechanism in human models. Here, we have shown that these parental ssDNA regions derives from a PrimPol-distinct repriming pathway mediated by Polα. We demonstrate that, in the absence of a functional RAD52, perturbed replication triggers an elevated engagement of Polα in chromatin, that is not related to its normal function in new origin firing, and is responsible for the accumulation of ssDNA gaps. We show that Polα recruitment in

absence of RAD52 involves the protein AND-1. Since AND-1 normally assists loading and retention of Polα during lagging strand synthesis, it is likely that loss of RAD52 triggers a peculiar repriming activity at lagging strand as opposed to that mediated by PrimPol that occurs at the leading strand. Of note, some PrimPol recruitment still occurs in the absence of RAD52 but it is not stimulated upon replication arrest significantly, as observed in RAD52-proficient cells and much more in BRCA2-depleted cells. Our data indicate that, under RAD52 deficiency, Polα binds the parental ssDNA downstream fork reversal, as its recruitment is strongly reduced by downregulation of SMARCAL1 or ZRANB3. Moreover, a significant portion of Polα is engaged after the pathological degradation of the nascent ssDNA exposed on the reversed fork mediated by the nuclease MRE11. These findings differentiate such Polα-mediated repriming from that mediated by PrimPol, which acts in a parallel pathway with the fork reversal (Quinet et al., 2020). In BRCA2-deficient cells, degradation of the reversed fork is followed by endonucleolytic cleavage by the MUS81/EME2 complex and BIR to promote restart of DNA synthesis (Kramara et al., 2018). Likewise, also loss of RAD52 promotes fork degradation, but does not induce fork cleavage because RAD52 also regulates MUS81-dependent DSBs (Murfuni et al., 2013). Depletion of MUS81 in BRCA2-deficient cells leads to extended fork degradation, which is the same observed in cells inhibited of RAD52 during replication arrest (Lemaçon et al., 2017; Malacaria et al., 2019). Our findings indicate that co-depletion of MUS81 and BRCA2 is sufficient to stimulate Polα recruitment at parental ssDNA following replication perturbation, recapitulating what happens when RAD52

is inhibited. This suggest that extended degradation, which might reset the reversed fork, could also promote repriming on both DNA strands as shown in yeast (Heller & Marians, 2006). Interestingly, we find that in absence of RAD52, Polα engagement strictly relies on RAD51 function, as its depletion impaired both Polα recruitment and gap accumulation only in RAD52i cells. Moreover, we have shown that RAD52 depletion enhanced Polα-RAD51 interaction. RAD51 has an important role in fork restart. Previous studies in *Xenopus* has shown that RAD51 interact with Polα, and this association is important to bind Polα at the fork (Kolinjivadi et al., 2017). However, our data indicate that RAD51-dependent Polα recruitment occurs downstream fork reversal/degradation and not before as a mechanism avoiding fork remodelling. Our findings also show that even a small reduction in the amount of RAD51 is sufficient to interfere with Polα recruitment and Polα-dependent gap accumulation. Analysis of proximity at the dsDNA allowed us to visualize Polα binding both at the active replication forks or far behind them. This binding is increased by RAD52 inhibition, and was dependent on both RAD51 and BRCA2. Since only the extensive RAD51 nucleation associated to strand invasion or fork protection is sensitive to even limited depletion (K. P. Bhat et al., 2018), our evidences suggests that Polα is recruited downstream a strand-invasion event. In yeast, mutations leading to extensive processing of RF can stimulate either Polα repriming or template-switching and repriming post strand invasion, which might be dependent on Polα primase if occurring on the lagging strand (Fumasoni et al., 2015). Thus, our findings could support a similar mechanism also in human cells, demonstrating that PrimPol is not

the only available repriming mechanism. Of note, the dependency of Polα recruitment on the nuclease MRE11 changes according to the distance from the active replication. At the replication fork, when replication is impaired and RAD52 absent, Polα engagement is MRE11-independent. On the contrary, Polα bindings that occurs far behind the forks is MRE11-dependent. This data suggests that there is a portion of Polα that may be bound directly on the slowed, unreverted forks, possibly after that other nucleases have processed the nascent DNA. Another pool of Polα, that found behind the forks, may be recruited after the RF are degraded by MRE11, either direcxtly on the resected forks or downstream the strand invasion mediated by BRCA2 and RAD51. If on one hand this peculiar repriming mediated by Polα generates single-stranded gaps along the DNA, it could be aimed to protect the cells from the increased levels of remodeled and deprotected replication forks, possibly avoiding DSBs formation late during the cell cycle. This could explain the significant increase in DSBs amount upon the combined treatment with RAD52i and Polαi. The presence of long ssDNA regions on the resected break ends of DSBs might favor chromatid fusion or chromosome exchanges by connecting two ends from different breaks (Llorens-Agost et al., 2021). Similar to what happens with DSBs, if the ssDNA gaps that accumulate after RAD52 inhibition persist until G2/M phase of the cell cycle, their repair through homology-directed pathways may result in the formation of wrong DNA intermediates and chromosomal fusions.

It is well established that extended regions of ssDNA are sensed and converted to a checkpoint signal (Branzei & Foiani, 2009; García-Rodríguez et al., 2018). First it was thought

that checkpoint kinases were activated only by ssDNA arising at stalled forks, either from the uncoupling between replicative helicase and DNA polymerase movement or between leading and lagging strand synthesis (Branzei & Foiani, 2009;). However, a work from Rodríguez *et al.* (2018) in yeast model proposed a post-replication checkpoint activation that senses ssDNA on daughter-strand gaps, left behind after passage of the replisome (García-Rodríguez et al., 2018). Here we observe that the ssDNA gaps raised during HU and RAD52i by Polα-repriming are conserved along the cell cycle, and elicit a post-replicative checkpoint response. Of note, our data demonstrate that the CHK1 phosphorylation occurring during HU is elicited in S-phase, as expected, while it occurs outside S-phase cells after recovery. From this point of view, our data are consistent with the studies from Rodríguez and colleagues, which observe late checkpoint activation during the G2-phase. To be correctly repaired, the ssDNA gaps exposed probably require a controlled resection by the exonuclease function of MRE11. Indeed, its inhibition significantly decrease ssDNA exposure after RAD52 depletion. This controlled resection could be regulated by the strand protecting function of RAD51, since its depletion results in a high increase in ssDNA signal. This processing of the gaps could be preparatory for the successive repair mechanism. We show that gaps filling in our background is regulated by PCNA mono- and poly-ubiquitination (PCNA-Ub/Ubn) mediated by RAD18. Recent evidences in yeast indicate that the E2 protein UBC13 drives the poly-ubiquitylation of PCNA on lysine-164 and promotes template switching (Ripley et al., 2020). Although Tirman *et al*. proposed that RAD18 and UBC13 act on gaps repair in different phase of the cell cycle,

we observe that the repair of ssDNA gaps derived from RAD52 deficiency are slightly dependent on UBC13 function even in G2-phase.

Altogether, our findings may be summarized in a model whereby replication perturbation in human cells, by uncoupling unwinding from DNA synthesis, stimulates the recruitment of RAD52 at the fork, probably at lagging strand. Recruitment of RAD52 functions as a gatekeeper limiting unscheduled and perhaps "error-prone" engagement of SMARCAL1, as previously demonstrated (Malacaria et al., 2019) (Fig. 19). In the absence of RAD52, the cell deals with this pathological condition stimulating an exceptional RAD51-dependent Polα recruitment on the lagging strand. If the replication fork is unreverted, Polα might bind directly to the ssDNA exposed on the uncoupled forks. In alternative, other unknown exonucleases may contribute to the digestion of the nascent strand, stimulating an unscheduled repriming by Polα. When the forks are reverted under RAD52 deficiency, they get degraded by MRE11, but cannot be cleaved by MUS81, leading to fork reset. Here, the uncontrolled processing of the RF exposes long stretches of nascent DNA that could function as a platform for the binding of Polα, that could restart the replication before the reannealing of the strands and the fork restoration. Another hypothesis is that, after MRE11 resection and fork reset, Polα repriming might occur on the parental ssDNA exposed on the lagging strand and restart the synthesis through a strand-invasion pathway mediated by Polα-RAD51. Thus, the Polα-mediated repriming mechanism may be an attempt to restart the forks and limit DNA damage that would accumulate upon the unscheduled processing of replication forks in the absence of

RAD52. However, since the quantity of RAD51 in the nucleus is limited, and is probably not sufficient to fulfil all its strand protection activities (Malacaria et al., 2019), the ssDNA gaps generated by fork degradation remain deprotected and exposed to nucleases attack. When the replication is repristinated, the gaps are maintained until a late phase of the cell cycle, where they activate a post-replicative checkpoint response that might regulate the gaps filling by PCNA-dependent TLS and TS (Fig. 19).

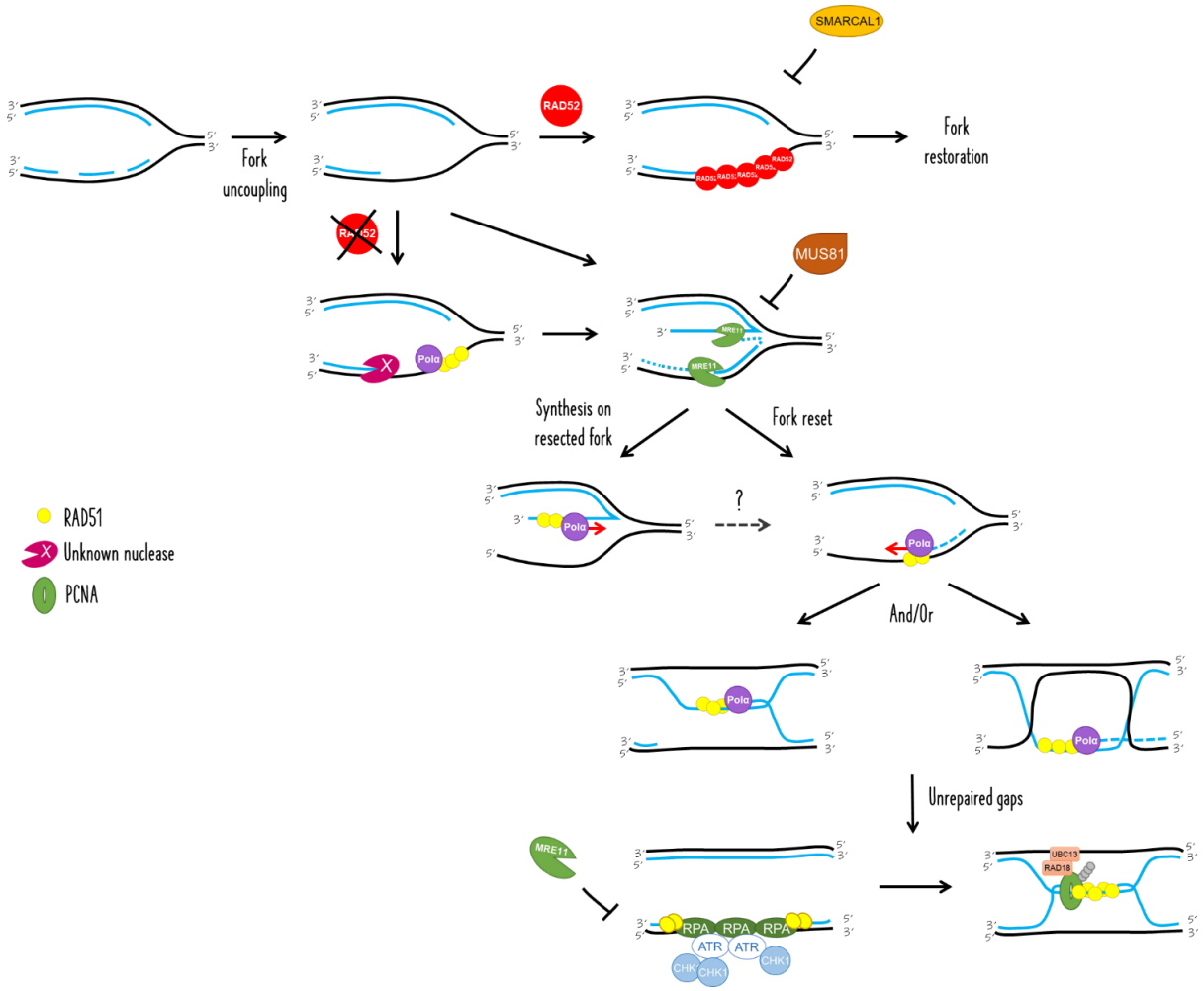

Fig. 19 – Summarizing model to illustrate the Pol*α*-mediated repriming under RAD52 deficiency.

In this thesis we proposed two novel functions of human RAD52, the first involved in regulating the restart of the replication forks in cells subjected to different level of replication stress, the second linked to the protection of the lagging strand integrity. Whether RAD52 could be involved also in the deposition or the processing of Okazaki fragments requires further investigations. The discovery of alternative pathways mediated by RAD52 is of fundamental importance, since its expression is often found

deregulated in tumor cells. RAD52 is overexpressed in several types of tumors, and correlates with a worse disease-free survival (P. Li et al., 2019). In other models, RAD52 function might serve to compensate for the defects in the DNA repair machinery, as it occurs in cells deficient for HR (Malacaria et al., 2020). Indeed, RAD52 depletion or inhibition in BRCA- or checkpoint deficient cells results in synthetic lethality (Lok et al., 2013; Chandramouly et al., 2015; F. Huang et al., 2016). Despite the many evidences regarding this genetic interaction, it is still unclear which of the many functions of RAD52 allow for survival and proliferation of HR-defective cells (Malacaria et al., 2020). A previous work demonstrated that, under BRCA2 deficiency, RAD52 is sufficient for the generation of RAD51 foci and HR reaction (Feng et al., 2011). Other studies proposed that RAD52 could compensate HR loss by driving alternative repair pathways like SSA (Grimme et al., 2010), BIR (Sakofsky & Malkova, 2017) or MMJ (Kelso et al., 2019). On the basis of our results, it would be interesting to determine if the survival of HR-defective cells correlates with the inability to perform RAD51-Polα-mediated repriming at distressed forks. Moreover, it would be interesting to assess if also in cancers that present a mutation in RAD52 is favoured the Polα-mediated repriming. In that case, the treatment with inhibitors of RAD51-Polα interaction could be an effective strategy to kill cancer cells that presents a mutation or lack the protein RAD52.

MATERIALS AND METHODS

Cell lines and culture conditions

The MRC5SV40 and human osteosarcoma cell line (U2OS) were maintained in Dulbecco's modified Eagle's medium (DMEM, Euroclone) supplemented with 10% fetal bovine serum (Euroclone) and incubated at 37 °C in a humidified 5% CO2 atmosphere. MRC5SV40 -/- PrimPol was a kind gift from Professor Aidan Doherty of Sussex University. MRC5 -/- MUS81 was obtained with the Crispr/Cas9 system by using two Alt-R® Crispr-Cas9 gRNA (Hs.Cas9.MUS81.1.AA and Hs.Cas9.MUS81.1.AB) and successively transfected with the WT protein. MRC5 shBRCA2 and U2OS shSMARCAL were transfected with lentiviruses expressing the shSMARCAL1/shBRCA2 cassette under the control of a doxycycline (Dox)-regulated promoter, at 0.5 of multiplicity of infection (MOI) (Dharmacon SmartVector inducible lentivirus, sequence code: V3SH11252-227970177 (shSMARCAL) and V3SH7669-226099147 (shBRCA2). After puromycin selection at 300 ng/ml, a single clone was selected and used throughout the study. SMARCAL1 overexpressing U2OS was obtained by the transfection of WT cells with the inducible PiggyBac/Transposase system, kindly donated by professor Alessandro Rosa from University La Sapienza, in

a proportion of 9:1. PEO1 and PEO4 tumoral lines (ATCC) were maintained in Roswell Park Memorial Institute 1640 medium (RPMI, Euroclone) supplemented with 10% fetal bovine serum (Euroclone) and incubated at 37 °C in a humidified 5% CO2 atmosphere. Cell lines were routinely tested for mycoplasma contamination and maintained in cultures for no more than one month.

Oligos and plasmids

siRNA
MUS81: 6 FlexiTube siRNA cat # SI04300877
BRCA2: ON TARGET PLUS SMARTpool siRNA #SO-2994934G
siWDHD1: MISSION esiRNA #EHU134421
ZRANB3: siGENOME siRNA D-010025-03-005 Dharmacon cat # 84083.
RAD51 (J11): ON TARGET PLUS siRNA #SO-2960294G
RAD18: FlexiTube siRNA #1027418
UBC13: siRNA sc-43551

Plasmids
peGFP-PrimPol WT
PiggyBac-SMARCAL1
pFLAG-MUS81 WT

Transfections

All the siRNAs were transfected using Interferin® 48 h before to perform experiments. WDHD1 siRNA was used at 10 nM. RAD51 siRNA (J11) was used at 2 and 20 pmol. MUS81, BRCA2, RAD18 and UBC13 siRNAs were used at 25 nM. ZRANB3 siRNA was used at 50 nM. peGFP-PrimPol, PiggyBac-SMARCAL1 and pFLAG-MUS81 were transfected in cell lines using Neon™ transfection system 48 h prior to perform experiments.

Chemicals

HU (Sigma-Aldrich) was added to culture medium at 2 mM or 0.5 mM from a 200 mM stock solution prepared in Phosphate-buffer saline solution (PBS 1X) to induce DNA

replication arrest or slowing. RAD52 inhibitor, Epigallocatechin (EGC - Sigma-Aldrich) was dissolved in DMSO at 100 mM, and stock solution was stored at −80° and was used at 50 μM. The B02 compound (Selleck), an inhibitor of RAD51 activity, was used at 27 μM. CDC7i (Selleck) was dissolved in sterile water and used 10 μM. Doxycycline (Sigma-Aldrich) was dissolved in DMSO and used 1μ/ml. MIRIN, the inhibitor of MRE11 exonuclease activity (Calbiochem), was used at 50 μM. Pol*α* inhibitor (ST1926 – Sigma-Aldrich) was dissolved in DMSO and used at the concentrations reported on the experiments. S1 nuclease (Invitrogen cat # 18001016) was diluted 1/100 in S1 buffer and used at 20 U/ml. CldU (Sigma-Aldrich) was dissolved in sterile water as a 200 mM stock solution and used at 50 μM. IdU (Sigma-Aldrich) was dissolved in sterile DMEM as a stock solution 2.5 mM and used at 100 or 250 μM. 5-ethynyl-2'-deoxyuridine (EdU) (Sigma-Aldrich) Was dissolved in DMSO and used at 10 μM for S-phase labeling or 100 μM for SIRF assay.

Western blot analysis

Western blots were performed using standard methods. Blots were incubated with primary antibodies against: anti-GFP (Santa Cruz Biotechnology, 1:500), anti-MUS81 (Santa Cruz Biotechnology, 1:1000), LAMINB1 (Abcam, 1:10,000), anti-RAD52 (Santa Cruz Biotechnology, 1:500), anti-GAPDH (Millipore, 1:5000), anti-RAD51 (Abcam 1:10,000), anti-SMARCAL1 (Bethyl 1:1500), anti-ZRANB3 (Proteintech 1:1000), anti-

RAD18 (Abcam, 1:1000), anti-UBC13 (Cell Signaling Technologies 1:1000), anti-BRCA2 (Bethyl 1:5000), anti-Polα (Bethyl, 1:500), anti-ZRANB3 (Proteintech, 1:1000), anti-WDHD1 (Novus Biologicals, 1:1000), anti-pCHK1 (Cell Signaling Technologies, 1:1500), anti-CHK1 (Santa Cruz Biotechnology, 1:300). After incubations with horseradish peroxidase-linked secondary antibodies (Jackson ImmunoResearch, 1:20,000), the blots were developed using the chemiluminescence detection kit ECL-Plus (Amersham) according to the manufacturer's instructions. Quantification was performed on blot acquired by ChemiDoc XRS+ (Bio-Rad) using Image Lab software, the normalization of the protein content was done through LAMIN B1 or GAPDH immunoblotting.

Chromatin isolation

After the treatments, cells (4×10^6 cells/ml) were resuspended in buffer A (10 mM HEPES, [pH 7.9], 10 mM KCl, 1.5 mM MgCl2, 0.34 M sucrose, 10% glycerol, 1 mM DTT, 50 mM sodium fluoride, protease inhibitors [Roche]). Then was added Triton X-100 at a final concentration of 0.1% and the cells were incubated for 5 min on ice. Nuclei were collected in pellet by low-speed centrifugation (4 min, 1300 × g, 4 °C) and washed once in buffer A. Nuclei were then lysed in buffer B (3 mM EDTA, 0.2 mM EGTA, 1 mM DTT, protease inhibitors) for 10 min on ice. Insoluble chromatin was collected by centrifugation (4 min, 1700 × g, 4 °C), washed once in buffer B + 50 mM NaCl, and

centrifuged again under the same conditions. The final chromatin pellet was resuspended in 2X Laemmli buffer and sonicated for 15 s in a Tekmar CV26 sonicator using a microtip at 50% amplitude.

Immunofluorescence

Cells were grown on 35-mm coverslips and harvested at the indicated times after treatments. For γH2AX IF, cells were fixed in 4% PFA/PBS 1X and subsequently permeabilized with 0.4% Triton X-100 in PBS 1X. After blocking in 3% bovine serum albumine (BSA)/PBS 1X for 15 min, staining was performed with rabbit monoclonal anti- γH2AX (Millipore, 1:1000). For pS345-CHK1 and EdU or Cyclin-B IF, cells were fixed with 4% PFA at RT for 10 min then permeabilized 10 minutes with 0,4% Triton X-100 in PBS. Staining was performed with rabbit polyclonal anti phospho-CHK1-Ser345 (Cell Signaling Technologies, 1:50) incubated over-night at 4°C. Cells were then washed with PBS and subjected to Click-iT™ reaction for 30 min at RT or incubated with mouse monoclonal anti-Cyclin B (Santa Cruz Biotechnology, 1:250) for 1 hour at 37#C. After 3 washes in PBS 1X, specie-specific fluorescein-conjugated secondary antibodies (Alexa Fluor 594 Goat Anti-Rabbit or Alexa Fluor 488 Goat Anti-Mouse, Life technologies, 1:200) were applied for 1h at RT. Eventually cells was counterstained with 0,5 μg/ml DAPI. All the antibodies, either primary or secondary, were diluted in 1% BSA/0,1% saponin in PBS. The reagents for the Click-iT™ reaction were diluted

according to the manufacturer's instructions. Nuclei were examined with Eclipse 80i Nikon Fluorescence Microscope, equipped with a VideoConfocal (ViCo) system and foci were scored at 40X magnification. Quantification was carried out using the ImageJ software.

EdU incorporation assay

U2OS were treated with 10 μM EdU 10 min before giving the treatment with ST1926 for 30 min at the indicated concentrations. After the treatment, cells were permeabilized with 0.5% TritonX-100 in PBS 1X for 10 minutes on ice, then fixed with 3% PFA, 2% sucrose in PBS 1X at room temperature (RT) for 15 min. For the EdU detection was applied the Click-iT™ EdU Alexa Fluor™ 488 Imaging Kit (Invitrogen) for 30 minutes at RT. The reagents for the Click-iT™ reaction were diluted according to the manufacturer's instructions. Nuclei were examined with Eclipse 80i Nikon Fluorescence Microscope, equipped with a VideoConfocal (ViCo) system and foci were scored at 40X magnification. Quantification was carried out using the ImageJ software.

Detection of ssDNA by native IdU assay

To detect parental ssDNA, cells were labelled for 20 hours with 100 μM IdU (Sigma-Aldrich), released in a fresh DMEM for 2 hours, then treated as indicated. For immunofluorescence, cells were washed with PBS, permeabilized with 0.5% Triton X-100 for 10 min at 4 °C and fixed in 3% PFA, 2% sucrose in PBS 1X. Fixed cells were then incubated with mouse anti-IdU antibody (Becton Dickinson, 1:80) for 1 h at 37 °C in 1% BSA/PBS, followed by species-specific fluorescein-conjugated secondary antibodies (Alexa Fluor 488 Goat Anti-Mouse IgG (H + L), highly cross-adsorbed—Life Technologies). Slides were analysed with Eclipse 80i Nikon Fluorescence Microscope, equipped with a Video Confocal (ViCo) system. For each time point, at least 100 nuclei. Quantification was carried out using the ImageJ software.

In situ PLA assay for ssDNA–protein interaction

The in situ PLA (OLINK, Bioscience) was performed according to the manufacturer's instructions. For parental ssDNA-protein interaction, cells were labelled with 100 μM IdU for 20 hours and then released in fresh medium for 2 hours. After treatment, cells were permeabilized with 0.5% Triton X-100 for 10 min at 4 °C, fixed with 3% PFA/2% sucrose in PBS 1X for 10 min and then blocked in 3% BSA/PBS for 15 min. After

washing with PBS, cells were incubated with the two relevant primary antibodies. The primary antibodies used were as follows: mouse monoclonal anti-RAD51 (GeneTex, 1:150), mouse monoclonal anti-IdU (Becton Dickinson, 1:50), rabbit polyclonal anti-Polα (Bioss, 1:50), rabbit polyclonal anti-GFP (Invitrogen 1:150), rabbit anti-WDHD1 (Novus Biologicals, 1:50). The negative control consisted of using only one primary antibody. Samples were incubated with secondary antibodies conjugated with PLA probes MINUS and PLUS: the PLA probe anti-mouse PLUS and anti-rabbit MINUS (OLINK Bioscience). The incubation with all antibodies was accomplished in a humidified chamber for 1 h at 37 °C. Next, the PLA probes MINUS and PLUS were ligated using two connecting oligonucleotides to produce a template for rolling-cycle amplification. After amplification, the products were hybridized with red fluorescence-labelled oligonucleotide. Samples were mounted in Prolong Gold anti-fade reagent with DAPI (blue). Images were acquired randomly using Eclipse 80i Nikon Fluorescence Microscope, equipped with a Video Confocal (ViCo) system.

In situ PLA assay for EdU (dsDNA)–protein interaction

Exponential growing cells were seeded onto microscope chamber slide. The day of experiment, cells were incubated with 100 μM EdU for 20 min and treated as indicated. After treatment, cells were pre-extracted in 0.5% TritonX-100 for 5 min on ice and fixed with 3% PFA, 2% sucrose in PBS 1X for 15 min at RT. Cells were then blocked in 3%

BSA/PBS for 15 min. For the EdU detection was applied the Click-iT™ EdU Alexa Fluor™ Imaging Kit (Invitrogen) using 5mM Biotin-Azide for 30 minutes at RT. The primary antibodies used were as follows: mouse monoclonal anti-RAD51 (GeneTex, 1:150), rabbit polyclonal anti-Polα (Bioss, 1:50), mouse anti-biotin (Invitrogen, 1:50) rabbit anti-biotin (Abcam, 1:50). The negative control consisted of using only one primary antibody. Samples were incubated with secondary antibodies conjugated with PLA probes MINUS and PLUS: the PLA probe anti-mouse PLUS and anti-rabbit MINUS (OLINK Bioscience). The incubation with all antibodies was accomplished in a humidified chamber for 1 h at 37 °C. Next, the PLA probes MINUS and PLUS were ligated using two connecting oligonucleotides to produce a template for rolling-cycle amplification. After amplification, the products were hybridized with red fluorescence-labelled oligonucleotide. Samples were mounted in Prolong Gold anti-fade reagent with DAPI (blue). Images were acquired randomly using Eclipse 80i Nikon Fluorescence Microscope, equipped with a Video Confocal (ViCo) system.

dSTORM immunofluorescence

U2OS cells were treated as indicated on the experimental scheme. After the treatment, cells were fixed and immunofluorescence was performed as described by Whelan & Rothenberg, 2021. EdU was detected with the Click-iT™ EdU Alexa Fluor™ Imaging Kit (Invitrogen) for 30 minutes at RT. Coverslips with fixed cells were stored for up to

1 week at 4 °C prior to dSTORM imaging. They were then mounted into a Concave Slides with STORM imaging buffer provided from ONI company. All images were acquired using Nanoimager microscope from ONI company (https://oni.bio).

Quantitative image-based cytometry (QIBC)

Cells were labelled for 20 hours with 100 μM IdU (Sigma-Aldrich), released in a fresh DMEM for 2 hours, then treated as indicated. For immunofluorescence, cells were washed with PBS, permeabilized with 0.5% Triton X-100 for 10 min at 4 °C and fixed in 3% PFA, 2% sucrose in PBS 1X. Fixed cells were then incubated with mouse anti-IdU antibody (Becton Dickinson, 1:80) for 1 h at 37 °C in 1% BSA/PBS, followed by species-specific fluorescein-conjugated secondary antibodies (Alexa Fluor 488 Goat Anti-Mouse IgG (H + L), highly cross-adsorbed—Life Technologies). After DAPI staining, Slides were analysed with Nikon microscope and analyzed with the NIS-elements software. The experiment was repeated two times and a total of 700 nuclei for each experiment was analyzed.

DNA fiber analysis

Cells were pulse-labelled with 50 μM CldU and then labelled with 250 μM IdU with or without treatment as reported in the experimental schemes. DNA fibers were prepared and spread out as described by Iannascoli et al., 2015. For immunodetection of labelled tracks, the following primary antibodies were used: rat anti-CldU/BrdU (Abcam 1:50) and mouse anti-IdU/BrdU (Becton Dickinson 1:10). Fiber assay using S1 nuclease was performed as indicated by Quinet et al., 2017. Briefly, cells were pulse labelled as described above. At end of treatment, cells were permeabilized with CSK buffer (100 mM NaCl, 10 mM PIPES pH 6.8, 1M EGTA, 3 mM MgCl2, 300 mM sucrose, 0.5% Triton X-100) for 10 min at RT, then were washed with PBS 1X and S1 nuclease buffer (30 mM sodium acetate, 10 mM zinc acetate, 5% glycerol, 50 mM NaCl) prior to add +/- S1 nuclease for 30 min at 37 °C in a humidified chamber. Cells were washed with S1 buffer then scraped with 0.1% BSA/PBS and collected pellets were used to perform fibers spreading. The labelling was performed as reported above. Images were acquired randomly from fields with untangled fibers using Eclipse 80i Nikon Fluorescence Microscope, equipped with a Video Confocal (ViCo) system. The length of labelled tracks was measured using the Image-Pro-Plus 6.0 software. A minimum of 100 individual fibers were analyzed for each experiment and each experiment was repeated two times.

Chromosomal aberrations

MRC5SV40 cells were treated with HU in combination or not with RAD52 inhibitor and/or Polα inhibitor at 37 °C for 4 h and allowed to recover for additional 24 h. Cell cultures were incubated with colcemid (0.2 μg/ml) at 37 °C for 3 h until harvesting. Cells for metaphase preparations were collected and prepared as previously reported by Iannascoli et al., 2015. For each time point, at least 50 chromosomes were examined and chromosomal damage scored at 100×.

Statistical analysis

All the data are presented as means of at least two pooled independent experiments. Statistical analyses were performed by one-sided analysis of variance (ANOVA) or Mann–Whitney test using the built-in tools in Prism 7 (GraphPad Inc.). $P < 0.05$ was considered as significant. Statistical significance was always denoted as follow: ns = not significant; *$P < 0.05$; **$P < 0.01$; ***$P < 0.001$; ***$P < 0.0001$. Any specific statistical analysis is reported in the relevant legend.

ACKNOWLEDGMENTS

I would like to thank Dr. Pietro Pichierri and Dr. Annapaola Franchitto for the opportunity they gave me to do the PhD in their lab. I would like to thank them also for their teachings, their constant support and advices. They let me grow at an experimental and personal level. I am grateful also to Dr. Maria Spies and Dr. Marco Muzi-Falconi for reading this manuscript and for their revisions and kind advices. Finally, I would like to thank all my colleagues of Genome Stability group, with which I shared happy and sad moments, for their constant help and support.

BIBLIOGRAPHY

Abdel-Samad, R., Aouad, P., Gali-Muhtasib, H., Sweidan, Z., Hmadi, R., Kadara, H., Luca D'andrea, E., Fucci, A., Pisano, C., & Darwiche, N. (2018). Mechanism of action of the atypical retinoid ST1926 in colorectal cancer: DNA damage and DNA polymerase α. In *Am J Cancer Res* (Vol. 8, Issue 1). www.ajcr.us/

Achar, Y. J., Balogh, D., & Haracska, L. (2011). Coordinated protein and DNA remodeling by human HLTF on stalled replication fork. *Proceedings of the National Academy of Sciences*, *108*(34), 14073–14078. https://doi.org/10.1073/pnas.1101951108

Adolph, M. B., Mohamed, T. M., Balakrishnan, S., Xue, C., Morati, F., Modesti, M., Greene, E. C., Chazin, W. J., & Cortez, D. (2021). RADX controls RAD51 filament dynamics to regulate replication fork stability. *Molecular Cell*, *81*(5), 1074-1083.e5. https://doi.org/10.1016/j.molcel.2020.12.036

Altmannova, V., Eckert-Boulet, N., Arneric, M., Kolesar, P., Chaloupkova, R., Damborsky, J., Sung, P., Zhao, X., Lisby, M., & Krejci, L. (2010). Rad52 SUMOylation affects the efficiency of the DNA repair. *Nucleic Acids Research*, *38*(14), 4708–4721. https://doi.org/10.1093/nar/gkq195

Bailey, L. J., Bianchi, J., & Doherty, A. J. (2019). PrimPol is required for the maintenance of efficient nuclear and mitochondrial DNA replication in human cells. *Nucleic Acids Research*, *47*(8), 4026–4038. https://doi.org/10.1093/nar/gkz056

Bainbridge, L. J., Teague, R., & Doherty, A. J. (2021). Repriming DNA synthesis: An intrinsic restart pathway that maintains efficient genome replication. In *Nucleic Acids Research* (Vol. 49, Issue 9, pp. 4831–4847). Oxford University Press. https://doi.org/10.1093/nar/gkab176

Barroso-González, J., García-Expósito, L., Hoang, S. M., Lynskey, M. L., Roncaioli, J. L., Ghosh, A., Wallace, C. T., Modesti, M., Bernstein, K. A., Sarkar, S. N., Watkins, S. C., & O'Sullivan, R. J. (2019). RAD51AP1 Is an Essential Mediator of Alternative Lengthening of Telomeres. *Molecular Cell*, *76*(1), 11-26.e7. https://doi.org/10.1016/j.molcel.2019.06.043

Bell, S. P., & Dutta, A. (2002). DNA replication in eukaryotic cells. In *Annual Review of Biochemistry* (Vol. 71, pp. 333–374). https://doi.org/10.1146/annurev.biochem.71.110601.135425

Berti, M., Teloni, F., Mijic, S., Ursich, S., Fuchs, J., Palumbieri, M. D., Krietsch, J., Schmid, J. A., Garcin, E. B., Gon, S., Modesti, M., Altmeyer, M., & Lopes, M. (2020). Sequential role of RAD51 paralog complexes in replication fork remodeling and restart. *Nature Communications*, *11*(1). https://doi.org/10.1038/s41467-020-17324-z

Bétous, R., Couch, F. B., Mason, A. C., Eichman, B. F., Manosas, M., & Cortez, D. (2013). Substrate-Selective Repair and Restart of Replication Forks by DNA Translocases. *Cell Reports*, *3*(6), 1958–1969. https://doi.org/10.1016/j.celrep.2013.05.002

Bhat, D. S., Spies, M. A., & Spies, M. (2022). A moving target for drug discovery: Structure activity relationship and many genome (de)stabilizing functions of the RAD52 protein. *DNA Repair*, *120*, 103421. https://doi.org/10.1016/j.dnarep.2022.103421

Bhat, K. P., Bétous, R., & Cortez, D. (2015). High-affinity DNA-binding domains of replication protein A (RPA) direct SMARCAL1-dependent replication fork remodeling. *Journal of Biological Chemistry*, *290*(7), 4110–4117. https://doi.org/10.1074/jbc.M114.627083

Bhat, K. P., & Cortez, D. (2018). RPA and RAD51: fork reversal, fork protection, and genome stability. *Nature Structural & Molecular Biology*, *25*(6), 446–453. https://doi.org/10.1038/s41594-018-0075-z

Bhat, K. P., Krishnamoorthy, A., Dungrawala, H., Garcin, E. B., Modesti, M., & Cortez, D. (2018). RADX Modulates RAD51 Activity to Control Replication Fork Protection. *Cell Reports*, *24*(3), 538–545. https://doi.org/10.1016/j.celrep.2018.06.061

Bianchi, J., Rudd, S. G., Jozwiakowski, S. K., Bailey, L. J., Soura, V., Taylor, E., Stevanovic, I., Green, A. J., Stracker, T. H., Lindsay, H. D., & Doherty, A. J. (2013). Primpol bypasses UV photoproducts during eukaryotic chromosomal DNA replication. *Molecular Cell*, *52*(4), 566–573. https://doi.org/10.1016/j.molcel.2013.10.035

Blair, K., Tehseen, M., Raducanu, V. S., Shahid, T., Lancey, C., Rashid, F., Creuhet, R., Hamdan, S. M., & de Biasio, A. (2022). Mechanism of human Lig1 regulation by PCNA in Okazaki fragment sealing. *Nature Communications*, *13*(1). https://doi.org/10.1038/s41467-022-35475-z

Boehm, E. M., Powers, K. T., Kondratick, C. M., Spies, M., Houtman, J. C. D., & Washington, M. T. (2016). The Proliferating Cell Nuclear Antigen (PCNA)-interacting Protein (PIP) Motif of DNA Polymerase η Mediates Its Interaction with the C-terminal Domain of Rev1. *Journal of Biological Chemistry*, *291*(16), 8735–8744. https://doi.org/10.1074/jbc.M115.697938

Branzei, D. (2011). Ubiquitin family modifications and template switching. In *FEBS Letters* (Vol. 585, Issue 18, pp. 2810–2817). https://doi.org/10.1016/j.febslet.2011.04.053

Branzei, D., & Foiani, M. (2009). The checkpoint response to replication stress. *DNA Repair*, *8*(9), 1038–1046. https://doi.org/10.1016/j.dnarep.2009.04.014

Branzei, D., & Szakal, B. (2016). DNA damage tolerance by recombination: Molecular pathways and DNA structures. In *DNA Repair* (Vol. 44, pp. 68–75). Elsevier B.V. https://doi.org/10.1016/j.dnarep.2016.05.008

Carreira, A., & Kowalczykowski, S. C. (2011). Two classes of BRC repeats in BRCA2 promote RAD51 nucleoprotein filament function by distinct mechanisms. *Proceedings of the National Academy of Sciences*, *108*(26), 10448–10453. https://doi.org/10.1073/pnas.1106971108

Centore, R. C., Yazinski, S. A., Tse, A., & Zou, L. (2012). Spartan/C1orf124, a Reader of PCNA Ubiquitylation and a Regulator of UV-Induced DNA Damage Response. *Molecular Cell*, *46*(5), 625–635. https://doi.org/10.1016/j.molcel.2012.05.020

Chandramouly, G., McDevitt, S., Sullivan, K., Kent, T., Luz, A., Glickman, J. F., Andrake, M., Skorski, T., & Pomerantz, R. T. (2015). Small-Molecule Disruption of RAD52 Rings as a Mechanism for Precision Medicine in BRCA-Deficient Cancers. *Chemistry and Biology*, *22*(11), 1491–1504. https://doi.org/10.1016/j.chembiol.2015.10.003

Choe, K. N., & Moldovan, G. L. (2017). Forging Ahead through Darkness: PCNA, Still the Principal Conductor at the Replication Fork. In *Molecular Cell* (Vol. 65, Issue 3, pp. 380–392). Cell Press. https://doi.org/10.1016/j.molcel.2016.12.020

Choe, K. N., Nicolae, C. M., Constantin, D., Imamura Kawasawa, Y., Delgado-Diaz, M. R., De, S., Freire, R., Smits, V. A., & Moldovan, G. (2016). HUWE 1 interacts with PCNA to alleviate replication stress . *EMBO Reports*, *17*(6), 874–886. https://doi.org/10.15252/embr.201541685

Chun, J., Buechelmaier, E. S., & Powell, S. N. (2013). Rad51 Paralog Complexes BCDX2 and CX3 Act at Different Stages in the BRCA1-BRCA2-Dependent Homologous Recombination Pathway. *Molecular and Cellular Biology*, *33*(2), 387–395. https://doi.org/10.1128/MCB.00465-12

Ciccia, A., Nimonkar, A. V., Hu, Y., Hajdu, I., Achar, Y. J., Izhar, L., Petit, S. A., Adamson, B., Yoon, J. C., Kowalczykowski, S. C., Livingston, D. M., Haracska, L., & Elledge, S. J. (2012). Polyubiquitinated PCNA Recruits the ZRANB3 Translocase to Maintain Genomic Integrity after Replication Stress. *Molecular Cell*, *47*(3), 396–409. https://doi.org/10.1016/j.molcel.2012.05.024

Claussin, C., & Chang, M. (2016). Multiple Rad52-Mediated Homology-Directed Repair Mechanisms Are Required to Prevent Telomere Attrition-Induced Senescence in Saccharomyces cerevisiae. *PLoS Genetics*, *12*(7). https://doi.org/10.1371/journal.pgen.1006176

Couch, F. B., Bansbach, C. E., Driscoll, R., Luzwick, J. W., Glick, G. G., Bétous, R., Carroll, C. M., Jung, S. Y., Qin, J., Cimprich, K. A., & Cortez, D. (2013). ATR phosphorylates SMARCAL1 to prevent replication fork collapse. *Genes & Development*, *27*(14), 1610–1623. https://doi.org/10.1101/gad.214080.113

Croteau, D. L., Popuri, V., Opresko, P. L., & Bohr, V. A. (2014). Human RecQ Helicases in DNA Repair, Recombination, and Replication. *Annual Review of Biochemistry*, *83*(1), 519–552. https://doi.org/10.1146/annurev-biochem-060713-035428

Daigaku, Y., Keszthelyi, A., Müller, C. A., Miyabe, I., Brooks, T., Retkute, R., Hubank, M., Nieduszynski, C. A., & Carr, A. M. (2015). A global profile of replicative polymerase usage. *Nature Structural & Molecular Biology*, *22*(3), 192–198. https://doi.org/10.1038/nsmb.2962

Díaz-Talavera, A., Montero-Conde, C., Leandro-García, L. J., & Robledo, M. (2022). PrimPol: A Breakthrough among DNA Replication Enzymes and a Potential New Target for Cancer Therapy. In *Biomolecules* (Vol. 12, Issue 2). MDPI. https://doi.org/10.3390/biom12020248

Ercilla, A., Benada, J., Amitash, S., Zonderland, G., Baldi, G., Somyajit, K., Ochs, F., Costanzo, V., Lukas, J., & Toledo, L. (2020). Physiological Tolerance to ssDNA Enables Strand Uncoupling during DNA Replication. *Cell Reports*, *30*(7), 2416-2429.e7. https://doi.org/10.1016/j.celrep.2020.01.067

Feng, Z., Scott, S. P., Bussen, W., Sharma, G. G., Guo, G., Pandita, T. K., & Powell, S. N. (2011). Rad52 inactivation is synthetically lethal with BRCA2 deficiency. *Proceedings of the National Academy of Sciences of the United States of America*, *108*(2), 686–691. https://doi.org/10.1073/pnas.1010959107

Friedberg, E. C., Aguilera, A., Gellert, M., Hanawalt, P. C., Hays, J. B., Lehmann, A. R., Lindahl, T., Lowndes, N., Sarasin, A., & Wood, R. D. (2006). DNA repair: From molecular mechanism to human disease. *DNA Repair*, *5*(8), 986–996. https://doi.org/10.1016/j.dnarep.2006.05.005

Friedberg, E. C., Lehmann, A. R., & Fuchs, R. P. P. (2005). Trading Places: How do DNA polymerases switch during translesion DNA synthesis? In *Molecular Cell* (Vol. 18, Issue 5, pp. 499–505). Cell Press. https://doi.org/10.1016/j.molcel.2005.03.032

Fu, Y. v., Yardimci, H., Long, D. T., Ho, V., Guainazzi, A., Bermudez, V. P., Hurwitz, J., van Oijen, A., Schärer, O. D., & Walter, J. C. (2011). Selective bypass of a lagging strand roadblock by the

eukaryotic replicative DNA helicase. *Cell*, *146*(6), 931–941. https://doi.org/10.1016/j.cell.2011.07.045

Fugger, K., Mistrik, M., Neelsen, K. J., Yao, Q., Zellweger, R., Kousholt, A. N., Haahr, P., Chu, W. K., Bartek, J., Lopes, M., Hickson, I. D., & Sørensen, C. S. (2015). FBH1 Catalyzes Regression of Stalled Replication Forks. *Cell Reports*, *10*(10), 1749–1757. https://doi.org/10.1016/j.celrep.2015.02.028

Fumasoni, M., Zwicky, K., Vanoli, F., Lopes, M., & Branzei, D. (2015). Error-Free DNA Damage Tolerance and Sister Chromatid Proximity during DNA Replication Rely on the Polα/Primase/Ctf4 Complex. *Molecular Cell*, *57*(5), 812–823. https://doi.org/10.1016/j.molcel.2014.12.038

García-Rodríguez, N., Morawska, M., Wong, R. P., Daigaku, Y., & Ulrich, H. D. (2018). Spatial separation between replisome- and template-induced replication stress signaling. *The EMBO Journal*, *37*(9). https://doi.org/10.15252/embj.201798369

Giannattasio, M., Zwicky, K., Follonier, C., Foiani, M., Lopes, M., & Branzei, D. (2014). Visualization of recombination-mediated damage bypass by template switching. *Nature Structural & Molecular Biology*, *21*(10), 884–892. https://doi.org/10.1038/nsmb.2888

González-Acosta, D., Blanco-Romero, E., Ubieto-Capella, P., Mutreja, K., Míguez, S., Llanos, S., García, F., Muñoz, J., Blanco, L., Lopes, M., & Méndez, J. (2021). PrimPol-mediated repriming facilitates replication traverse of DNA interstrand crosslinks. *The EMBO Journal*, *40*(14). https://doi.org/10.15252/embj.2020106355

Grimme, J. M., Honda, M., Wright, R., Okuno, Y., Rothenberg, E., Mazin, A. v., Ha, T., & Spies, M. (2010). Human Rad52 binds and wraps single-stranded DNA and mediates annealing via two hRad52-ssDNA complexes. *Nucleic Acids Research*, *38*(9), 2917–2930. https://doi.org/10.1093/nar/gkp1249

Guilliam, T. A. (2021). Mechanisms for Maintaining Eukaryotic Replisome Progression in the Presence of DNA Damage. In *Frontiers in Molecular Biosciences* (Vol. 8). Frontiers Media S.A. https://doi.org/10.3389/fmolb.2021.712971

Guilliam, T., & Doherty, A. (2017). PrimPol—Prime Time to Reprime. *Genes*, *8*(1), 20. https://doi.org/10.3390/genes8010020

Guo, C., Sonoda, E., Tang, T. S., Parker, J. L., Bielen, A. B., Takeda, S., Ulrich, H. D., & Friedberg, E. C. (2006). REV1 Protein Interacts with PCNA: Significance of the REV1 BRCT Domain In Vitro and In Vivo. *Molecular Cell*, *23*(2), 265–271. https://doi.org/10.1016/j.molcel.2006.05.038

Ha, T., Hengel, S. R., Malacaria, E., Folly, L., Constantino, S., Bain, F. E., Diaz, A., Koch, B. G., Yu, L., Wu, M., Pichierri, P., Spies, M. A., & Spies, M. (2016). *Small-molecule inhibitors identify the RAD52-ssDNA interaction as critical for recovery from replication stress and for survival of BRCA2 deficient cells*. https://doi.org/10.7554/eLife.14740.001

Han, J., Liu, T., Huen, M. S. Y., Hu, L., Chen, Z., & Huang, J. (2014). SIVA1 directs the E3 ubiquitin ligase RAD18 for PCNA monoubiquitination. *Journal of Cell Biology*, *205*(6), 811–827. https://doi.org/10.1083/jcb.201311007

Hanamshet, K., & Mazin, A. V. (2020). The function of RAD52 N-terminal domain is essential for viability of BRCA-deficient cells. *Nucleic Acids Research*, *48*(22), 12778–12791. https://doi.org/10.1093/nar/gkaa1145

Hanamshet, K., Mazina, O. M., & Mazin, A. v. (2016). Reappearance from obscurity: Mammalian Rad52 in homologous recombination. In *Genes* (Vol. 7, Issue 9). MDPI AG. https://doi.org/10.3390/genes7090063

Hargreaves, D. C., & Crabtree, G. R. (2011). ATP-dependent chromatin remodeling: genetics, genomics and mechanisms. *Cell Research*, *21*(3), 396–420. https://doi.org/10.1038/cr.2011.32

Heller, R. C., Kang, S., Lam, W. M., Chen, S., Chan, C. S., & Bell, S. P. (2011). Eukaryotic origin-dependent DNA replication in vitro reveals sequential action of DDK and S-CDK kinases. *Cell*, *146*(1), 80–91. https://doi.org/10.1016/j.cell.2011.06.012

Heller, R. C., & Marians, K. J. (2006). Replication fork reactivation downstream of a blocked nascent leading strand. *Nature*, *439*(7076), 557–562. https://doi.org/10.1038/nature04329

Helmer, L., Farrell, P., Hendy, I., Harding, S., Robertson, M., & Preston, J. (2019). Active management is required to turn the tide for depleted *Ostrea edulis* stocks from the effects of overfishing, disease and invasive species. *PeerJ*, *7*, e6431. https://doi.org/10.7717/peerj.6431

Higgs, M. R., Reynolds, J. J., Winczura, A., Blackford, A. N., Borel, V., Miller, E. S., Zlatanou, A., Nieminuszczy, J., Ryan, E. L., Davies, N. J., Stankovic, T., Boulton, S. J., Niedzwiedz, W., & Stewart, G. S. (2015). BOD1L Is Required to Suppress Deleterious Resection of Stressed Replication Forks. *Molecular Cell*, *59*(3), 462–477. https://doi.org/10.1016/j.molcel.2015.06.007

Holloman, W. K. (2011). Unraveling the mechanism of BRCA2 in homologous recombination. In *Nature Structural and Molecular Biology* (Vol. 18, Issue 7, pp. 748–754). https://doi.org/10.1038/nsmb.2096

Honda, M., Okuno, Y., Yoo, J., Ha, T., & Spies, M. (2011). Tyrosine phosphorylation enhances RAD52-mediated annealing by modulating its DNA binding. *The EMBO Journal*, *30*(16), 3368–3382. https://doi.org/10.1038/emboj.2011.238

Howard-Flanders, P., Rupp, W. D., Wilkins, B. M., & Cole, R. S. (1968). DNA Replication and Recombination after UV Irradiation. *Cold Spring Harbor Symposia on Quantitative Biology*, *33*(0), 195–207. https://doi.org/10.1101/SQB.1968.033.01.023

Huang, F., Goyal, N., Sullivan, K., Hanamshet, K., Patel, M., Mazina, O. M., Wang, C. X., An, W. F., Spoonamore, J., Metkar, S., Emmitte, K. A., Cocklin, S., Skorski, T., & Mazin, A. v. (2016). Targeting BRCA1-and BRCA2-deficient cells with RAD52 small molecule inhibitors. *Nucleic Acids Research*, *44*(9), 4189–4199. https://doi.org/10.1093/nar/gkw087

Huang, M., Zhou, B., Gong, J., Xing, L., Ma, X., Wang, F., Wu, W., Shen, H., Sun, C., Zhu, X., Yang, Y., Sun, Y., Liu, Y., Tang, T. S., & Guo, C. (2018). RNA-splicing factor SART3 regulates translesion DNA synthesis. *Nucleic Acids Research*, *46*(9), 4560–4574. https://doi.org/10.1093/nar/gky220

Iannascoli, C., Palermo, V., Murfuni, I., Franchitto, A., & Pichierri, P. (2015). The WRN exonuclease domain protects nascent strands from pathological MRE11/EXO1-dependent degradation. *Nucleic Acids Research*, *43*(20), 9788–9803. https://doi.org/10.1093/nar/gkv836

Jalan, M., Olsen, K. S., & Powell, S. N. (2019). Emerging roles of RAD52 in genome maintenance. In *Cancers* (Vol. 11, Issue 7). MDPI AG. https://doi.org/10.3390/cancers11071038

Kaochar, S., Shanks, L., & Weinert, T. (2010). Checkpoint genes and Exo1 regulate nearby inverted repeat fusions that form dicentric chromosomes in Saccharomyces cerevisiae. *Proceedings of*

the National Academy of Sciences of the United States of America, *107*(50), 21605–21610. https://doi.org/10.1073/pnas.1001938107

Keen, B. A., Bailey, L. J., Jozwiakowski, S. K., & Doherty, A. J. (2014). Human PrimPol mutation associated with high myopia has a DNA replication defect. *Nucleic Acids Research*, *42*(19), 12102–12111. https://doi.org/10.1093/nar/gku879

Kelso, A. A., Lopezcolorado, F. W., Bhargava, R., & Stark, J. M. (2019). Distinct roles of RAD52 and POLQ in chromosomal break repair and replication stress response. *PLoS Genetics*, *15*(8). https://doi.org/10.1371/journal.pgen.1008319

Khanna, K. K., & Jackson, S. P. (2001). *DNA double-strand breaks: signaling, repair and the cancer connection*. http://genetics.nature.com

Kile, A. C., Chavez, D. A., Bacal, J., Eldirany, S., Korzhnev, D. M., Bezsonova, I., Eichman, B. F., & Cimprich, K. A. (2015). HLTF's Ancient HIRAN Domain Binds 3' DNA Ends to Drive Replication Fork Reversal. *Molecular Cell*, *58*(6), 1090–1100. https://doi.org/10.1016/j.molcel.2015.05.013

Kilkenny, M. L., Simon, A. C., Mainwaring, J., Wirthensohn, D., Holzer, S., & Pellegrini, L. (2017). The human CTF4-orthologue AND-1 interacts with DNA polymerase a/primase via its unique C-Terminal HMG box. *Journal of the Royal Society Interface*, *7*(136). https://doi.org/10.1098/rsob.170217

Kim, Y.-J., Kim, T.-W., Park, S.-R., Kim, H.-T., Ryu, S.-Y., & Jung, J.-Y. (2015). Expression of the Mre11–Rad50–Nbs1 complex in cisplatin nephrotoxicity. *Environmental Toxicology and Pharmacology*, *40*(1), 12–17. https://doi.org/10.1016/j.etap.2015.04.018

Kobayashi, K., Guilliam, T. A., Tsuda, M., Yamamoto, J., Bailey, L. J., Iwai, S., Takeda, S., Doherty, A. J., & Hirota, K. (2016). Repriming by PrimPol is critical for DNA replication restart downstream of lesions and chain-terminating nucleosides. *Cell Cycle*, *15*(15), 1997–2008. https://doi.org/10.1080/15384101.2016.1191711

Kojic, M., Kostrub, C. F., Buchman, A. R., & Holloman, W. K. (2002). BRCA2 Homolog Required for Proficiency in DNA Repair, Recombination, and Genome Stability in Ustilago maydis 1998b; Wong et al., 1997). Expression of DNA fragments encoding individual BRC repeats disrupts the BRCA2-Rad51 complex, conferring a dominant-negative radia-tion hypersensitivity and an inability to form radiation-induced Rad51 nuclear foci (Chen et al., 1999). Synthetic. In *Molecular Cell* (Vol. 10). http://searchlauncher.bcm.tmc.edu/cgi-bin/

Kolinjivadi, A. M., Sannino, V., De Antoni, A., Zadorozhny, K., Kilkenny, M., Técher, H., Baldi, G., Shen, R., Ciccia, A., Pellegrini, L., Krejci, L., & Costanzo, V. (2017). Smarcal1-Mediated Fork Reversal Triggers Mre11-Dependent Degradation of Nascent DNA in the Absence of Brca2 and Stable Rad51 Nucleofilaments. *Molecular Cell*, *67*(5), 867-881.e7. https://doi.org/10.1016/j.molcel.2017.07.001

Kondratick, C. M., Washington, M. T., & Spies, M. (2021). Making choices: DNA replication fork recovery mechanisms. *Seminars in Cell & Developmental Biology*, *113*, 27–37. https://doi.org/10.1016/j.semcdb.2020.10.001

Kramara, J., Osia, B., & Malkova, A. (2018). Break-Induced Replication: The Where, The Why, and The How. *Trends in Genetics*, *34*(7), 518–531. https://doi.org/10.1016/j.tig.2018.04.002

Krijger, P. H. L., Lee, K. Y., Wit, N., van den Berk, P. C. M., Wu, X., Roest, H. P., Maas, A., Ding, H., Hoeijmakers, J. H. J., Myung, K., & Jacobs, H. (2011). HLTF and SHPRH are not essential for PCNA

polyubiquitination, survival and somatic hypermutation: Existence of an alternative E3 ligase. *DNA Repair*, *10*(4), 438–444. https://doi.org/10.1016/j.dnarep.2010.12.008

Kuchta, R. D., Reid, B., & Chang, L. M. S. (1990). DNA primase. Processivity and the primase to polymerase α activity switch. *Journal of Biological Chemistry*, *265*(27), 16158–16165. https://doi.org/10.1016/s0021-9258(17)46202-8

Kuchta, R. D., & Stengel, G. (2010). Mechanism and evolution of DNA primases. In *Biochimica et Biophysica Acta - Proteins and Proteomics* (Vol. 1804, Issue 5, pp. 1180–1189). https://doi.org/10.1016/j.bbapap.2009.06.011

Laurini, E., Marson, D., Fermeglia, A., Aulic, S., Fermeglia, M., & Pricl, S. (2020). Role of Rad51 and DNA repair in cancer: A molecular perspective. *Pharmacology & Therapeutics*, *208*, 107492. https://doi.org/10.1016/j.pharmthera.2020.107492

Lazarchuk, P., Roy, S., Schlacher, K., & Sidorova, J. (2019). Detection and quantitation of acetylated histones on replicating DNA using in situ proximity ligation assay and click-it chemistry. In *Methods in Molecular Biology* (Vol. 1983, pp. 29–45). Humana Press Inc. https://doi.org/10.1007/978-1-4939-9434-2_3

Lee, J.-H., Mand, M. R., Kao, C.-H., Zhou, Y., Ryu, S. W., Richards, A. L., Coon, J. J., & Paull, T. T. (2018). ATM directs DNA damage responses and proteostasis via genetically separable pathways. *Science Signaling*, *11*(512). https://doi.org/10.1126/scisignal.aan5598

Lee, J.-H., & Paull, T. T. (2021). Cellular functions of the protein kinase ATM and their relevance to human disease. *Nature Reviews Molecular Cell Biology*, *22*(12), 796–814. https://doi.org/10.1038/s41580-021-00394-2

Lemaçon, D., Jackson, J., Quinet, A., Brickner, J. R., Li, S., Yazinski, S., You, Z., Ira, G., Zou, L., Mosammaparast, N., & Vindigni, A. (2017). MRE11 and EXO1 nucleases degrade reversed forks and elicit MUS81-dependent fork rescue in BRCA2-deficient cells. *Nature Communications*, *8*(1), 860. https://doi.org/10.1038/s41467-017-01180-5

Leuzzi, G., Marabitti, V., Pichierri, P., & Franchitto, A. (2016). <scp>WRNIP</scp> 1 protects stalled forks from degradation and promotes fork restart after replication stress. *The EMBO Journal*, *35*(13), 1437–1451. https://doi.org/10.15252/embj.201593265

Li, M., Larsen, L., & Hedglin, M. (2020). Rad6/Rad18 Competes with DNA Polymerases η and δ for PCNA Encircling DNA. *Biochemistry*, *59*(4), 407–416. https://doi.org/10.1021/acs.biochem.9b00938

Li, P., Xu, Y. Z., Zhang, Q., Li, Y., Jia, W., Wang, X., Xie, Z., Liu, J., Zhao, D., Shao, M., Chen, S., Mo, N., Jiang, Z., Li, L., Liu, R., Huang, W., Chang, L., Chen, S., Li, H., … Yang, X. (2019). Evaluating the role of RAD52 and its interactors as novel potential molecular targets for hepatocellular carcinoma. *Cancer Cell International*, *19*(1). https://doi.org/10.1186/s12935-019-0996-6

Liao, H., Ji, F., Helleday, T., & Ying, S. (2018). Mechanisms for stalled replication fork stabilization: new targets for synthetic lethality strategies in cancer treatments. *EMBO Reports*, *19*(9). https://doi.org/10.15252/embr.201846263

Lin, S. H. S., Wang, X., Zhang, S., Zhang, Z., Lee, E. Y. C., & Lee, M. Y. W. T. (2013). Dynamics of enzymatic interactions during short flap human Okazaki fragment processing by two forms of human DNA polymerase δ. *DNA Repair*, *12*(11), 922–935. https://doi.org/10.1016/j.dnarep.2013.08.008

Ling, C., Huang, J., Yan, Z., Li, Y., Ohzeki, M., Ishiai, M., Xu, D., Takata, M., Seidman, M., & Wang, W. (2016). Bloom syndrome complex promotes FANCM recruitment to stalled replication forks and facilitates both repair and traverse of DNA interstrand crosslinks. *Cell Discovery*, *2*(1), 16047. https://doi.org/10.1038/celldisc.2016.47

Ling, J. A., Frevert, Z., & Washington, M. T. (2022). Recent Advances in Understanding the Structures of Translesion Synthesis DNA Polymerases. *Genes*, *13*(5), 915. https://doi.org/10.3390/genes13050915

Llorens-Agost, M., Ensminger, M., Le, H. P., Gawai, A., Liu, J., Cruz-García, A., Bhetawal, S., Wood, R. D., Heyer, W. D., & Löbrich, M. (2021). POLθ-mediated end joining is restricted by RAD52 and BRCA2 until the onset of mitosis. *Nature Cell Biology*, *23*(10), 1095–1104. https://doi.org/10.1038/s41556-021-00764-0

Lok, B. H., Carley, A. C., Tchang, B., & Powell, S. N. (2013). RAD52 inactivation is synthetically lethal with deficiencies in BRCA1 and PALB2 in addition to BRCA2 through RAD51-mediated homologous recombination. *Oncogene*, *32*(30), 3552–3558. https://doi.org/10.1038/onc.2012.391

Lopes, M., Foiani, M., & Sogo, J. M. (2006). Multiple mechanisms control chromosome integrity after replication fork uncoupling and restart at irreparable UV lesions. *Molecular Cell*, *21*(1), 15–27. https://doi.org/10.1016/j.molcel.2005.11.015

Lord, C. J., & Ashworth, A. (2016). BRCAness revisited. *Nature Reviews Cancer*, *16*(2), 110–120. https://doi.org/10.1038/nrc.2015.21

Lovejoy, C. A., & Cortez, D. (2009). Common mechanisms of PIKK regulation. *DNA Repair*, *8*(9), 1004–1008. https://doi.org/10.1016/j.dnarep.2009.04.006

MacKay, C., Toth, R., & Rouse, J. (2009). Biochemical characterisation of the SWI/SNF family member HLTF. *Biochemical and Biophysical Research Communications*, *390*(2), 187–191. https://doi.org/10.1016/j.bbrc.2009.08.151

Maga, G., Villani, G., Tillement, V., Stucki, M., Locatelli, G. A., Frouin, I., Spadari, S., & Hü, U. (2001). *Okazaki fragment processing: Modulation of the strand displacement activity of DNA polymerase by the concerted action of replication protein A, proliferating cell nuclear antigen, and flap endonuclease-1*. https://www.pnas.org

Malacaria, E., Honda, M., Franchitto, A., Spies, M., & Pichierri, P. (2020). Physiological and pathological roles of RAD52 at DNA replication forks. In *Cancers* (Vol. 12, Issue 2). MDPI AG. https://doi.org/10.3390/cancers12020402

Malacaria, E., Pugliese, G. M., Honda, M., Marabitti, V., Aiello, F. A., Spies, M., Franchitto, A., & Pichierri, P. (2019). Rad52 prevents excessive replication fork reversal and protects from nascent strand degradation. *Nature Communications*, *10*(1). https://doi.org/10.1038/s41467-019-09196-9

Maréchal, A., & Zou, L. (2013). DNA damage sensing by the ATM and ATR kinases. *Cold Spring Harbor Perspectives in Biology*, *5*(9). https://doi.org/10.1101/cshperspect.a012716

Matsumoto, Y., Brooks, R. C., Sverzhinsky, A., Pascal, J. M., & Tomkinson, A. E. (2020). Dynamic DNA-bound PCNA complexes co-ordinate Okazaki fragment synthesis, processing and ligation. *Journal of Molecular Biology*, *432*(24). https://doi.org/10.1016/j.jmb.2020.10.032

Matsuoka, S., Ballif, B. A., Smogorzewska, A., McDonald, E. R., Hurov, K. E., Luo, J., Bakalarski, C. E., Zhao, Z., Solimini, N., Lerenthal, Y., Shiloh, Y., Gygi, S. P., & Elledge, S. J. (2007). ATM and ATR Substrate Analysis Reveals Extensive Protein Networks Responsive to DNA Damage. *Science*, *316*(5828), 1160–1166. https://doi.org/10.1126/science.1140321

McKinnon, P. J. (2004). ATM and ataxia telangiectasia. *EMBO Reports*, *5*(8), 772–776. https://doi.org/10.1038/sj.embor.7400210

Mijic, S., Zellweger, R., Chappidi, N., Berti, M., Jacobs, K., Mutreja, K., Ursich, S., Ray Chaudhuri, A., Nussenzweig, A., Janscak, P., & Lopes, M. (2017). Replication fork reversal triggers fork degradation in BRCA2-defective cells. *Nature Communications*, *8*(1). https://doi.org/10.1038/s41467-017-01164-5

Mohiuddin, M., Evans, T. J., Rahman, M. M., Keka, I. S., Tsuda, M., Sasanuma, H., & Takeda, S. (2018). SUMOylation of PCNA by PIAS1 and PIAS4 promotes template switch in the chicken and human B cell lines. *Proceedings of the National Academy of Sciences of the United States of America*, *115*(50), 12793–12798. https://doi.org/10.1073/pnas.1716349115

Moldovan, G. L., Pfander, B., & Jentsch, S. (2007). PCNA, the Maestro of the Replication Fork. In *Cell* (Vol. 129, Issue 4, pp. 665–679). Elsevier B.V. https://doi.org/10.1016/j.cell.2007.05.003

Mourón, S., Rodriguez-Acebes, S., Martínez-Jiménez, M. I., García-Gómez, S., Chocrón, S., Blanco, L., & Méndez, J. (2013). Repriming of DNA synthesis at stalled replication forks by human PrimPol. *Nature Structural and Molecular Biology*, *20*(12), 1383–1389. https://doi.org/10.1038/nsmb.2719

Murfuni, I., Basile, G., Subramanyam, S., Malacaria, E., Bignami, M., Spies, M., Franchitto, A., & Pichierri, P. (2013). Survival of the Replication Checkpoint Deficient Cells Requires MUS81-RAD52 Function. *PLoS Genetics*, *9*(10). https://doi.org/10.1371/journal.pgen.1003910

Neelsen, K. J., & Lopes, M. (2015). Replication fork reversal in eukaryotes: from dead end to dynamic response. *Nature Reviews Molecular Cell Biology*, *16*(4), 207–220. https://doi.org/10.1038/nrm3935

Panzarino, N. J., Krais, J. J., Cong, K., Peng, M., Mosqueda, M., Nayak, S. U., Bond, S. M., Calvo, J. A., Doshi, M. B., Bere, M., Ou, J., Deng, B., Zhu, L. J., Johnson, N., & Cantor, S. B. (2021). Replication gaps underlie BRCA deficiency and therapy response. *Cancer Research*, *81*(5), 1388–1397. https://doi.org/10.1158/0008-5472.CAN-20-1602

Parplys, A. C., Seelbach, J. I., Becker, S., Behr, M., Wrona, A., Jend, C., Mansour, W. Y., Joosse, S. A., Stuerzbecher, H.-W., Pospiech, H., Petersen, C., Dikomey, E., & Borgmann, K. (2015). High levels of RAD51 perturb DNA replication elongation and cause unscheduled origin firing due to impaired CHK1 activation. *Cell Cycle*, *14*(19), 3190–3202. https://doi.org/10.1080/15384101.2015.1055996

Pellegrini, L., & Venkitaraman, A. (2004). Emerging functions of BRCA2 in DNA recombination. In *Trends in Biochemical Sciences* (Vol. 29, Issue 6, pp. 310–316). https://doi.org/10.1016/j.tibs.2004.04.009

Peng, M., Cong, K., Panzarino, N. J., Nayak, S., Calvo, J., Deng, B., Zhu, L. J., Morocz, M., Hegedus, L., Haracska, L., & Cantor, S. B. (2018). Opposing Roles of FANCJ and HLTF Protect Forks and Restrain Replication during Stress. *Cell Reports*, *24*(12), 3251–3261. https://doi.org/10.1016/j.celrep.2018.08.065

Perera, R. L., Torella, R., Klinge, S., Kilkenny, M. L., Maman, J. D., & Pellegrini, L. (2013). Mechanism for priming DNA synthesis by yeast DNA Polymerase α. *ELife*, *2013*(2). https://doi.org/10.7554/eLife.00482

Piberger, A. L., Bowry, A., Kelly, R. D. W., Walker, A. K., González-Acosta, D., Bailey, L. J., Doherty, A. J., Méndez, J., Morris, J. R., Bryant, H. E., & Petermann, E. (2020). PrimPol-dependent single-stranded gap formation mediates homologous recombination at bulky DNA adducts. *Nature Communications*, *11*(1), 5863. https://doi.org/10.1038/s41467-020-19570-7

Pichierri, P., Franchitto, A., & Rosselli, F. (2004). BLM and the FANC proteins collaborate in a common pathway in response to stalled replication forks. *The EMBO Journal*, *23*(15), 3154–3163. https://doi.org/10.1038/sj.emboj.7600277

Pilzecker, B., Buoninfante, O. A., & Jacobs, H. (2019). DNA damage tolerance in stem cells, ageing, mutagenesis, disease and cancer therapy. In *Nucleic Acids Research* (Vol. 47, Issue 14, pp. 7163–7181). Oxford University Press. https://doi.org/10.1093/NAR/GKZ531

Poole, L. A., & Cortez, D. (2017). Functions of SMARCAL1, ZRANB3, and HLTF in maintaining genome stability. *Critical Reviews in Biochemistry and Molecular Biology*, *52*(6), 696–714. https://doi.org/10.1080/10409238.2017.1380597

Povlsen, L. K., Beli, P., Wagner, S. A., Poulsen, S. L., Sylvestersen, K. B., Poulsen, J. W., Nielsen, M. L., Bekker-Jensen, S., Mailand, N., & Choudhary, C. (2012). Systems-wide analysis of ubiquitylation dynamics reveals a key role for PAF15 ubiquitylation in DNA-damage bypass. *Nature Cell Biology*, *14*(10), 1089–1098. https://doi.org/10.1038/ncb2579

Prado, F. (2014). Homologous recombination maintenance of genome integrity during DNA damage tolerance. *Molecular & Cellular Oncology*, *1*(2), e957039. https://doi.org/10.4161/23723548.2014.957039

Qiu, S., Jiang, G., Cao, L., & Huang, J. (2021). Replication Fork Reversal and Protection. In *Frontiers in Cell and Developmental Biology* (Vol. 9). Frontiers Media S.A. https://doi.org/10.3389/fcell.2021.670392

Quinet, A., Carvajal-Maldonado, D., Lemacon, D., & Vindigni, A. (2017). DNA Fiber Analysis: Mind the Gap! In *Methods in Enzymology* (Vol. 591, pp. 55–82). Academic Press Inc. https://doi.org/10.1016/bs.mie.2017.03.019

Quinet, A., Lemaçon, D., & Vindigni, A. (2017). Replication Fork Reversal: Players and Guardians. *Molecular Cell*, *68*(5), 830–833. https://doi.org/10.1016/j.molcel.2017.11.022

Quinet, A., Martins, D. J., Vessoni, A. T., Biard, D., Sarasin, A., Stary, A., & Menck, C. F. M. (2016). Translesion synthesis mechanisms depend on the nature of DNA damage in UV-irradiated human cells. *Nucleic Acids Research*, *44*(12), 5717–5731. https://doi.org/10.1093/nar/gkw280

Quinet, A., Tirman, S., Cybulla, E., Meroni, A., & Vindigni, A. (2021). To skip or not to skip: choosing repriming to tolerate DNA damage. In *Molecular Cell* (Vol. 81, Issue 4, pp. 649–658). Cell Press. https://doi.org/10.1016/j.molcel.2021.01.012

Quinet, A., Tirman, S., Jackson, J., Šviković, S., Lemaçon, D., Carvajal-Maldonado, D., González-Acosta, D., Vessoni, A. T., Cybulla, E., Wood, M., Tavis, S., Batista, L. F. Z., Méndez, J., Sale, J. E., & Vindigni, A. (2020). PRIMPOL-Mediated Adaptive Response Suppresses Replication Fork Reversal in BRCA-Deficient Cells. *Molecular Cell*, *77*(3), 461-474.e9. https://doi.org/10.1016/j.molcel.2019.10.008

Ripley, B. M., Gildenberg, M. S., & Todd Washington, M. (2020). Control of DNA damage bypass by ubiquitylation of PCNA. In *Genes* (Vol. 11, Issue 2). MDPI AG. https://doi.org/10.3390/genes11020138

Rizzo, A. A., & Korzhnev, D. M. (2019). The Rev1-Polζ translesion synthesis mutasome: Structure, interactions and inhibition. In *Enzymes* (Vol. 45, pp. 139–181). Academic Press. https://doi.org/10.1016/bs.enz.2019.07.001

Rodrigue, A., Lafrance, M., Gauthier, M.-C., McDonald, D., Hendzel, M., West, S. C., Jasin, M., & Masson, J.-Y. (2006). Interplay between human DNA repair proteins at a unique double-strand break in vivo. *The EMBO Journal*, *25*(1), 222–231. https://doi.org/10.1038/sj.emboj.7600914

Sakofsky, C. J., & Malkova, A. (2017). Break induced replication in eukaryotes: mechanisms, functions, and consequences. In *Critical Reviews in Biochemistry and Molecular Biology* (Vol. 52, Issue 4, pp. 395–413). Taylor and Francis Ltd. https://doi.org/10.1080/10409238.2017.1314444

Sale, J. E. (2013). Translesion DNA synthesis and mutagenesis in eukaryotes. *Cold Spring Harbor Perspectives in Biology*, *5*(3). https://doi.org/10.1101/cshperspect.a012708

Sale, J. E., Lehmann, A. R., & Woodgate, R. (2012). Y-family DNA polymerases and their role in tolerance of cellular DNA damage. In *Nature Reviews Molecular Cell Biology* (Vol. 13, Issue 3, pp. 141–152). https://doi.org/10.1038/nrm3289

Schiavone, D., Jozwiakowski, S. K., Romanello, M., Guilbaud, G., Guilliam, T. A., Bailey, L. J., Sale, J. E., & Doherty, A. J. (2016). PrimPol Is Required for Replicative Tolerance of G Quadruplexes in Vertebrate Cells. *Molecular Cell*, *61*(1), 161–169. https://doi.org/10.1016/j.molcel.2015.10.038

Schlacher, K., Christ, N., Siaud, N., Egashira, A., Wu, H., & Jasin, M. (2011). Erratum: Double-strand break repair-independent role for BRCA2 in blocking stalled replication fork degradation by MRE11 (Cell (2011) 145 (529-542)). In *Cell* (Vol. 145, Issue 6, p. 993). Elsevier B.V. https://doi.org/10.1016/j.cell.2011.05.021

Schlacher, K., Wu, H., & Jasin, M. (2012). A Distinct Replication Fork Protection Pathway Connects Fanconi Anemia Tumor Suppressors to RAD51-BRCA1/2. *Cancer Cell*, *22*(1), 106–116. https://doi.org/10.1016/j.ccr.2012.05.015

Sinha, A. K., Possoz, C., & Leach, D. R. F. (2020). The Roles of Bacterial DNA Double-Strand Break Repair Proteins in Chromosomal DNA Replication. *FEMS Microbiology Reviews*, *44*(3), 351–368. https://doi.org/10.1093/femsre/fuaa009

Somyajit, K., Saxena, S., Babu, S., Mishra, A., & Nagaraju, G. (2015). Mammalian RAD51 paralogs protect nascent DNA at stalled forks and mediate replication restart. *Nucleic Acids Research*, gkv880. https://doi.org/10.1093/nar/gkv880

Stallons, L. J., & McGregor, W. G. (2010). Translesion synthesis polymerases in the prevention and promotion of carcinogenesis. In *Journal of Nucleic Acids* (Vol. 2010). https://doi.org/10.4061/2010/643857

Stefanovie, B., Hengel, S. R., Mlcouskova, J., Prochazkova, J., Spirek, M., Nikulenkov, F., Nemecek, D., Koch, B. G., Bain, F. E., Yu, L., Spies, M., & Krejci, L. (2020). DSS1 interacts with and stimulates RAD52 to promote the repair of DSBs. *Nucleic Acids Research*, *48*(2), 694–708. https://doi.org/10.1093/nar/gkz1052

Su, F., Mukherjee, S., Yang, Y., Mori, E., Bhattacharya, S., Kobayashi, J., Yannone, S. M., Chen, D. J., & Asaithamby, A. (2014). Nonenzymatic Role for WRN in Preserving Nascent DNA Strands after Replication Stress. *Cell Reports*, *9*(4), 1387–1401. https://doi.org/10.1016/j.celrep.2014.10.025

Šviković, S., Crisp, A., Tan-Wong, S. M., Guilliam, T. A., Doherty, A. J., Proudfoot, N. J., Guilbaud, G., & Sale, J. E. (2019). R-loop formation during S phase is restricted by PrimPol-mediated repriming. *The EMBO Journal*, *38*(3). https://doi.org/10.15252/embj.201899793

Symington, L. S. (2002). Role of RAD52 Epistasis Group Genes in Homologous Recombination and Double-Strand Break Repair . *Microbiology and Molecular Biology Reviews*, *66*(4), 630–670. https://doi.org/10.1128/mmbr.66.4.630-670.2002

Taglialatela, A., Alvarez, S., Leuzzi, G., Sannino, V., Ranjha, L., Huang, J. W., Madubata, C., Anand, R., Levy, B., Rabadan, R., Cejka, P., Costanzo, V., & Ciccia, A. (2017). Restoration of Replication Fork Stability in BRCA1- and BRCA2-Deficient Cells by Inactivation of SNF2-Family Fork Remodelers. *Molecular Cell*, *68*(2), 414-430.e8. https://doi.org/10.1016/j.molcel.2017.09.036

Taglialatela, A., Leuzzi, G., Sannino, V., Cuella-Martin, R., Huang, J.-W., Wu-Baer, F., Baer, R., Costanzo, V., & Ciccia, A. (2021). REV1-Polζ maintains the viability of homologous recombination-deficient cancer cells through mutagenic repair of PRIMPOL-dependent ssDNA gaps. *Molecular Cell*, *81*(19), 4008-4025.e7. https://doi.org/10.1016/j.molcel.2021.08.016

Terai, K., Abbas, T., Jazaeri, A. A., & Dutta, A. (2010). CRL4Cdt2 E3 Ubiquitin Ligase Monoubiquitinates PCNA to Promote Translesion DNA Synthesis. *Molecular Cell*, *37*(1), 143–149. https://doi.org/10.1016/j.molcel.2009.12.018

Thangavel, S., Berti, M., Levikova, M., Pinto, C., Gomathinayagam, S., Vujanovic, M., Zellweger, R., Moore, H., Lee, E. H., Hendrickson, E. A., Cejka, P., Stewart, S., Lopes, M., & Vindigni, A. (2015). DNA2 drives processing and restart of reversed replication forks in human cells. *Journal of Cell Biology*, *208*(5), 545–562. https://doi.org/10.1083/jcb.201406100

Tian, T., Bu, M., Chen, X., Ding, L., Yang, Y., Han, J., Feng, X. H., Xu, P., Liu, T., Ying, S., Lei, Y., Li, Q., & Huang, J. (2021). The ZATT-TOP2A-PICH Axis Drives Extensive Replication Fork Reversal to Promote Genome Stability. *Molecular Cell*, *81*(1), 198-211.e6. https://doi.org/10.1016/j.molcel.2020.11.007

Tirman, S., Quinet, A., Wood, M., Meroni, A., Cybulla, E., Jackson, J., Pegoraro, S., Simoneau, A., Zou, L., & Vindigni, A. (2021). Temporally distinct post-replicative repair mechanisms fill PRIMPOL-dependent ssDNA gaps in human cells. *Molecular Cell*, *81*(19), 4026-4040.e8. https://doi.org/10.1016/j.molcel.2021.09.013

Toma, M., Sullivan-Reed, K., Śliwiński, T., & Skorski, T. (2019). RAD52 as a potential target for synthetic lethality-based anticancer therapies. In *Cancers* (Vol. 11, Issue 10). MDPI AG. https://doi.org/10.3390/cancers11101561

Ulrich, H. D. (2000). Two RING finger proteins mediate cooperation between ubiquitin-conjugating enzymes in DNA repair. *The EMBO Journal*, *19*(13), 3388–3397. https://doi.org/10.1093/emboj/19.13.3388

Uziel, T. (2003). Requirement of the MRN complex for ATM activation by DNA damage. *The EMBO Journal*, *22*(20), 5612–5621. https://doi.org/10.1093/emboj/cdg541

Vaisman, A., McDonald, J. P., & Woodgate, R. (2012). Translesion DNA Synthesis. *EcoSal Plus*, *5*(1). https://doi.org/10.1128/ecosalplus.7.2.2

Vaisman, A., & Woodgate, R. (2017). Translesion DNA polymerases in eukaryotes: what makes them tick? *Critical Reviews in Biochemistry and Molecular Biology*, *52*(3), 274–303. https://doi.org/10.1080/10409238.2017.1291576

Vallerga, M. B., Mansilla, S. F., Federico, M. B., Bertolin, A. P., & Gottifredi, V. (2015). Rad51 recombinase prevents Mre11 nuclease-dependent degradation and excessive PrimPol-mediated elongation of nascent DNA after UV irradiation. *Proceedings of the National Academy of Sciences*, *112*(48). https://doi.org/10.1073/pnas.1508543112

Van, C., Yan, S., Michael, W. M., Waga, S., & Cimprich, K. A. (2010). Continued primer synthesis at stalled replication forks contributes to checkpoint activation. *Journal of Cell Biology*, *189*(2), 233–246. https://doi.org/10.1083/jcb.200909105

Verma, P., Dilley, R. L., Zhang, T., Gyparaki, M. T., Li, Y., & Greenberg, R. A. (2019). RAD52 and SLX4 act nonepistatically to ensure telomere stability during alternative telomere lengthening. *Genes and Development*, *33*(3–4), 221–235. https://doi.org/10.1101/gad.319723.118

Vujanovic, M., Krietsch, J., Raso, M. C., Terraneo, N., Zellweger, R., Schmid, J. A., Taglialatela, A., Huang, J. W., Holland, C. L., Zwicky, K., Herrador, R., Jacobs, H., Cortez, D., Ciccia, A., Penengo, L., & Lopes, M. (2017). Replication Fork Slowing and Reversal upon DNA Damage Require PCNA Polyubiquitination and ZRANB3 DNA Translocase Activity. *Molecular Cell*, *67*(5), 882-890.e5. https://doi.org/10.1016/j.molcel.2017.08.010

West, S. C. (2003). Molecular views of recombination proteins and their control. In *Nature Reviews Molecular Cell Biology* (Vol. 4, Issue 6, pp. 435–445). https://doi.org/10.1038/nrm1127

Weston, R., Peeters, H., & Ahel, D. (2012). ZRANB3 is a structure-specific ATP-dependent endonuclease involved in replication stress response. *Genes & Development*, *26*(14), 1558–1572. https://doi.org/10.1101/gad.193516.112

Whelan, D. R., & Rothenberg, E. (2021). *Super-Resolution Imaging of Homologous Recombination Repair at Collapsed Replication Forks* (pp. 355–363). https://doi.org/10.1007/978-1-0716-0644-5_24

Wong, R. P., Petriukov, K., & Ulrich, H. D. (2021). Daughter-strand gaps in DNA replication – substrates of lesion processing and initiators of distress signalling. *DNA Repair*, *105*. https://doi.org/10.1016/j.dnarep.2021.103163

Xu, X., Xu, Y., Guo, R., Xu, R., Fu, C., Xing, M., Sasanuma, H., Li, Q., Takata, M., Takeda, S., Guo, R., & Xu, D. (2021). Fanconi anemia proteins participate in a break-induced-replication-like pathway to counter replication stress. *Nature Structural & Molecular Biology*, *28*(6), 487–500. https://doi.org/10.1038/s41594-021-00602-9

Yang, W., & Gao, Y. (2018). Translesion and Repair DNA Polymerases: Diverse Structure and Mechanism. *Annual Review of Biochemistry*, *87*(1), 239–261. https://doi.org/10.1146/annurev-biochem-062917-012405

Yasuda, T., Kagawa, W., Ogi, T., Kato, T. A., Suzuki, T., Dohmae, N., Takizawa, K., Nakazawa, Y., Genet, M. D., Saotome, M., Hama, M., Konishi, T., Nakajima, N. I., Hazawa, M., Tomita, M., Koike, M., Noshiro, K., Tomiyama, K., Obara, C., … Tajima, K. (2018). Novel function of HATs and HDACs in homologous recombination through acetylation of human RAD52 at double-strand break sites. *PLOS Genetics*, *14*(3), e1007277. https://doi.org/10.1371/journal.pgen.1007277

Yasuhara, T., Kato, R., Hagiwara, Y., Shiotani, B., Yamauchi, M., Nakada, S., Shibata, A., & Miyagawa, K. (2018). Human Rad52 Promotes XPG-Mediated R-loop Processing to Initiate Transcription-Associated Homologous Recombination Repair. *Cell*, *175*(2), 558-570.e11. https://doi.org/10.1016/j.cell.2018.08.056

Yeeles, J. T. P., Deegan, T. D., Janska, A., Early, A., & Diffley, J. F. X. (2015). Regulated eukaryotic DNA replication origin firing with purified proteins. *Nature*, *519*(7544), 431–435. https://doi.org/10.1038/nature14285

Yeeles, J. T. P., & Marians, K. J. (2011). The *Escherichia coli* Replisome Is Inherently DNA Damage Tolerant. *Science*, *334*(6053), 235–238. https://doi.org/10.1126/science.1209111

Zaher, M. S., Rashid, F., Song, B., Joudeh, L. I., Sobhy, M. A., Tehseen, M., Hingorani, M. M., & Hamdan, S. M. (2018). Missed cleavage opportunities by FEN1 lead to Okazaki fragment maturation via the long-flap pathway. *Nucleic Acids Research*, *46*(6), 2956–2974. https://doi.org/10.1093/nar/gky082

Zellweger, R., Dalcher, D., Mutreja, K., Berti, M., Schmid, J. A., Herrador, R., Vindigni, A., & Lopes, M. (2015). Rad51-mediated replication fork reversal is a global response to genotoxic treatments in human cells. *Journal of Cell Biology*, *208*(5), 563–579. https://doi.org/10.1083/jcb.201406099

Zhang, H., Schaub, J. M., & Finkelstein, I. J. (2020). RADX condenses single-stranded DNA to antagonize RAD51 loading. *Nucleic Acids Research*, *48*(14), 7834–7843. https://doi.org/10.1093/nar/gkaa559

Zhang, Y., Lee, J.-H., Paull, T. T., Gehrke, S., D'Alessandro, A., Dou, Q., Gladyshev, V. N., Schroeder, E. A., Steyl, S. K., Christian, B. E., & Shadel, G. S. (2018). Mitochondrial redox sensing by the kinase ATM maintains cellular antioxidant capacity. *Science Signaling*, *11*(538). https://doi.org/10.1126/scisignal.aaq0702

Zhou, B. B. S., & Bartek, J. (2004). Targeting the checkpoint kinases: Chemosensitization versus chemoprotection. In *Nature Reviews Cancer* (Vol. 4, Issue 3, pp. 216–225). Nature Publishing Group. https://doi.org/10.1038/nrc1296

Zhu, W., Ukomadu, C., Jha, S., Senga, T., Dhar, S. K., Wohlschlegel, J. A., Nutt, L. K., Kornbluth, S., & Dutta, A. (2007). Mcm10 and And-1/CTF4 recruit DNA polymerase α to chromatin for initiation of DNA replication. *Genes and Development*, *21*(18), 2288–2299. https://doi.org/10.1101/gad.1585607